# Elucidating the Effects of Interstitial Fluid Flow on Hepatocellular Carcinoma Invasion

A Dissertation

Submitted to the Faculty of

Drexel University

by

Arpit D. Shah

in partial fulfillment of the

requirements for the degree of

Doctor of Philosophy

June 2017

© Copyright 2017

Arpit D. Shah.  All Rights Reserved.

## DEDICATIONS

*This work is dedicated to my mother, father, and sister. Without their unconditional love, support, and patience, I would not be where I am today. I am forever grateful for all of the sacrifices you have made.*

## ACKNOWLEDGMENTS

The completion of this dissertation would not have been possible without the guidance and support of many people. I would like to express my heartfelt thanks to all of you who played such an integral role in my success.

First and foremost, I would like to express my sincerest gratitude to my PhD advisor, Dr. Adrian Shieh. Thank you for taking me on as a PhD student and believing in me during this entire journey. Your continuous support and infinite patience has allowed me to grow as an engineer, scientist, and most importantly a person. You have constantly challenged my scientific knowledge and writing (especially my writing), bringing out the best in me during my graduate work. I will forever be indebted to you for the guidance you have provided and the time you have invested in me.

To my committee members, Drs. Wheatley, Han, Bouchard, Clyne, and Barbee, thank you all for your time and constructively challenging my research and ideas. Your input and feedback has been a tremendous help.

I would also like to acknowledge and express my deep appreciation to two faculty members who have not only impacted my research, but have served as mentors during both my undergraduate and graduate studies. Dr. Fred Allen, I sat in your class as a freshmen with a minimal understanding of biomedical engineering or even a clear idea of what I wanted to do professionally. After that first class, I knew I wanted to be a BME who possessed as much enthusiasm and passion into my craft as you did. You took me on as a teaching assistant and I cannot thank you enough for the opportunity and tutelage you provided during this journey. Additionally, I would like to acknowledge, Dr. Jaimie Dougherty, who was that one TA that wielded a red pen tearing through my lab reports and

docking points when I was an undergraduate student. However, you always took the time to explain my short comings and provided feedback to help improve my work as a student. You continued to provide guidance and feedback during my graduate work. Thank you for caring and challenging me to be a better student.

To the lab members of the Laboratory of Tumor Mechanobiology and Microenvironment, thank you all for your help and stimulating conversations in lab during the long days and late nights. I owe a special thank you to a few of my lab members who played a critical role in my research. First, thank you Dr. Alimatou Tchafa, who trained and helped refine my technical skills in lab. Your commitment and dedication to the lab, pushed me to be a better researcher and PhD student. I appreciate the mentoring and time you took to discuss my research to help me progress forward. Christine 'Tubs' Ho, thank you for always being hungry and willing to get food, irrespective of how late it was. Your friendship and encouragement has helped me complete this dissertation. Harry Bach, thank you for your help during your STAR summer research, your contributions in lab directly impacted this dissertation. Also thank you for bleaching and sterilizing the incubators whenever they got contaminated.

To the biomedical engineering staff, you have treated me like family providing guidance and emotional support throughout my entire time at Drexel. I would like to acknowledge a few of you who have impacted my life academically, professionally, and personally. Caryn Glaser, thank you for believing in me during my worst. You have served not only as my academic advisor, but a great friend who has provided invaluable guidance and support. I will never forget the life lessons you have provided (i.e. 'Hey is for horses!'). Natalia Broz, better known as 'Rainy Day', thank you for always listening and reminding

me that things will be okay whenever I had an emotional or dramatic outburst (like last Saturday). You have been selfless with your time in making sure your students succeed and go on to make an impact in this world. I am forever indebted to you for your support. Lisa Williams, thank you for always making sure I got paid on time. This dissertation would not exist if you had not recommended me for a position in Dr. Shieh's lab when I first started graduate school. More importantly, thank you for always listening to me and emotionally supporting me when I didn't believe I could make it. Danielle Crocker, by no means would this dissertation be completed without your help. Thank you for taking a chance a decade ago by hiring me as your work study; without that job I would never have been able to build the relationships I did with the faculty and staff at biomed. I will miss walking into the office and being greeted with "hello my prince!". Bob Matthews, thank you for being the best 'work-wife' a person could have; I appreciate all of the lunches that turned into me just venting to you about my problems. I appreciate your friendship and willingness to listen. Steve Detofsky, thank you for always reminding me that I could just do stand-up comedy if this did not work out. Thank you for punishing me with some of those puns, I truly appreciate the laughs and your comedic insight. Dolores Conover, thank you for sharing your expansive technical expertise to help troubleshoot any of the problems I experienced. You have been essential to my success since my co-op days and I could not have finished this dissertation without your help. Also all those prayers worked! Frank Kepics, thank you for your help in the lab over the years, your ability to fix just about anything in the lab has allowed me to complete my work. I appreciate all the conversations we had over the years and every time I walked away learning something new and useful.

Estella Angle, thank you for always being helpful whenever I had questions. Laurie Lenz, thank you for allowing me to be a peer mentor and always baking cookies.

To all of my friends (you know who you are), thank you all for your constant emotional support and reminders that there is a light at the end of the tunnel. Thank you all for your encouragement and helping me stay sane during my PhD.

Last, but certainly not least, I would like to thank my family for all of the sacrifices they have made in order to make my academic goals a reality. Thank you for your unconditional love and unending support, you have been my source of strength and motivation during the darkest times on this journey. To my parents, Dipak and Parul Shah, thank you for everything you have done and sacrificed for me to be in this position today. Watching both of you work so hard your entire lives so that I could have a future is a debt that I will never be able to repay. To my sister, Pooja Shah, while I may not express it, but I am so proud of the woman you have matured into. Every day I am impressed with how successful you have become on your own. Thank you for putting up with me growing up and even dealing with my shenanigans now.

# TABLE OF CONTENTS

# LIST OF TABLES

## LIST OF FIGURES

## LIST OF ABBREVIATIONS

| | |
|---|---|
| HCC | hepatocellular carcinoma |
| IFF | interstitial fluid flow |
| CXCR4 | C-X-C chemokine receptor type 4 |
| CXCL12 | C-X-C motif chemokine ligand 12 |
| ERK | extracellular signal-regulated kinase |
| RTK | receptor tyrosine kinase |
| EGFR | epidermal growth factor receptor |
| PDGFR | platelet-derived growth factor receptor |
| VEGFR | vascular endothelial growth factor receptors |
| VEGF | vascular endothelial growth factor |
| IGF | insulin growth factor |
| PTEN | phosphatase and tensin homolog (PTEN) |
| MMP | matrix metalloproteinase |
| TME | tumor microenvironment |
| EMT | epithelial to mesenchymal transition |
| TGF-β | transforming growth factor beta |
| CAFs | cancer-associated fibroblasts |
| EGF | epidermal growth factor |
| HGF | hepatocyte growth factor |
| FGF | fibroblast growth factor |
| SDF-1α | stromal cell-derived factor 1 alpha |
| IL-6 | interleukin 6 |

| | |
|---|---|
| IL-8 | interleukin 8 |
| HSCs | hepatic stellate cells |
| PDGF | platelet-derived growth factor |
| TNF-α | tumor necrosis factor alpha |
| NF-κB | nuclear factor kappa-light-chain-enhance of activated B cells |
| Akt | protein kinase B |
| ICAM-1 | intercellular adhesion molecule-1 |
| RPMI | Roswell Park Memorial Institute |
| FBS | fetal bovine serum |
| MEM | minimal essential medium |
| NEAA | non-essential amino acids |
| PRH | primary rat hepatocytes |
| ITS | insulin/transferrin/selenium |
| DMSO | dimethyl sulfoxide |
| DAPI | 4’,6-diamidino-2-phenylindole |
| RIPA | radioimmunoprecipitation assay |
| ELISA | enzyme-linked immunosorbent assay |
| SEM | standard error of mean |
| ANOVA | analysis of variance |
| SDF-1 | stromal cell-derived factor 1 |
| mRNA | messenger RNA |
| FAK | focal adhesion kinase |
| MAPK | mitogen-activated protein kinase |

| | |
|---|---|
| AGE | advanced glycation end product |

# ABSTRACT

Elucidating the Effects of Interstitial Fluid Flow on Hepatocellular Carcinoma Invasion
Arpit D. Shah
Adrian C. Shieh, Ph.D.

Over the last two decades with advancements in research, detection, and treatment of all cancer types in the United States, resulting in an overall 23% decrease in cancer related deaths, liver cancer has gone against this trend possessing an increased death rate. Globally, hepatocellular carcinoma (HCC), the most common form of liver cancer, ranks as the second leading cause of cancer related deaths with approximately 788,000 deaths annually. In recent years much emphasis has been placed on understanding the process of HCC cell invasion; however, it has become apparent that the progression of this disease is not solely dependent on just the cancer cells or biological factors, but also their interaction with the tumor microenvironment. A significant number of studies have shown that changes in biomechanical forces within the tumor microenvironment can alter cancer progression. Previous research has demonstrated that interstitial fluid flow (IFF), one of the biomechanical forces that is altered during tumor growth, can promote cancer cell invasion. The findings in this work elucidate the effects of IFF in HCC cell invasion.

Using our 3D *in vitro* flow invasion assay, we demonstrate that IFF increases cellular invasion through autologous gradient formation of chemokines (CXCR4/CXCL12) that promote migration, a mechanism known as autologous chemotaxis. We also demonstrated that MEK/ERK signaling affects IFF-induced invasion; however, this pathway was separate from CXCR4/CXCL12 signaling. Increased matrix metalloproteinase (MMP) expression is a hallmark for cancer progression and poor

prognosis. Biomechanical forces have been observed to increase the secretion of these proteolytic enzymes, which promote extracellular matrix degradation and tumor cell invasion. We observed an increase in MMP-9 and MMP-2 activity in HCC cells exposed to IFF. In total these findings indicate multiple mechanisms are at play in HCC flow-induced invasion, further emphasizing the significance biomechanical forces play in disease progression.

Finally, by modifying our 3D *in vitro* flow invasion assay, we examined IFF in a relevant cell-based disease model where HCC cells are embedded in a stiff matrix. The increase in matrix stiffness is a result of tumor growth, shown to disturb the mechanical forces and biochemical signaling that occurs in the microenvironment, effectively promoting disease progression. HCC also possesses a very unique disease profile and risk factors; nearly 80% of HCCs occur from patients who suffer from chronic fibrosis or cirrhosis, where inflammation and hepatic wound-healing response attributes to the hepatocarcinogenesis. Many studies have observed cellular behavior of hepatocytes and HCC cells in a stiff matrix; however, none have observed the effect of IFF and a stiff microenvironment in HCC cells. The findings in this chapter confirm a synergistic relationship between IFF and matrix stiffness on HCC cell invasion. Ultimately the findings in this study provide a better foundational and mechanistic understanding of IFF and its effects on HCC cell invasion adding to the mounting evidence of how biomechanical forces in the tumor microenvironment influence cancer progression.

# INTRODUCTION

In recent years much emphasis has been placed on understanding the process of hepatocellular carcinoma (HCC) invasion; however, it has become apparent that the progression of this disease is not solely dependent on just the cancer cells or biological factors, but also the tumor microenvironment (TME). A significant number of studies have shown that changes in biomechanical forces within the tumor microenvironment can alter cancer progression. Previous research has demonstrated that interstitial fluid flow (IFF), one of the biomechanical forces that is altered during tumor growth, can promote cancer cell invasion. The findings in this dissertation provide greater insight into understanding the effects of IFF in HCC cell invasion.

This dissertation is organized into five main chapters. The first chapter provides a thorough background and literature review on the etiology and development of HCC, followed by a discussion on the TME, IFF, and finally the mechanisms of IFF mechanosensing. The proceeding three chapters contain findings and observations uncovered in this study highlighting the effects of IFF on HCC invasion. In Chapter 2, the 3D invasion assay was utilized with multiple HCC cell lines, which resulted in a greater invasive response to fluid flow. I also uncovered higher fluid flow velocities correlate with HCC cell invasion, which could serve as a prognostic marker for HCC progression since elevated fluid flow velocity has been correlated with poor prognosis in many other cancers. Furthermore in Chapter 2 I uncovered autologous chemotaxis via the CXCR4/CXCL12 signaling axis as a mechanism for flow-induced HCC invasion. In the process I determined that MEK/ERK signaling is also required in flow-induced HCC cell invasion, but was independent of the autologous chemotaxis mechanism. In Chapter 3, I describe how the

proteolytic activity of MMP-9 and MMP-2 is increased when HCC cells are exposed to IFF, while MMP-2/9 expression does not change. Furthermore we confirmed that this elevated MMP-9 and MMP-2 activity is independent of the autologous chemotaxis mechanism, suggesting multiple mechanisms could be driving IFF-induced invasion of Huh7 cells.

Chapter 4 observed the effects of IFF in a physiological disease relevant HCC cell based model where HCC cells are embedded in a stiff matrix. The increase in matrix stiffness as a result of tumor growth, shown to disturb the mechanical forces and biochemical signaling that occurs in the microenvironment, effectively promoting disease progression. HCC also possesses a very unique disease profile and risk factors; nearly 80% of HCCs occur in patients who suffer from chronic fibrosis or cirrhosis where inflammation and hepatic wound-healing response attributes to the hepatocarcinogenesis. Many studies have observed cellular behavior of hepatocytes and HCC cells in a stiff matrix; however, none have observed the effect of IFF and a stiff microenvironment in HCC cells. The findings in this chapter confirmed a synergistic relationship between IFF and matrix stiffness on HCC cell invasion.

Finally, Chapter 5 discussed the main findings from this work and the significance in uncovering multiple mechanisms and signaling pathways that can regulate flow-induced HCC cell invasion. This work contributes to the mounting evidence of how biomechanical forces in the TME influence cancer progression.

# CHAPTER 1: BACKGROUND

[†]Portions of this chapter were published in the book, 'Cells, Forces, and the Microenvironment': Shah, A., & Shieh, A. (2015). Interstitial Fluid Flow Mechanosensing: Mechanisms and Consequences *Cells, Forces, and the Microenvironment* (pp. 127-154): Pan Stanford

## 1.1 Hepatocellular carcinoma

Cancer is a complex multi-step disease that occurs when abnormal cells divide in a dysregulated fashion. Cancer cells continuously divide and many times begin to show invasive characteristics; these cells are capable of dislodging themselves from a primary tumor site and eventually metastasizing to another tissue site via the lymphatic system or the bloodstream [1]. Consequently, a majority of cancer related deaths are due to the uncontrolled proliferation and invasive nature of these cancer cells. The World Health Organization estimates 1 in 6 deaths are due to cancer, making it the second leading cause of death worldwide. Hepatocellular carcinoma (HCC) is the most common form of liver cancer, which is the second leading cause of cancer-related deaths estimated by the World Health Organization with over 788,000 deaths annually. In the United States, liver cancer has tripled in incidence since 1980, and it is estimated that there will be 40,710 new cases of liver cancer with 28,920 deaths in 2017 [2]. It is important to note that over the last two decades there have been significant advancements in research, detection, and treatment of all cancer types in the United States, resulting in an overall 23% decrease in cancer related deaths, but liver cancer has gone against the trend, with an increased death rate of 3% per year since 2000 [2]. Treatment of HCC remains a challenge, with 5 year survival rates for patients with stages IIC and IVA (regional HCC) of 10% and for patients with stage IVB (distant HCC) as low as 3% [3]. At the present time, the natural history of HCC is not well pronounced until it is diagnosed as it has been observed to be clinically indolent in its

infancy; notably there is a severe dearth of knowledge in the mechanism of hepatocytes transitioning to a neoplastic state, often attributed to its diverse risk profile [4, 5].

The high mortality rate in patients with HCC is attributed to undetected tumor progression and the formation of metastases, which is encouraged by underlying chronic liver disease [4]. Chronic hepatitis B (HBV) and C virus infection account for nearly 85% of HCC cases worldwide, primarily occurring in countries lacking HBV vaccination programs such as sub-Saharan Africa and southeast Asia [6, 7]. Cirrhosis is a major contributor in the progression of HCC; however, it is not only observed in patients who suffer from chronic viral hepatitis, but also from patients who suffer from type 2 diabetes, alcoholism, and non-alcoholic fatty liver disease often observed in developed countries [4, 8, 9]. Chronic hepatitis and metabolic disorders are not the only risk factors associated with the development of HCC; many other unique risk factors have been identified over the years (Figure 1) [4]. Due to the diverse risk profile associated with HCC, there is a lack of screening for the general population, making early detection and diagnosis very difficult.

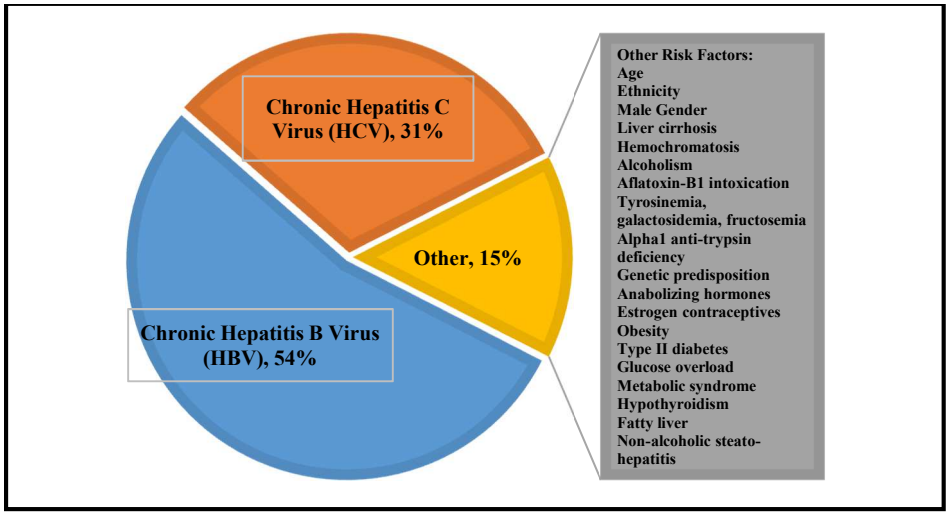


**Figure 1: Distribution of risk factors associated with development of hepatocellular carcinoma.**

**1.2 Normal liver function and hepatocellular carcinoma development**

The liver has two major functions: 1) synthesis, metabolism, and clearance of protein and various chemicals and 2) secretion of bile for waste removal. Liver function is often compromised during the transition to HCC where the dysregulation of hepatocytes to HCC cell proliferation is thrown off balance. To date many risk factors associated with the development of HCC have been identified and studied (Figure 1); however, the exact mechanisms of the transition from normal healthy hepatocytes to malignant neoplasms have not been elucidated. Chronic HBV infection is the most common cause of HCC as the virus genome possesses four overlapping open reading frames where the partially double-stranded DNA encodes the viral envelope, preCore, core, polymerase, and HBx proteins [10, 11]. The most common characteristic observed during chronic liver injury is the continuous cycle of cell death and regeneration that is often a result of inflammation. In the event of HCV which is an RNA virus that replicates in hepatocyte cytoplasm's with a rapid virus turnover and spreading from one cell to the next [12]. Both of these viruses are leading causes for chronic liver disease and the eventual progression to HCC. Additionally, alcohol-induced hepatocarcinogenesis, where the consumption of alcohol in large volumes results in production of proinflammatory cytokines and prolonged circulation of endotoxins. Often the transition of a healthy liver to the development of HCC by either viral or alcohol-induced hepatocarcinogenesis is accompanied by cirrhosis of the liver and ultimate loss of function by this vital organ [13, 14]. The development of HCC is often a slow one over the course of decades for most patients who suffer from any chronic liver injury. Accordingly similarities in signaling pathways involved HCC development have been identified and implicated in underlying liver disease: Ras and

Raf/MEK/ERK, PI3K/AKT/mTOR, and WNT/β-catenin. Additionally with the use of integrative transcriptome analysis, 3 molecular subclasses of HCC have been identified from analysis of 603 patients with HCC. The first subclass, S1, possessed a distinct activation of WNT. The second subclass, S2, upon analysis possessed HCCs with proliferative characteristics via AKT activation, and the S3 subclass was related more towards hepatocyte differentiation [15].

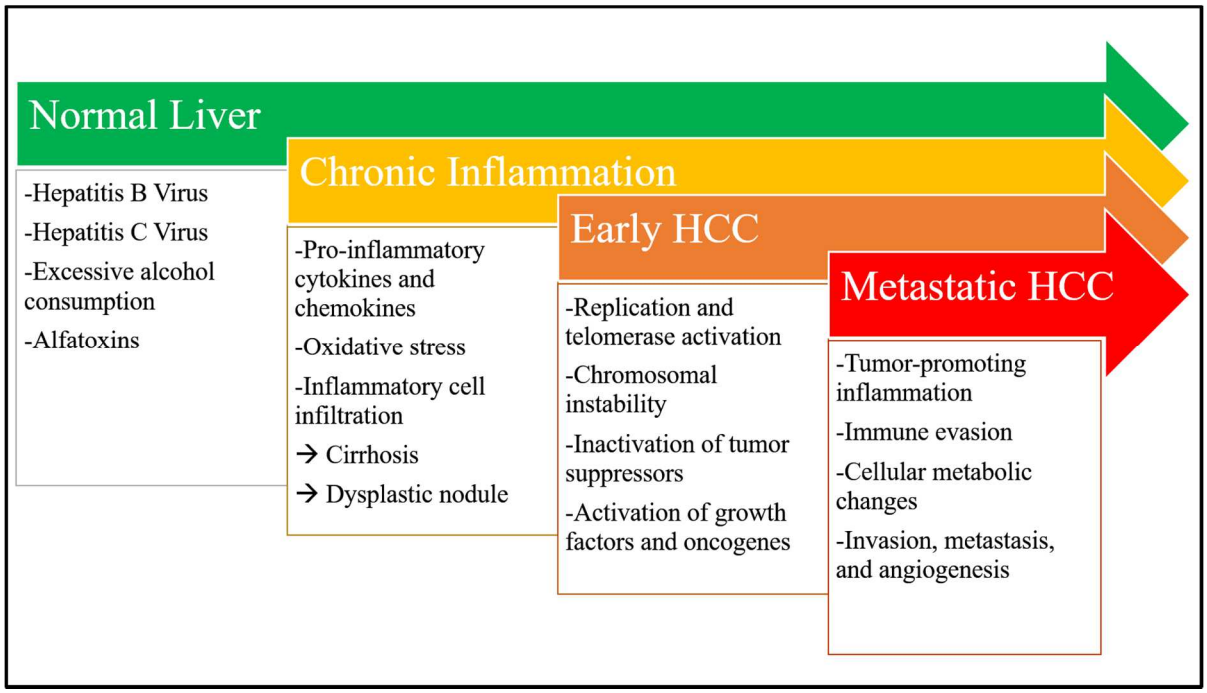


**Figure 2: Biological multi-step process of hepatocellular carcinoma development. (Adaptation of Figure 2 from Cetin-Atalay et al 2015 [16])**

The Ras/Raf/MEK/ERK signaling cascade is a popular therapeutic target for treating HCC as it has been shown to be constitutively activated; in other solid tumors components from this pathway have been shown to be overexpressed or activated resulting in tumorigenesis, disease progression, and metastasis of the cancer [17, 18]. In primary

liver cancer HBV X protein (HBx) integration is involved in the transformation process of malignant HCC [19]. This viral protein is also shown to activate the Ras/Raf/MEK/ERK signaling pathway where they cohesively alter regulation of cell cycle check points as well as activate of several oncogenes in the cytoplasm [20-22]. The Ras/Raf/MEK/ERK pathway has been shown to be activated by a multitude of upstream receptor tyrosine kinases (RTKs) such as epidermal growth factor receptor (EGFR), platelet-derived growth factor receptor (PDGFR), and vascular endothelial growth factor receptors (VEGFR) [23]. Nearly 30% of HCCs possess a Ras mutation resulting in downstream activation of the critical molecular signaling regulator Raf; more specifically one of its three isoforms: ARAF, BRAF, or CRAF [24]. Ras/Raf signaling has been shown to be a critical pathway in sustaining proliferation aiding in the development of HCC [25]. Constitutively elevated MEK/ERK activity has been observed in HCC cells, HCC tissue, as well as other carcinomas resulting in altered cell proliferation, differentiation, and apoptosis [26, 27].

Similar to Ras/Raf/MEK/ERK signaling cascade, the PI3K/AKT/mTOR pathway has been observed to be constitutively activated in many solid tumors often playing a critical role in tumor cell growth, proliferation, and survival [28]. In HCC, 30-50% of all HCCs possess activated PI3K signaling, and this signaling cascade is often over activated by receptor tyrosine kinases such as insulin growth factor (IGF) receptors often observed in cirrhotic livers [29, 30]. In turn this activated PI3K signaling cascade can simultaneously activate Raf/MEK/ERK and the WNT/β-catenin signaling cascades [30, 31]. The PI3K signaling cascade in HCC has been observed to be activated due to abnormal phosphatase and tensin homolog (PTEN) function while during normal liver function, PTEN has been often observed to be negatively regulated [32]. The loss of PTEN

regulation with overexpression of pAKT and p-mTOR in some cases has been shown to result in HCC tumor differentiation, intrahepatic metastasis, and MMP-2/9 upregulation [32-34]. Notably, mTOR signaling is disrupted by the over activation of PI3K/AKT in HCC resulting in increased cell proliferation [35].

Activation of the WNT/β-catenin signaling pathway has been observed to play an important role in some early carcinogenic events in HCC development via abnormal regulation of the transcription factor β-catenin [36]. In normal physiology, the WNT signaling cascade is responsible for various cellular process such as homeostasis, cell proliferation, differentiation, motility, and even cell apoptosis [37]. Early HCC due to HBV, HCV, and alcoholic liver cirrhosis in some cases has been observed to possess WNT activation due to a β-catenin mutation [38]. In cases of HCCs directly caused by chronic HCV infection approximately, 50-70% of tumors possessed greater β-catenin levels in the cytoplasm [39, 40]. This increased WNT activity and increased activated β-catenin in the cells has been correlated to increased invasion and metastatic potential [41].

### 1.3 Tumor microenvironment in hepatocellular carcinoma progression

A significant body of literature has demonstrated the importance of investigating the liver tumor microenvironment (TME). These studies have highlighted that the cross-talk between tumor cells and the surrounding stroma plays a key role in HCC progression, EMT, tumor growth, invasion, and metastatic spread [42, 43]. Investigating the cellular and non-cellular components within the TME of the liver has resulted in a better understanding of HCC progression and the mechanisms involved, and has also provided physicians with a better understanding of HCC tumor progression, staging, and therapeutic

strategies [42, 44, 45]. Notably investigating the TME of HCC is often a difficult one as most HCCs develop in the presence of chronic liver injury adding to the complexity of studying the ever-changing TME and malignancy.

Many studies have shown that chronic liver injury promotes the development of fibrosis and cirrhosis and this eventually progresses to HCC [46-48]. The mechanical and molecular events that occur during fibrosis, scarring of the liver, essentially provide a pro-carcinogenic effect in the liver microenvironment. There have been a variety of risk factors identified for liver fibrosis such as metabolic syndrome/fatty liver disease and even heavy alcohol consumption. However to date, untreated chronic viral infections such as hepatitis B and C are the two greatest risk factors for development of liver fibrosis [48].

The ECM of the liver plays a significantly dynamic role in liver function. The ECM proteins mechanically play an important role in the liver by providing tensile strength and resilience. From an architectural standpoint these ECM proteins can alter diffusive properties and regulate cellular movement [49]. In liver fibrosis, the increased production and accumulation of ECM proteins is the hallmark response to this acute injury in order to protect the parenchymal cells. Dysregulation of this balanced response within the liver disrupts normal healthy function and this excessive accumulation of ECM proteins is often regarded as an indicator of a pathological state [49-51]. A complex set of mechanical and molecular events occur during hepatic fibrosis; initially a wound-healing response occurs in the presence of an acute liver injury. On a cellular level this wound-healing response results in an initial response from inflammatory lymphocytes which infiltrate the parenchyma of the liver [52, 53]. Simultaneously regeneration of parenchymal cells occurs in order to replace any apoptotic hepatocytes and activation of Kupffer cells which

modulate proinflammatory and fibrogenic mediators like TNF-α and IL-6 shown to regulated hepatocyte survival [13, 54-57]. HSCs found in the perisinusoidal space of Disse make up nearly 10% of all cells in the liver and serve as the primary source of ECM proteins, where once they are activated, these cells help coordinate the repair efforts of the injury site [51, 58-60]. In a persistent chronic injury state from viral infections like HBV or HCV, the activated HSCs transdifferentiate into myofibroblast-like cells and continue to deposit fibrillar and non-fibrillar collagens along with other ECM proteins by migrating to the injured sites [61]. These cells acquire proinflammatory and fibrogenic properties, ultimately resulting in dysregulated ECM degradation and continuous fibrillar collagen deposition over hepatocytes, thus distorting liver function and architecture [56, 59, 60]. Soluble factors such as inflammatory cytokines and growth factors like, TNF-α and TGF-β, contribute and help maintain the activated fibrogenic state and perpetuate a reciprocating relationship between inflammatory and fibrogenic cells [62].

The accumulation of these ECM proteins has been shown to alter the availability of soluble factors which in turn affects cellular functions such as cell growth, survival, adhesion, migration, and even differentiation [63-65]. As discussed previously, fibrosis in the liver results in changes to the physical architecture of the tissue, notably the increased accumulation of ECM proteins (eight-fold higher than healthy livers) has been shown to alter the hepatocyte microenvironment and cell behavior [66]. The increased accumulation of ECM proteins results in a remodeled matrix that is much stiffer. A variety of normal cell types are capable of observing and responding to changes in stiffness within their microenvironment; the mechanosensing of this specific environmental change occurs through many different mechanisms often altering the balance of mechanical forces and

molecular signaling in turn effecting cell behavior [67]. Furthermore, the transformed ECM functions as a reservoir for various growth factors and proteolytic enzymes like MMPs, which have been shown to aid differentiation of hepatocytes to HCCs [68, 69]

The cross-talk between the cellular and the non-cellular components such as cytokines, growth factors, ECM proteins, and proteolytic enzymes play a substantial role in HCC progression. Understanding the interplay between these components and the altered biomechanical forces in the TME could lead to the identification of new and effective treatment options.

### *1.3.1 Cellular components*

#### *Cancer-associated fibroblasts*

Cancer-associated fibroblasts (CAFs), activated by TGF-β, are located in the tumor stroma and play a critical role in ECM protein deposition and remodeling which attribute to metastatic spread [70]. Tumor-stromal interactions often involve CAFs and HCC cells which have been shown to possess a reciprocating relationship where the presence of CAFs, promotes HCC cell growth and in turn these malignant cells aid in proliferation of CAFs [71]. Additionally CAFs promote tumor progression with the production of growth factors like EGF, HGF, FGF; chemokines such as stromal-derived factor-1α (SDF-1α); and cytokines such as interleukin-6 (IL-6), and interleukin-8 (IL-8) [35, 72-74].

#### *Hepatic stellate cells*

As previously discussed, the development of HCC is often in the presence of underlying chronic liver injury such as fibrosis, and quiescent hepatic stellate cells (HSCs)

are activated by this repeated liver injury [75]. Located in the Space of Disse of the liver, HSCs, also known as peri-sinusoidal or Ito cells, are activated in the presence of repeated liver injury, hepatic toxins, or viral infections, and play a vital role in fibrosis development where they are responsible for collagen synthesis and trans-differentiate into myofibroblast-like cells [51, 76]. Upon activation, HSCs experience a phenotypic transformation where they increase proliferation, secretion of ECM proteins, production various cytokines, chemokines, and growth factors [46, 51, 52, 77, 78]. Dormant HSCs protect the liver when it is damaged by hepatic toxins or a viral infection in their activated state by secreting cytokines, growth factors, and ECM proteins [77]. It is important to note that this response form HSCs is due to chronic liver injury; the activated HSCs possess the ability to penetrate the stroma and settle around the liver sinusoids, fibrous septa, and capsules of the tumor [79, 80]. Furthermore, these activated HSCs play a prominent role in hepatic immune responses as they are capable of suppressing the immune response of monocytes during inflammation and promoting HCC cell growth [81-83]. Activated HSCs in the tumor microenvironment induce HCC cell proliferation and migration (via NF-κB and ERK), and ultimately tumor growth, enhancing HCC progression and poor clinical outcomes [82].

*Tumor-associated endothelial cells*

The vascular endothelium is comprised of blood vessels that aid in the transport of nutrients found in blood to the tissues in the body. These blood vessels are comprised of tightly formed continuous monolayers of endothelial cells, which in normal healthy tissues can express angiogenic receptors and C-X-C chemokine receptors [84-88]. Binding of

these ligands to their respective angiogenic and chemokine receptors affects the signaling cascade that regulates cellular functions such as survival, proliferation, and migration [88-90]. Additionally, it is important to note that the liver is one of the most vascular organs in the body and HCC is one of the most vascular solid tumors. Furthermore, these endothelial cells behave much differently in HCC tissues compared to normal tissue, and as a result endothelial cells found in the TME are referred to as tumor-associated endothelial cells [91]. Tumor-associated endothelial cells behave and function much differently than normal endothelial cells as they are observed to possess rapid cell turn over, increased TGF-β1expression, and dysregulation of cellular functions like survival, proliferation, and invasion [92-94]. These tumor-associated endothelial cells are observed to possess irregular morphology and variation in size which results in the formation of leaky blood vessels within the tumor [95]. Many human HCC cases have been observed to possess increased upregulation of VEGF expression which promotes tumor progression by increasing angiogenesis via tumor endothelial cells [89, 96, 97].

*1.3.2 Non-cellular components*

The TME is a complex environment in which the tumor and surrounding cellular components interact in a reciprocating manner activating various signaling pathways resulting in dysregulated cellular processes. However, this is a very complex process where the non-cellular components in the tumor microenvironment assist in the growth and sustainability of the tumor and the eventual loosening and degradation of the tumor cell from the ECM. Chemoattractants provide chemical signaling cues to the cell, where these tumor cells' invasive nature result in their eventual spread to another organ [90]. This

spreading or progression of the tumor cells to a secondary site is not possible without the non-cellular components such as cytokines and growth factors, which serve to help tumor cells evade immune cells, but also allow for sustained growth [98-100]. ECM proteins and MMPs serve as non-cellular components which play a significant role in the migration and invasion of the tumor cells [101, 102].

*Cytokines*

Researchers over the years have identified cytokines to be vital contributors HCC in the liver tumor microenvironment. Most HCC cases in the liver arise from underlying chronic liver injury often in the presence of inflammation and scarring of the liver, and inflammatory cytokines are produced in response to this injury. These cytokines have been observed to induce proliferation in various cell types and also contribute to the migration of tumor cells [103, 104]. Kupffer cells are liver macrophages that are capable of producing a variety of cytokines which regulate regenerative and proliferative processes in the liver by activating receptors found on hepatocytes. In a malignant state, these receptors are often activated by a variety of cells altering, immune cell response to viruses and inhibiting apoptosis in cancer cells. IL-6 is an inflammatory cytokine that is observed to be in the presence of hepatocyte death and also contributes to hepatocyte proliferation by Kupffer cells [105]. The increase in IL-6 in patients with cirrhosis is correlated with increased HCC and poor prognosis of individuals suffering from HCC [98, 105]. Tumor necrosis factor-alpha (TNF-α) is a prominent cytokine that is expressed in the presence of liver injury activating downstream NF-κB and Akt [106, 107]. Similar to IL-6, TNF-α is activated during inflammation, and studies show high expression levels are correlated to

HCC recurrence in patients [108, 109]. Various pro-inflammatory cytokines have been investigated and shown to play a role in HCC progression and can be produced by both cancerous and non-cancerous cells. A robust review by Wang and colleagues has outlined in detail the role of cytokines in HCC progression or HBV/HCV associated HCC [110].

*Growth factors*

The interactions between the components of the microenvironment have been shown to often result in a pro-metastatic state; however, the molecular mechanisms involved are not fully elucidated. Growth factors such as TGF-β, VEGF, HGF, FGF, and PDGF play an indispensable role in regulating cell processes and tumor progression [46, 92, 111-115]. Before the development of HCC, TGF-β plays the role of a tumor suppressor by regulating apoptotic signals to modulate proliferation through TGF-β1 [116, 117]. TGF-β plays a vital role in liver fibrogenesis and hepatocarcinogenesis as it has been shown to be up-regulated in liver tissue with HCC and peri-neoplastic stroma [117, 118]. The presence of the HBx protein and even HCV have been shown to shift TGF-β signaling from its tumor-suppressive state to an activated state via c-Jun N-terminal kinase (JNK) [112, 119]. Due to the vascular nature of HCC, VEGF has been observed to be a critical growth factor stimulating angiogenesis by promoting proliferation of endothelial cells to drive HCC progression [114]. Tumor-stromal interactions are mediated by HGF expressed by HSCs and have been shown to increase HCC cell proliferation and invasion [114].

*Extracellular matrix proteins*

The ECM is analogous to a structural scaffold as it provides physical support and anchorage sites for parenchymal and non-parenchymal cells. The ECM and the proteins that comprise it are no longer recognized as passive components in cancer progression. Collagen is the most abundant ECM protein in the liver; activated HSCs have been identified to be the main cellular source for collagen [120]. This fibrillar protein provides structural support for cells, but in the presence of chronic liver injury, collagen is overexpressed resulting in a stiff matrix. In HCC, collagen can promote cell migration and proliferation [121]. Laminins are ECM proteins that form web-like structures to mediate tensile forces that occur in the basal lamina via basement membrane assembly. Laminin is also involved in cellular processes like cell migration, growth, and differentiation [122]. In HCC, lamin-5 is found in HCC nodules and expressed in HCCs associated with a metastatic phenotype [123]. Integrins are found on cell surfaces serving as heterodimeric transmembrane receptor proteins mediating cell adhesion. To date, there are more than 20 different integrin heterodimers, but specific integrin subunits have been identified to mediate cellular processes in HCC cells [124]. The β3 subunit has been found to play a role in cell growth and apoptosis while the overexpression of integrins with the β1 subunit inhibit HCC cell proliferation, migration, and invasion [125-127]. Proteoglycans are found in the ECM and play a vital role in intracellular communication, maintain the ECM framework, and serve as a reservoir for growth factor storage. Heparan sulfate proteoglycans are involved in the pathogenesis of HCC by storing growth factors (FGF, HGF, PDGF, and VEGF) which have been shown to contribute to HCC progression [46,

113, 114, 128]. The ECM proteins described here play a critical role in regulating various cellular process and ultimately promoting HCC progression.

*Matrix metalloproteinases*

MMPs play a central role in mediating changes to the tumor microenvironment through various physiological processes and signaling events. Since their discovery in 1962, a total of 23 different MMPs have been identified in humans and have been investigated as therapeutic targets for treating cancer and inflammatory diseases [129, 130]. Various tumor and stromal cells are capable of producing these MMPs, which have been categorized into the following subtypes based on their domain structure and function: collagenases (MMP-1/8/13), gelatinases (MMP-9/2), matrylisins (MMP-7/26), membrane type MMPs (MMP-14/15/16/17/24/25), and stromelysins (MMP-3/10/11) [131]. These proteolytic enzymes function as integral communicators between the tumor and stroma to drive tumor progression. MMPs degrade the structural frame work of the ECM creating an escape route for tumor cells to migrate, thus their elevated expression is often correlated with poor prognosis in cancer [132]. MMPs are expressed in an enzymatically inactive state due to the presence of an unpaired cysteine residue at the C-terminal end of the pro-domain and a zinc ion found in the catalytic or active-site. These zinc-dependent endopeptidases become proteolytically activate by a mechanism known as the cysteine switch, where the pro-domain is removed or the cysteine residue chemically modified, allowing the active-site to cleave substrates [133]. Proteolytic activity of MMPs can be regulated at various levels from gene expression, zymogen conversion, extracellular

activation by activated MMPs, presences of serine proteinases, localization on cell surfaces, or even by endogenous inhibitors like TIMP [134].

In the TME, MMPs not only aid in the remodeling of the hepatic architecture, but play key roles in pro- and anti-inflammation, tumor cell growth, invasion, and metastasis [90]. The expression of the gelatinases (MMP-9 and MMP-2) have been correlated to increased HCC invasion and pathological parameters like tumor size, stage, and probability of HCC recurrence [135-137]. In HCC, MMP-9 and MMP-2 have been observed to regulate chemokine and cytokine recruitment in response to inflammation, bioavailability of VEGF for angiogenesis, and modulate EMT by activating TGF-β1, resulting in HCC tumorigenesis [99, 138, 139]. Inhibition of these active MMPs is regulated by TIMPs which prevent excessive degradation of the ECM, but also regulate cell proliferation, apoptosis, and the activation of MMPs. The balance between TIMPs and the gelatinases is tightly regulated and any dysregulation of this relationship has been observed to result in detrimental outcomes in HCC [32, 140].

### 1.4 Basics of interstitial fluid flow†

Interstitial fluid flows through intercellular spaces of the extracellular matrix between blood and lymphatic capillaries, where it is eventually collected and drained by the lymphatic system as lymph [141, 142]. Convective forces facilitate transport of molecules while simultaneously maintaining tissue fluid balance [142]. This fluid flow through the interstitium also generates biophysical forces that may directly affect cells [143]. Theoretical or computational models of interstitial flow are complicated by the nature of interstitial flow; at each location in the interstitium where fluid flow occurs, the

structure and properties of the matrix can vary considerably, along with the shape and orientation of affected cells. However, despite these complexities, several governing principles can be considered to better understand IFF in a quantitative fashion.

*1.4.1 Interstitial flow velocity*

One of the fundamental ways to characterize fluid flow is by the velocity. In the case of interstitial flow, there have been a number of experimental measurements and computational models to estimate flow velocity *in vivo*. Utilizing the technique, fluorescence recovery after photobleaching (FRAP), resulted in a IFF velocity range of 0.1 - 2 μm/s in a rabbit ear chamber with bovine serum albumin conjugated with fluorescein isothiocyanate tracer [144]. An *in vivo* study examined the effect of overexpression of $VEGF_{165}$ and its role on peritumoral fluid convection and lymphatic drainage. Magnetic resonance imaging (MRI) of the $VEGF_{165}$-overexpressing tumors revealed IFF velocities of approximately 0.2 - 0.3 μm/s. Overall there was increased interstitial convection, vascular permeability, and lymphatic drainage in tumors [145]. Dynamic contrast-enhanced MRI (DCE-MRI) has also been used to measure fluid-flow velocity at the edge of cervical carcinoma xenografts in mice and cervical tumors in humans by wash out of gadolinium-based contrast agents. Flow at the tumor edge is of particular interest, since there is dramatic gradient in fluid pressure between the high pressure tumor and the lower pressure surrounding tissue. This pressure gradient resulted in an approximated flow velocity of 5 μm/s at an interstitial fluid pressure of 20 mmHg in mouse xenografts, while human cervical cancer patients with pelvic lymph node metastases showed flow velocities

as high as 50 μm/s [146]. Other models have shown that the periphery of a tumor can have interstitial-fluid velocities as high as 10 μm/s as well [147].

To date there is much uncertainty in regards to determining quantitatively the flow velocity, many of these studies correlate it to various parameters such as convective transport of macromolecules or shear stress that is generated on the cell surface. Overall there are many challenges for current computational models and *in vivo* measurements of interstitial-flow velocities. The internal forces and interstitial spaces of various tissues are highly heterogeneous, thus making it very difficult to determine the characteristics of interstitial flow without identifying and understanding all local parameters. Nevertheless, quantitatively determining flow velocity (and other flow characteristics) would provide a greater understanding of the effects interstitial flow may exert on cells and tissues.

### *1.4.2 Starling's Equation*

To characterize IFF, we need to first understand the phenomenon of capillary filtration. It is widely known that oncotic (colloid osmotic) and hydrostatic pressure gradients play a major role in the movement of fluid. In 1846, Ernest Henry Starling determined that forces such as tissue fluid pressure ($P_t$), capillary fluid pressure ($P_c$), tissue colloid osmotic pressure ($\pi_t$), and plasma colloid osmotic pressure($\pi_p$), known as Starling forces, were responsible for driving capillary filtration [148, 149]. In humans, typical colloid osmotic pressure is 28 mmHg for the capillaries and 8 mmHg for the interstitium, while hydrostatic pressure is 20 mmHg for the capillaries and -1 to -3 mmHg for the interstitium [150]. Oncotic pressure is an important indicator for identifying potential diseases; elevated oncotic pressure is associated with pulmonary edema [151].

Additionally in cancer, studies in rats have shown that both oncotic and interstitial-fluid pressure are elevated in solid tumors [152].

Using these hydrostatic and oncotic pressures, Starling's equation predicts fluid filtration across capillary membranes:

$$J_v = K_{f,c}[(P_c - P_t) - \sigma(\Pi_c - \Pi_t)]$$

$J_v$ is the transcapillary fluid flow, $K_{f,c}$ is the capillary filtration coefficient, and σ is the capillary protein reflection coefficient. The reflection coefficient represents the degree to which the capillary is impermeable to the proteins generating the oncotic pressure gradient [153]. If the capillary was permeable to all plasma proteins, then the reflection coefficient would be 0, whereas a completely impermeable capillary would have a reflection coefficient of 1. A majority of the fluid filtered through the capillary wall is reabsorbed by downstream post-capillary venules; however a small fraction of this fluid remains within the tissue interstitium [154, 155]. This fluid is ultimately converted into lymph once it is drained from the interstitium by the initial lymphatic capillaries. However, while Starling's equation describes capillary fluid filtration, it does not model interstitial flow within the tissue. For this, we turn to civil engineering and models of flow through porous media.

### *1.4.3 Darcy's law and Brinkman's equation*

IFF depends on many factors, such as pressure gradients within the interstitium and the structure and properties of the tissue. Darcy's Law was developed to characterize fluid flowing through a porous medium. In 1856 Henry Darcy examined the flow of groundwater through sand-beds that assisted in filtration [155]:

$$\bar{v} = -\frac{k}{\mu}\nabla P$$

The equation is comprised of $\bar{v}$ , the bulk-averaged velocity; $k$, the permeability (measured in $m^2$); $\mu$, the fluid viscosity; and $P$, the fluid pressure [156]. Collagen gels have been shown to have permeability values ranging from $10^{-7}$ to $10^{-8}$ $cm^2$, with gel permeability increasing with increasing culture time [157]. The permeability of gels made from Matrigel was found to be approximately $10^{-8}$ $cm^2$ [158]. Tissue permeability ranges between $10^{-8}$ and $10^{-12}$ $cm^2$ [141].

The equation that Darcy developed for one-dimensional flow is helpful in determining average flow velocity; however, it is not sufficient in understanding complex permeability and flow in tissues. Brinkman's equation was developed by Henry Brinkman in 1949, when he modified Darcy's equation to take into consideration changes in viscosity, viscous shear effects, and the presence of a boundary layer [143]:

$$\nabla P = -\frac{\mu}{k}\bar{v} + \mu\nabla^2\bar{v}$$

The Darcy-Brinkman equation helps characterize flow of fluid through porous media where fluid viscosity is factored in with boundary layer effects. These fundamental equations allow for analysis of fluid flow through the interstitium due to pressure gradients that are developed. However, these equations normally assume constant matrix permeabilities, and do not consider the heterogeneity in tissue structure and properties [159]. This can result in large local variations in interstitial flow. Regardless of these limitations these two equations have helped create a fundamental understanding of how interstitial fluid flows through tissues.

*1.4.4 Shear stress*

IFF generates direct stress on cells within a microenvironment along with indirect forces transmitted via the matrix [143]. These direct and indirect forces result in biochemical and biophysical cues that can lead to profound changes to the cell and its normal function [144, 154, 160-169]. Forces such as fluid shear stress are exerted on surfaces due to a tangential stress caused by fluid viscosity and flow [170]. However, the intensity of the shear stress is dramatically less on the cell due to extracellular matrix fibers that shield the cell from direct fluid shear [154]. Fluid shear stress that occurs on cells may be transmitted through structures such as the glycocalyx – an extracellular coat of glycoproteins, glycolipids, and proteoglycans that has been shown to transduce fluid flow-induced shear stress in endothelial cells [171]. Given estimated interstitial flow velocities, it is generally assumed that the resulting shear stresses are comparatively low. It has been hypothesized that interstitial flow can result in shear stresses of 0.1 dyne $cm^{-2}$ or even lower; however this does not mean that they can be neglected [172]. Computational fluid dynamic simulations of flow through *in vitro* collagen gels have shown that maximum shear stresses are three times higher and average shear stress two times higher than values predicted by Brinkman's equation [154]. Average shear stress can be calculated with consideration of high porosity matrices, cell profile, and fibers on the cell membrane [154]:

$$\tau_{avg} = \frac{3\pi}{8} \cdot \frac{(U_0 \mu)}{a} \cdot \left(1 + \frac{1}{\sigma}\right)$$

The average shear stress is denoted by $\tau_{avg}$, free stream velocity is noted as $U_0$, viscosity is $\mu$, the cell radius is represented by $a$, and $\sigma$ is the dimensionless

permeability[154]. Shear stress plays a major role in triggering various biochemical signals [166, 173-178].

*1.4.5 Convective mass transport*

Convection has been examined in many models, from transport of fluid through sediment to convective transport in tumors [179, 180]. As noted earlier gradients created by interstitial pressure play a role in transcapillary exchange of fluid and macromolecules. The dimensionless Peclet number can be used to determine if convection can be neglected for mass transport in a particular setting or system. The Peclet number is a dimensionless ratio that determines the relative importance of convective versus diffusive mass transport of a species, and is defined as the following:

$$P_e = \frac{Lu_i}{D_t}$$

L is the characteristic length, $u_i$ is the bulk convective velocity of the solute, and $D_t$is the diffusion coefficient [156]. When $P_e$<<1 diffusion is the dominant form of transport, while for $P_e$>>1 convection is the driving force for transport. The utilization of the Peclet number in the study showed that when there was a high Peclet ratio with increased velocities or decreased diffusion coefficients of secreted proteins, a biased transcellular gradient formed [181]. However, even at low Peclet numbers (less than 1), interstitial flow may still generate biologically relevant, asymmetric pericellular morphogen gradients [181].

## 1.5 Effects of interstitial flow in biological systems †

Interstitial fluid flow plays a significant role in various physiological and disease systems. This section highlights examples of the effects of IFF in three systems: blood vessels, lymphatic vessels, and cancer. Blood and lymphatic vessels are constantly exposed to mechanical forces and IFF plays an important role in cellular behavior, signaling, lymphangiogenesis, and angiogenesis [170, 172, 182-185]. In cancer, IFF may cause reorganization of extracellular matrices and promote tumor cell invasion mediated by autologous chemotaxis [186, 187].

We would like to note that one system where IFF mechanotransduction has been extensively studied is in bone. Unlike many other tissues described here, where interstitial flow is driven primarily by the pressure differences between blood capillaries, the interstitium, and lymphatic vessels, interstitial flow in bone occurs in response to external mechanical loading. These external loads result in transient pressure gradients that drive dynamic and often oscillatory interstitial flow through the extensive lacunae-canaliculi network, simulating osteocyte and osteoblast cell processes. There are many nuances to interstitial flow mechanosensing that are qualitatively and quantitatively different from those in other tissues, and extensive research has been conducted in this area. We point the reader to specific treatments of this topic [164, 188-196].

### *1.5.1 Blood vessels*

Pressure differences across the vascular wall can result in transmural interstitial flow, potentially affecting the behavior of vascular smooth muscle cells and adventitial fibroblasts. Interstitial flow has been shown to play an intimate yet indirect role on smooth

muscle cell biochemical signaling and responsiveness [184, 185]. Transmural pressure differentials drive interstitial flow velocities of nearly 0.1 – 1.0μm/s [197]. The fluid shear stress generated by IFF can be 100 times greater near fenestral pores in the vicinity of smooth muscle cells. This increased shear stress can trigger changes such as increased production of prostaglandin $I_2/E_2$ by smooth muscle cells in collagen gels [185]. Physiologically IFF was also shown to initiate signaling crosstalk between the blood vessel lumen and smooth muscle cells. These results demonstrated that IFF and shear stress may affect smooth muscle cell proliferation and local vascular tone [185]. Further work suggested that interstitial flow can directly govern contraction and relaxation of smooth muscle. It was determined that smooth muscle cells which were exposed to 11 dyn/cm$^2$ shear stress for 15 minutes exhibited increased contractility via a $Ca^{2+}$-independent, Rho/Rho-kinase-dependent mechanism. This study was one of the first of its kind to reveal that interstitial flow shear stresses could affect myogenic responses in smooth muscle cells [197].

In addition to effects on smooth muscle cell function, interstitial flow may also affect the motility of vascular cells via the upregulation of MMP-1 [172]. Exposure to an approximate interstitial flow velocity of 0.5 μm/s (under a pressure of 1 cm $H_2O$) increased migration of myofibroblasts, fibroblasts, and smooth muscle cells [172]. In this experiment, cells were initially stimulated by interstitial flow, and then exposed to a chemotactic gradient (without flow) to quantify changes in cell motility. Flow-induced increases in cell migration were related to increased MMP-1 production and activity in response to interstitial flow in smooth muscle cells and fibroblasts [172, 198]. Furthermore, it was concluded that upregulation of MMPs was dependent on downstream

activity of ERK1/2 and transcription factor c-Jun activation [198]. Heparan sulfate proteoglycans are components of the glycocalyx that may serve as shear stress sensors [199-201]. These glycocalyx heparan sulfate proteoglycans have been shown to mediate the mechanotransduction of interstitial flow-induced forces through the FAK-ERK pathway in smooth muscle cells [202]. Modulation of smooth muscle cell marker genes under interstitial (1 $cmH_20$, 0.05 $dyn/cm^2$) was similarly dependent on ERK1/2 activity and heparan sulfate proteoglycans, as demonstrated by enzymatic treatment with heparinase [203]. These results, in total, shed light on a possible mechanism of interstitial flow mechanotransduction mediated by the heparan sulfate proteoglycans in the glycocalyx, integrin and FAK activation, and downstream ERK 1/2 signaling. These findings shed light on the role of interstitial flow-induced fluid shear stress in regulating vascular wall cell phenotypes [198, 202, 203].

*1.5.2 Lymphatic vessels*

Given the function of lymphatic vessels in interstitial fluid drainage, it should come as no surprise that interstitial flow can modulate the behavior of lymphatic endothelial cells. Lymphatic drainage and transport of interstitial fluid is important for maintaining tissue fluid balance and may also aid in innate and adaptive immunity [156, 204]. Important physiological events such as inflammation or tissue injury generate rapid responsive measures that include increased vascular permeability, leading to elevated interstitial flow and downstream lymphatic drainage. Increased interstitial flow has been shown to upregulate intercellular adhesion molecule-1 (ICAM-1) and E-selectin on lymphatic endothelial cells, which in turn promoted dendritic cell migration in the presence of flow.

There were also associated increases in secretion of the chemokine CCL21 and alterations in lymphatic endothelial cell junction proteins such as VE-cadherin. During tissue injury or inflammation, the hyperpermeability of blood vessels and concomitant increases in IFF can affect lymphatic endothelial cells by increasing chemokine secretion, up-regulating of adhesion molecules, and facilitating dendritic cell transmigration [205].

IFF also appears to have a significant role in the process of lymphangiogenesis. Lymphatic endothelial cells are capable of systematically organizing into working lymphatic capillaries, which is crucial for lymphangiogenesis. This study was conducted *in vivo* in mice; a small 2-mm-wide band of skin was removed from the tail and replaced with a collagen dermal equivalent and sealed with surgical glue. Fluorescently labeled macromolecules were used to trace fluid flow channels and lymphatic capillaries via fluorescence microlymphangiography. Using these approaches, it was observed that fluid channeling occurred prior to formation a new lymphatic capillary network [182]. In addition, cell migration, vascular endothelial growth factor C (VEGF-C) expression, and ultimately lymphatic capillary formation appeared driven by primarily in the direction of interstitial flow, suggesting that flow was required to dictate the organization of new lymphatic vessels. These findings were corroborated by *in vitro* results that showed that IFF had morphological consequences on blood and lymphatic endothelial cells [183]. Interstitial flow (10 μm/s flow velocity) stimulated formation of vacuoles associated with geodesic actin networks and dendritic extensions in lymphatic endothelial cells, while in blood endothelial cells interstitial flow caused enhanced multicellular tubule formation and cell alignment. Endothelial cell organization and structure formation was further enhanced by interstitial flow when cells were seeded in fibrin gels with fibrin-bound vascular

endothelial growth factor (VEGF), suggesting an interstitial flow-induced gradient formation mechanism [206]. In addition to understanding how interstitial flow might affect lymphangiogenesis and angiogenesis, these findings are important in the broader sense that IFF could be utilized to organize endothelial cells into a functional network as part of *in vitro* and *in vivo* regenerative medicine strategies [183, 206].

### *1.5.3 Cancer*

The tumor microenvironment is very different from normal healthy tissue structures. Tumor growth causes physical changes to the structure of the microenvironment, resulting in matrix stresses, increased matrix stiffness, elevated fluid pressure, and alterations to fluid flow [186]. When tumors reach a critical size, they promote new blood vessel formation via secretion of VEGF [207]. The permeability of the new blood vessels and lymphatic capillaries, along with structural changes to the extracellular matrix, generate an increase in interstitial fluid pressure in tumor [208]. Tumors can possess an interstitial fluid pressure anywhere between 10 mmHg to 20 mmHg higher than normal tissue [170]. At the center of a tumor, the interstitial fluid pressure is at its highest, creating at large pressure differential across the tumor edge and driving IFF into the surrounding tumor stroma [145, 174, 179]. Thus, interstitial flow may have effects not only on the cancer cells themselves, but the various cell types (fibroblasts, endothelial cells, immune cells) in the tumor microenvironment.

Interstitial flow can potentially alter the behavior of tumor cells directly, and a seminal study demonstrated that flow and autocrine signaling worked synergistically to promote melanoma and breast cancer cell invasion to lymphatics via autologous

chemotaxis [209]. The more invasive cell lines expressed high levels of the chemokine receptor CCR7, which has been implicated in lymph node metastasis [187], and secreted elevated levels of its ligand CCL21. Under IFF (0.2μm/s), this resulted in increased invasion and cell polarization in the direction of flow, which could be neutralized by function-blocking antibodies for CCR7 and CCL21. This response was further enhanced by the presence of downstream lymphatic endothelial cells, which also secrete CCL21, suggesting combined effects of autologous and paracrine gradients. Invasive glioma cells showed similar increases in invasion due to an interstitial flow and CXCR4-dependent mechanism. Invasive glioma cells under fluid flow were much more invasive due to the expression of CXCR4 and autocrine secretion of CXCL12. These *in vitro* findings were linked to interstitial flow patterns in the brain, which themselves have been correlated with glioma invasion *in vivo* [210]. A recent study has further concluded that different mechanisms govern fluid flow responsiveness in glioblastoma stem cells in a single patient where a subpopulation of these cells respond via CD44-dependent invasion or CXCR4-CXCL12 autologous chemotaxis [211]. Elevated IFP has been observed to drive IFF in solid tumors, recent findings state elevated pressure can alter gene expression associated with epithelial-to-mesenchymal transition which promotes collective invasion in MDA-MB-231 human breast cancer cells [212]. Furthermore, recent findings have indicated ERBB2-expressing breast cancer cells exposed to IFF, which have also undergone epithelial-to-mesenchymal transition, invade via PI3K activation and require CXCR4 [213]. These studies demonstrate that IFF plays an active role in tumor cell invasion, potentially through the mechanism of autologous chemotaxis.

In addition to autologous chemotaxis, there is evidence that interstitial flow may drive cancer cell invasion via other mechanisms. In prior work using a microfluidic cell culture system, changes in cell migration and morphology were observed in response to low velocity IFF [214]. Interestingly, migration both with and against the direction of flow was observed, and each seemed to involve different mechanisms. While migration downstream was CCR7-dependent, migration upstream was mediated by integrins and driven by focal adhesion kinase (FAK) activation [214]. Models incorporating interstitial flow and extracellular matrix fiber architecture suggest that FAK activation could be the result of fluid drag-induced matrix tension transmitted to integrins [215]. Another mechanism for regulating tumor invasion may involve degradation and remodeling of the extracellular matrix via MMP activity, as demonstrated in smooth muscle cells and fibroblasts [172, 198, 216]. FAK-ERK pathway activation has been shown to upregulate MMP expression in response to flow, resulting in enhanced renal carcinoma cell migration [217]. However, there is also evidence that interstitial flow can suppress migration of CNS-1, U87, and U251 glioma cells by downregulating MMP-1 and MMP-2. These results are contrary to most findings that interstitial flow promotes cancer cell invasion, but it brings to light the potential for a spectrum of tumor cell responses to IFF [218].

In healthy tissues, fibroblasts are dynamic contributors to extracellular matrix remodeling [219]. In cancer, fibroblasts also drive matrix remodeling and are key contributors to tumor progression [220]. Thus, considering the responses of non-tumor cells in the microenvironment will also be highly relevant to understanding the role of interstitial flow in cancer progression. In previous work, fibroblasts were seeded in collagen gels and exposed to IFF in a radial flow chamber, resulting in varying average

flow velocities across the chamber (average fluid velocity of 13μm/s near the inlet and 3.6μm/s at the outlet). Exposure to interstitial flow for 72 hours caused fibroblasts to align perpendicular to the flow direction and adopt a more spindle-shaped morphology [142]. Changes in cell alignment were matched by changes in matrix alignment as well [142]. These morphological changes that resulted from the alignment of fibroblasts and the matrix could be a major component in controlling permeability within the microenvironment. In addition to cell and matrix alignment, interstitial flow also induced myofibroblast differentiation via a transforming growth factor (TGF)–β1-dependent mechanism [221]. When IFF rates are elevated, e.g., during inflammation and cancer, fibroblasts may differentiate or begin to reorganize the extracellular matrix. The effect of interstitial flow on fibroblast-to-myofibroblast differentiation was particularly significant because it suggests a role in cancer, which is often characterized by fibrotic stroma and the presence of myofibroblasts [220, 221].

More recently, studies have examined the potential interactions of tumor cells and stromal fibroblasts in the presence of interstitial flow. Experiments with metastatic melanoma cells co-cultured with dermal fibroblasts revealed that both tumor cells and fibroblasts invaded in response to interstitial flow [216]. Fibroblast invasion was driven largely by increased activation of TGF- β1 and increased degradation of collagen by MMPs [216]. Tumor cell invasion, in turn, was facilitated by fibroblast invasion and simultaneous "matrix priming" via Rho-dependent fibroblast contractility. This matrix priming would lead to local remodeling of the architecture of the cellular microenvironment and promote tumor cell invasion.

There are many clinical benefits that could be potentially derived from examining the role of IFF in cancer progression, given the growing evidence of its effects on tumor cell invasion. There is already clinical evidence that elevated interstitial flow velocities at the periphery of cervical tumors correlates with increased lymph node metastasis, suggesting the potential use of interstitial flow as a diagnostic or prognostic indicator [146]. Novel therapeutic agents could prevent or reduce migration of cancer cells by specifically targeting pathways stimulated by interstitial flow. More broadly, better understanding the context in which a tumor grows and progresses, which necessarily must include the contributions of interstitial flow, could lead to advances in a wide array of detection and treatment methods for cancer.

### 1.6 Mechanisms of interstitial fluid flow mechanosensing†

Many studies have shown that biomechanical forces indisputably play a significant role within the cellular microenvironment; IFF is one of these forces that can drive biochemical and biophysical changes within the cellular microenvironment [142, 145, 181, 184, 190, 195, 222-226]. The mechanisms by which cells sense and respond to interstitial flow remain elusive; currently, there are three major hypothesized mechanisms for interstitial flow mechanosensing: shear stress sensing via the glycocalyx, autologous gradient formation, and integrin activation due to matrix tension [154, 164, 181, 214, 227-229].

*1.6.1 Glycocalyx shear stress sensing*

Cells subjected to interstitial flow may be stimulated by the shear stresses acting on their surface [154]. It is typically assumed that the shear stresses resulting from interstitial would be relatively low, especially compared to better understand systems such as blood vessels; however, heterogeneous matrix architecture and cell orientation could result in localized elevated stresses. One of the ways that cells may sense shear stress is through a structure known as the glycocalyx. The glycocalyx is a membrane-bound coating of proteoglycans, glycoproteins, hyaluronic acid, and glycolipids [230]. In endothelial cells, shear stress can be sensed via the glycocalyx resulting from blood flow. The stress is transmitted via core proteins of the glycocalyx, which in turn can initiate signals for production of nitric oxide, leading to many downstream affects [229]. These core proteins are part of a "bush-like" structure that experiences the drag force at the core protein tips, which is amplified on the cortical cytoskeleton due to its length (Figure 3). Prior studies in vascular smooth muscle cells suggest that heparan sulfate proteoglycans in the glycocalyx (i.e., syndecans and glypicans) are critical to cellular responses to interstitial flow, mediated by integrins, focal adhesion kinase (FAK), and extracellular signal-related kinase (ERK) [202, 203]. These findings are supported by modeling of interstitial flow and shear stress on the glycocalyx, where the solid shear stress transmitted by the glycocalyx can be as much as one to two orders of magnitude greater than the predicated fluid shear stress applied to the cell [231]. The model also predicts that glycocalyx thickness and permeability would strongly affect the solid shear stress, raising the possibility that shear stress sensing could be tuned or disrupted by modifying the structure and composition of the glycocalyx. These findings suggest that while the fluid shear stresses applied by

interstitial flow may be relatively low, the glycocalyx could amplify and transmit those stresses to the cell [231].

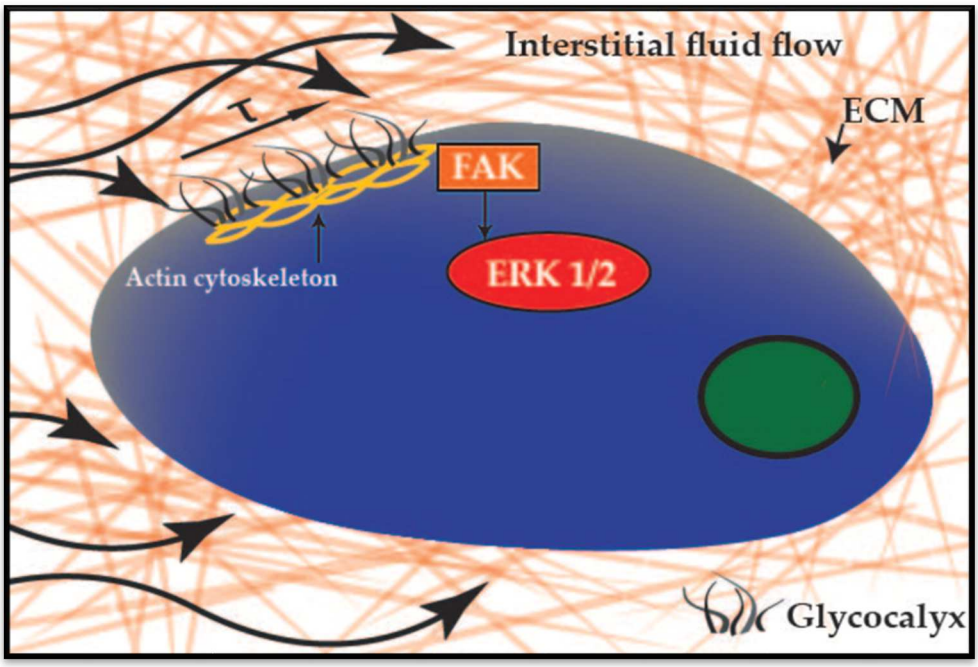


**Figure 3: Glycocalyx-mediated shear stress sensing by a cell exposed to IFF.**

*1.6.2 Autologous gradient formation*

Another potential mechanism for interstitial flow sensing revolves around the convective mass transport associated with flow. During fluid flow, molecules are transported through the tissue interstitium where they are needed; this can cause the formation of extracellular gradients, to which cells are exquisitely sensitive [181, 232]. Fluid flow can be sensed by solute transport in intervertebral discs; this convective transport of molecules provides nutritional needs to the cells allowing them to function normally [227]. Similarly, joint loading alters soluble macromolecule distribution in articular cartilage via fluid flow. This redistribution of macromolecules alters the

regulation of matrix protein formation and degradation of the extracellular matrix of cartilage [233].

Models of interstitial flow and autocrine morphogen secretion of a single cell demonstrate that convective forces alone can establish transcellular autologous gradients and bias protein concentrations that can change cellular behavior (Figure 4). These gradients can be amplified if the secreted morphogen is matrix binding; these morphogens can then be liberated or activated by cell-secreted proteases. Under interstitial flow conditions, these proteins released from the extracellular matrix result in amplified gradients downstream compared to the soluble form of the same protein [181]. Amplified gradients of these morphogens possess capabilities of signaling via receptor tyrosine kinases and G-protein coupled receptors [234]. The model demonstrated that biologically relevant gradients can result for IFF velocities ranging from 0.12 - 6.0 μm/s, even if the Peclet number suggests that diffusion is the dominant mechanism of mass transport. If the secreted factor is a chemoattractant, these autologous gradients can drive directed cell migration via a mechanism called autologous chemotaxis [209, 235]. While sensing of autologous gradients generated by interstitial flow may not fit the traditional definition of mechanosensing (which generally involves transmission of stresses or strains), it nonetheless represents a mechanism by which cells can transduce the physical phenomenon of interstitial flow into an intracellular biochemical signal.

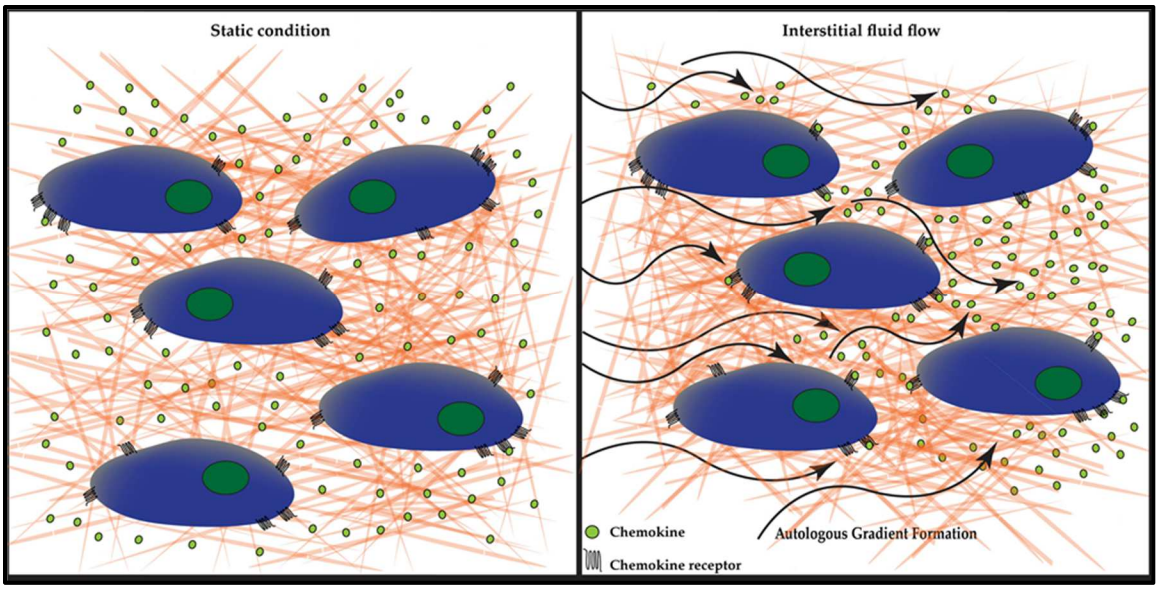


**Figure 4: Transcellular autologous gradient generated by convective forces (right). Under static conditions, no autologous gradient is generated (left).**

*1.6.3 Matrix tension and integrin activation*

IFF is known to create pressure forces on cells within a three-dimensional environment, leading to transcellular stress gradients and asymmetric forces between the cell and extracellular matrix [214, 215]. IFF can also create drag forces on matrix fibers found on the extracellular matrix [154]. The forces can generate relatively high shear stresses on these fibers that can, in turn, be transmitted to engaged integrin receptors (Figure 5). This may represent a distinct mechanism from the activation of integrins by shear stress transmitted via the glycocalyx, as described above. Integrins have been shown to play important roles in mechanosensing in various systems, such as endothelial cells [236] and tumor cells [237]. Cells can sense this fluid drag-induced matrix tension and respond via increased integrin and FAK activation [214]. Interestingly, the glycocalyx may potentially play a role in this mechanism as well, as models have suggested that integrin clustering can be regulated by the glycocalyx [238]. However, compared to glycocalyx

shear stress sensing and autologous gradient formation, there is considerably less experimental evidence for this hypothetical mechanism.

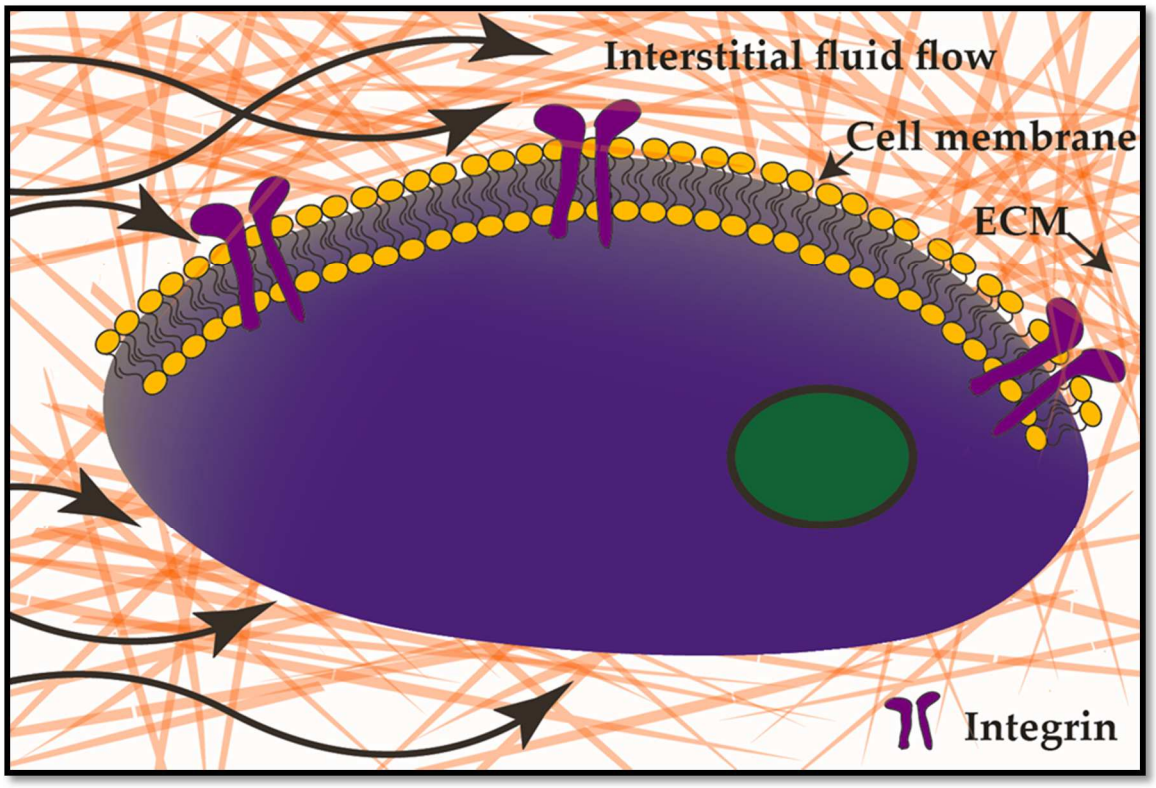


**Figure 5: A cell anchored to the matrix experiences tensile forces stress upstream of IFF. Integrin receptors are able to sense this tension that is transmitted through the matrix.**

### 1.7 Outstanding questions

In the last 20 years, HCC is one of the only three major cancer types observed to have increased mortality and possess a steady increase in incidence regardless of the current advances in cancer detection and treatment. The progression of this deadly malignancy is often in the background of underlying chronic injury making it difficult to detect in early stages. In recent years, much emphasis has been placed on understanding

the process of HCC cell invasion; however, it has become apparent that the progression of this disease is not solely dependent on just the cancer cells or biological factors, but also their interaction with surrounding cells and tissue [43, 223, 239-242]. A growing body of evidence has shown us that cells respond to changes in their microenvironment, resulting in altered cellular behavior that can contribute to cancer progression. However, these changes in the TME, specifically biomechanical forces like IFF in particular, are severely understudied. IFF is observed to be elevated within the tumor resulting in increased tumor cell invasion [209, 213, 216, 243-247]. The goal of this research is to elucidate the effects of IFF on HCC invasion and identify the key molecular components involved. Uncovering the synergistic effect of both matrix stiffness and IFF in the liver TME will establish a significant physiological understanding of how mechanical forces and molecular signaling pathways alter HCC cell invasion.

# CHAPTER 2: INTERSTITIAL FLUID FLOW INCREASES HEPATOCELLULAR CARCINOMA CELL INVASION THROUGH CXCR4/CXCL12 AND MEK/ERK SIGNALING†

†The content of this chapter was published in the Public Library of Science (PLoS): Shah, A. D., Bouchard, M. J., & Shieh, A. C. (2015). Interstitial Fluid Flow Increases Hepatocellular Carcinoma Cell Invasion through CXCR4/CXCL12 and MEK/ERK Signaling. *PLoS One, 10*(11), e0142337. doi:10.1371/journal.pone.0142337

## 2.1 Introduction

Worldwide, HCC is the second leading cause of cancer-related deaths with over 746,000 deaths annually [248]. In the United States, it is estimated that there will be 35,560 new cases of HCC in 2015, making it one of the few types of cancer that is still increasing in incidence at a rate of approximately 3% per year [249]. Treatment of HCC remains a challenge, with 5 year survival rates for patients with stages IIC and IVA (regional HCC) of 10% and for patients with stage IVB (distant HCC) as low as 3% [3]. Chronic hepatitis B or C virus infection, non-alcoholic fatty liver disease, alcoholism, obesity, type 2 diabetes, exposure to alfatoxins, and anabolic steroids may all play a role in the development and progression of HCC [250]. The formation of intrahepatic metastases, which occurs in 51-75% of HCC tumors, is an indicator of poor prognosis [251]. Furthermore intrahepatic metastasis can be aggressive as observed in a study of 148 patients with intrahepatic HCC (stage IVA or III tumors), nearly 86% of the patients developed extrahepatic metastases occurring most frequently in the lungs [252]. Identification of early stage HCC provides the best opportunities for effectively treating this cancer; however, even if detected early, the most successful curative treatment options are limited to resection of the diseased liver tissue or liver transplantation [253]. Unfortunately, studies have shown that HCC redevelops in more than 50% of patients with intrahepatic or extrahepatic metastases within the first year [254]. Treatments for late stage

or recurring HCC are also limited; palliative treatment options include transarterial chemoembolization or pharmaceutical interventions such as Sorafenib, a kinase inhibitor which has been shown in a Phase III clinical trial of 602 patients to only improve overall survival by 12 weeks. [253, 255]. Poor outcomes have been attributed to the dearth of HCC screening in the general population, limited treatment options, and invasiveness of the cancer [256]. Therefore, a better understanding of the molecular mechanisms that affect HCC development and progression is needed to develop more effective strategies for diagnosing and treating HCC.

In recent years, many studies have emphasized the importance of the tumor microenvironment in HCC progression [43]. Factors such as chronic inflammation, liver fibrosis, and cellular activity of hepatic stellate cells have been observed to alter the liver microenvironment [79]. However, the role of mechanical forces within the HCC tumor microenvironment remains poorly understood. Within the tumor microenvironment, changes in biomechanical forces such as solid stress [257], fluid pressure [146], and fluid flow [154, 214, 215, 218] have been shown to alter cancer progression [223, 258]. Interstitial fluid flow (IFF) is one of these altered forces in the tumor microenvironment.

High permeability of tumor-associated vasculature has been shown to alter fluid movement, likely due to changes in hydrostatic and oncotic pressure [223]. Previous studies identified that most solid tumors have increased interstitial fluid pressure [150]. Interstitial fluid pressure in a healthy liver was found to be -2.2 mmHg, while the interstitial fluid pressure in a hepatoma ranged between 0-30 mmHg [259]. The resulting increase in tumor interstitial fluid pressure leads to a steep pressure gradient between the tumor and stroma that drives elevated IFF [144, 223]. Computational models have predicted IFF

velocities between 0.1 – 6.0 μm/s under various conditions [181]. IFF velocity in mice with $VEGF_{165}$-expressing tumors was measured to be 0.1 - 0.5 μm/s, and even greater velocities (1.0 – 8.0 μm/s) were observed in mice with human cervical carcinoma and melanoma xenografts [145, 146]. *In vivo* IFF velocities in cervical cancer patients with pelvic lymph node metastases were measured to be between 10 – 55 μm/s [146]. IFF has been shown to affect various cellular processes such as differentiation [244], morphogenesis [183, 214], and protein secretion [144, 235]. In cancer, IFF can promote cancer cell invasion [209, 245], alter stromal fibroblast behavior [216], and increase MMP secretion [218]. Previous studies have revealed that cells can sense interstitial flow through glycocalyx-mediated shear-stress sensing [229], autologous-gradient formation [181], and integrin activation due to fluid-drag forces and cell-matrix adhesion [214]. In a mechanism referred to as 'autologous chemotaxis', IFF combines with autocrine chemoattractant secretion to form an autologous gradient that directs tumor-cell migration [181, 209, 216, 235, 244, 247]. Computational models have shown that slow-moving fluid, in combination with cell-secreted proteins, can generate a pericellular chemoattractant gradient that is sufficient to trigger a physiological response such as chemotaxis [181, 209]. Previous studies have also shown that human breast cancer cell lines exhibit increased invasion in the direction of IFF via a CCR7-dependent mechanism, while glioma cell invasion can occur through CXCR4-dependent autologous chemotaxis [209, 235]. In HCC, studies have shown that CXCR4 and CXCL12 play a pivotal role in extrahepatic metastasis [260], migration [261, 262], and patient prognosis [263]. To date, however, no studies have examined the role of interstitial flow and autologous chemotaxis (potentially via CXCR4/CXCL12) in HCC cell invasion.

The increase in IFF in tumors results in increased tumor cell invasion in various cancer types; however, to date there is no study that has investigated the effects of IFF in HCC [213, 216, 235, 247]. We hypothesized that increased IFF induces greater HCC invasion in a velocity-dependent fashion. IFF velocity in various solid tumors has been observed to be significantly higher than flow rates found in normal tissue [145]. Consequently, peritumoral IFF velocity has been observed to be an indicator of low survival in human cervical carcinoma patients [146]. Understanding and profiling IFF velocity on HCC cell invasion could serve as a potential prognostic indicator for HCC progression and patient survival. Furthermore, we hypothesized that HCC cells invade in response to IFF through the autologous formation of a CXCL12 chemokine gradient. In the studies described here, we have analyzed the effects of IFF on HCC cell invasion and have identified a key molecular pathway that is involved in liver cancer cell invasion. We show that IFF-induced HCC invasion is dependent on an autologous chemotaxis via CXCR4 and CXCL12, as well as MEK/ERK activation. The results of our studies suggest a potential role for IFF in the invasive potential of HCC.

## 2.2 Methods

*Cell Isolation and Culture*

Hepatoma-derived Huh7 and Hep3B cells were cultured in Roswell Park Memorial Institute (RPMI) 1640 with L-glutamine (Cellgro, Manassas, VA) supplemented with 10% fetal bovine serum (FBS) and 1% penicillin/streptomycin. HepG2 hepatoblastoma-derived cells were cultured in Minimal Essential Medium (MEM) (Cellgro) supplemented with 10% FBS, 1% non-essential amino acids (NEAA), 1% sodium pyruvate, and 1%

penicillin/streptomycin on collagen-coated cell-culture plates. Rat hepatocytes (PRHs) were isolated from 5-7 week old male Sprague-Dawley rats using a 2-step perfusion method [264]. Surgery and isolation of rat hepatocytes were approved by the Institutional Animal Care and Use Committee of Drexel University College of Medicine and complied with the Animal Welfare Act, the Public Health Service Policy of Humane Care and Use of Laboratory Animals, and the National Institutes of Health (United States) Guide for the Care and Use of Laboratory Animals [265, 266]. PRHs were used within 3 hours of isolation to prevent hepatocyte de-differentiation. The PRHs were maintained in Williams E medium (Life Technologies, Carlsbad, CA) supplemented with 2 mM L-glutamine, 1 mM sodium pyruvate, 4 μg/ml insulin/transferrin/selenium (ITS), 5 μg/ml hydrocortisone, 5 ng/ml epidermal growth factor (EGF), 10 μg/ml gentamycin, and 2% dimethyl sulfoxide (DMSO). All cells were maintained in a humidified 37˚C environment with 5% $CO_2$.

*3D Interstitial Flow Invasion Assay*

The liver cells (5.0 x $10^5$ cells/ml gel) were encapsulated in a gel comprised of 1.3 mg/ml rat tail tendon type I collagen (BD Biosciences, San Jose, CA) and 1 mg/ml Matrigel (BD Biosciences) and seeded into 12 mm diameter, 8 μm pore diameter culture inserts (Millipore, Bellerica, MA). Static and flow conditions were generated over the course of 24 hours by following a previously described method [209, 216, 267]. For the static condition, the level of basal medium outside of the transwell was level with the medium inside the transwell, resulting in little to no hydrostatic pressure difference. The IFF condition was created by adding more basal medium to the inside of that transwell than the outside, resulting in a hydrostatic pressure difference of approximately 1 mm Hg. This

drove IFF through the collagen gel, with an average velocity of approximately 0.05 – 0.1 μm/s (based on average volumetric flow rate and the cross-sectional area of the gel). This velocity is on the lower end of velocities measured in or modeled for tumors, but much higher than the IFF velocities predicted for normal hepatic lobules [145, 146, 268]. Cells that transmigrated through the porous membrane were fixed with 4% paraformaldehyde (Sigma-Aldrich, St. Louis, MO) and stained with DAPI (2 μg/ml, MP Biomedicals, Santa Ana, CA). Fixed and stained cells were imaged by fluorescence microscopy. Both static and flow conditions were analyzed by counting five locations on the fixed membranes. Percent invasion was calculated with the following equation:

$$\%\ Invasion = \left[\frac{(Average\ cell\ count) * (Membrane\ surface\ area)}{(Image\ area) * (Number\ of\ cells\ seeded)}\right] * 100$$

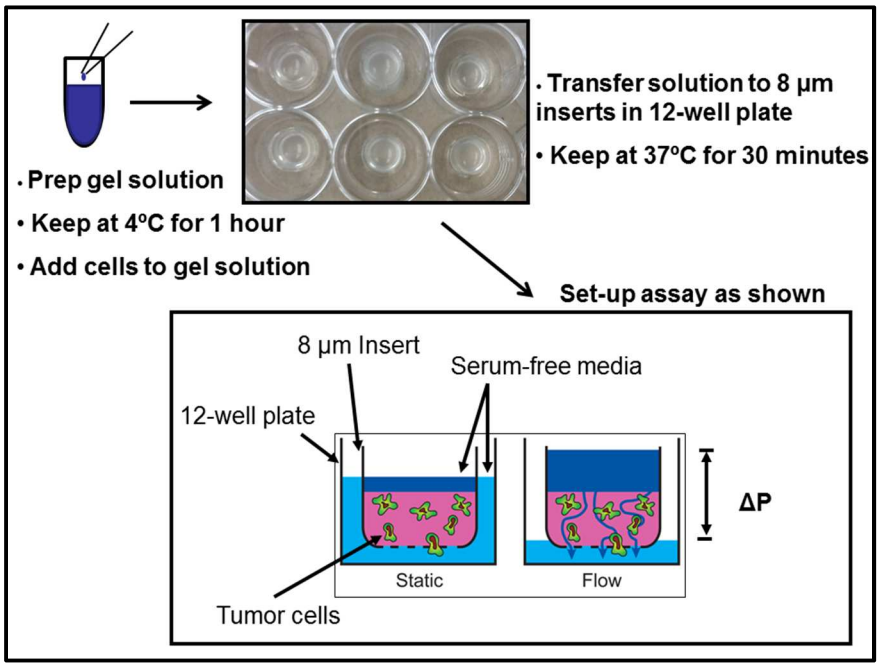


**Figure 6: Schematic of the 3D invasion assay. The collagen/Matrigel matrix (pink) is seeded with HCC cells (green). Interstitial flow is simulated with basal media (blue) and the fluid flow is drive by the pressure head generated by the basal media.**

For specific experiments, pharmacological inhibitors, neutralizing antibodies, or recombinant proteins were added to the cell/gel mixture before gel polymerization and in the media used for the experiment at their respective target concentrations (Table 1).

**Table 1: List of pharmacological inhibitors and neutralizing antibodies.**

| Agent | Source | Target | Concentration |
|---|---|---|---|
| AMD3100 | R&D Systems | CXCR4 | 12.6 μM |
| CXCL12 neutralizing antibody | R&D Systems | CXCL12 | 3 μg/ml |
| U0126 | Selleckchem | MEK1/2 | 25 μM |
| FR180204 | Tocris | ERK1/2 | 10 μM |

*Measurement and calculation of IFF velocity*

To determine IFF velocity, the normal 3D invasion assay with Huh7 cells was set up as described previously was utilized with varying velocity conditions: static, low flow, medium flow, medium-high flow, and high flow conditions. To achieve a broader range of flow velocities, we increased the permeability of the collagen matrix by removing Matrigel, and confirming that IFF still induces invasion in the absence of Matrigel and all the factors it contains. IFF velocity was determined by collecting the basal medium that flowed through the Boyden chamber and measuring its volume. Every hour the basal medium was collected and replenished to the respective volume for low flow – 162.5 μl, medium flow – 325 μl, medium-high flow – 487.5 μl, and high flow – 650 μl. This was repeated for 6 hours and finally the cells were fixed, stained, and imaged for quantification of flow-induced HCC invasion. It is important to note that normal invasion experiments were conducted for 24 hours without refill of Boyden chambers. The volume of basal

medium collected each hour was measured and recorded. This value was utilized to determine fluid flow velocity as described in the following equation:

$$Q = v * A$$

*Q: volumetric flow rate; v: mean velocity; A: cross-sectional area of flow:* $A = 1.131 * 10^{-4} m^2$

*Western Blot*

Western blot was used to measure changes in total and phosphorylated protein levels in response to IFF and specific inhibitors. Cells were lysed with radioimmunoprecipitation assay (RIPA) buffer containing Halt protease and phosphatase inhibitor cocktail (Thermo Scientific, Waltham, MA). For 3D samples, cells were first digested out of the gels with collagenase D (0.5625 U/ml, Roche Life Science, Indianapolis, IN) for 45 minutes and then centrifuged for 10 minutes at 1,000 RPM. The following primary antibodies were used to detect the proteins of interest: anti-CXCR4 (1:1,000, Abcam, Cambridge, England), MEK1/2 (1:1,000, Cell Signaling Technology, Beverly, MA), phospho-MEK1/2 (Ser217/221) (1:1,000, Cell Signaling Technology, Beverly, MA), ERK1/2 (1:1,000, Cell Signaling Technology, Beverly, MA), phospho-ERK1/2 (Thr202/Tyr204) (1:1,000, Cell Signaling Technology, Beverly, MA), and β-actin (13E5) (1:2,000, Cell Signaling Technology, Beverly, MA). The following secondary antibodies were used: rabbit anti-mouse IgG-HRP (1:10,000, Abcam, Cambridge, England), goat anti-rabbit IgG-HRP (1:10,000, Abcam, Cambridge, England), and anti-rabbit IgG (1:2,000, Cell Signaling Technology, Beverly, MA). Chemiluminescence imaging was conducted with a FluorChem M imaging system (Proteinsimple, San Jose,

California) and quantified with AlphaView (Proteinsimple, San Jose, California). Target protein levels were normalized to β-actin.

*CXCL12 Chemotaxis Assay*

Huh7 cells (1.25 x $10^5$ cells/ml gel) were added to the same type of gel and cell-culture inserts used for the 3D flow invasion assay. Cells were exposed to a gradient of recombinant human CXCL12 in a checkerboard method, by adding a known concentration of CXCL12 (10 nM) in the medium only above, below, or above and below the gel (or a control condition with no CXCL12) for 24 hours at 37˚C with 5% $CO_2$. Cells that migrated through the membrane of the cell-culture insert were fixed and stained. Invasion was quantified following the same method described for the 3D flow invasion assay.

*Enzyme-linked immunosorbent assay (ELISA)*

Protein from 2D cell lysates and medium were collected from approximately 8.0-11 x $10^6$ HCC cells after 4 days of incubation at 37˚C and 5% $CO_2$ in a T75 flask with full media. Protein from 3D cell lysates and medium were collected from 5.0 x $10^5$ liver cells after 1 day of incubation at 37˚C and 5% $CO_2$ in a collagen/Matrigel matrix. Protease inhibitors were added to all cell lysates and media. CXCL12 levels were quantified using a commercially available DuoSet ELISA kit (R&D Systems, Minneapolis, MN). Standard curves were generated using known concentrations of recombinant human CXCL12 and data were fit with a four parameter logistic curve in MATLAB (MathWorks, Natick, MA).

*Statistical Analysis*

All data are presented as mean ± standard error of the mean (SEM). All results for invasion assays are based on a minimum of two independent experiments with sample size $n \geq 3$ for each experiment. Statistical significance between two groups was determined by conducting a Student's t-test. For three or more groups, one or two-factor AVOVA with a Bonferroni or Tukey's multiple comparison test was utilized. GraphPad Prism 5 (San Diego, CA) was used to perform statistical analyses.

## 2.3 Results

*IFF enhances HCC cell invasion*

A panel of human liver-derived cell lines consisting of Huh7 (human hepatoma cells), HepG2 (human hepatoblastoma cells), and Hep3B (human hepatoma cells with integrated hepatitis B virus genome), along with PRHs, were exposed to IFF in the 3D flow invasion assay to quantify the effects of IFF on cell invasion. Huh7, Hep3B, and HepG2 cells exposed to IFF showed increased invasion in comparison to cells in static (no IFF) conditions (Figure 7A). Notably, the percent invasion of Huh7 cells exposed to IFF was much higher than Hep3B, HepG2, and PRHs (Figure 7A). When data were normalized to their respective static controls, the hepatoma-derived Huh7 and Hep3B cells showed the most dramatic response to interstitial flow, with nearly a 5.5 fold increase in invasion due to IFF (Figure 7B). In contrast, HepG2 cells showed only a 2.1 fold increase in cellular invasion in response to IFF (Figure 7B). PRHs exposed to IFF did not show any significant changes in invasion.

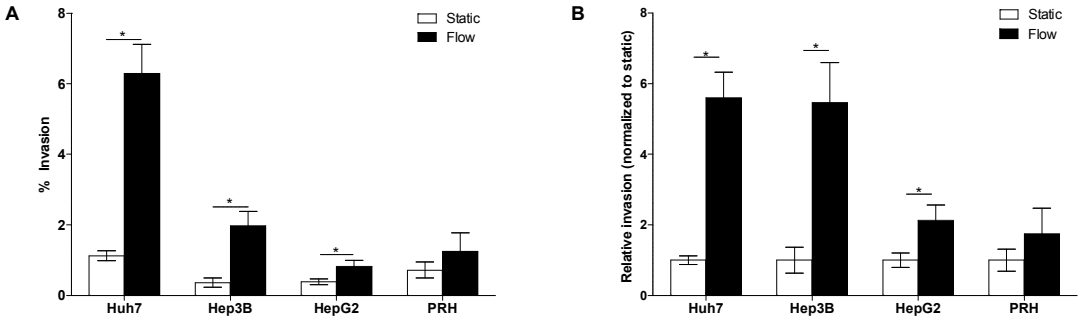


**Figure 7: Interstitial flow induces invasion of HCC cell lines.** (A) Percentage of HCC and PRHs that have invaded in response to fluid flow. Huh7, n=23 (static and flow); Hep3B, n=15/21 (static/flow); HepG2, n=21/19 (static/flow); PRH, n=9 (static and flow). *, $p < 0.05$. (B) Invasion results (identical to A) presented as normalized to each cell type's respective static condition.

*Flow-induced HCC cell invasion is velocity-dependent*

In order to vary the fluid flow velocity, two major parameters were changed to simulate physiologically relevant fluid flow velocities. First, Matrigel was removed from the matrix and the Huh7 cells were encapsulated solely in type I collagen (Samples B-E, Figure 8A), resulting in decreased matrix permeability allowing increased basal medium to flow through. Next, altering the hydrostatic pressure within the Boyden chamber by adjusting the volume of basal medium placed inside would result in changes to the fluid flow rate, ultimately varying the velocity. Four different velocities along with a static control was utilized to observe the effects of the varying flow velocities of basal medium on the invasiveness of the encapsulated cells. Our results indicate that there is a correlative relationship between fluid flow velocity and Huh7 cell invasion (Figure 8A). Additionally it is apparent that the overall invasion percentage is much lower than the invasion results observed in (Figure 8A). It is important to keep in mind that the set of experiments examining velocity were only conducted for a 6 hour period with constant fluid flow, while

the traditional 3D invasion assay required 24 hours with decreasing fluid flow velocity. Additionally linear regression analysis established a positive relationship with fluid flow velocity and Huh7 cell invasion (Figure 8B, $R^2 = 0.2763$).

A.

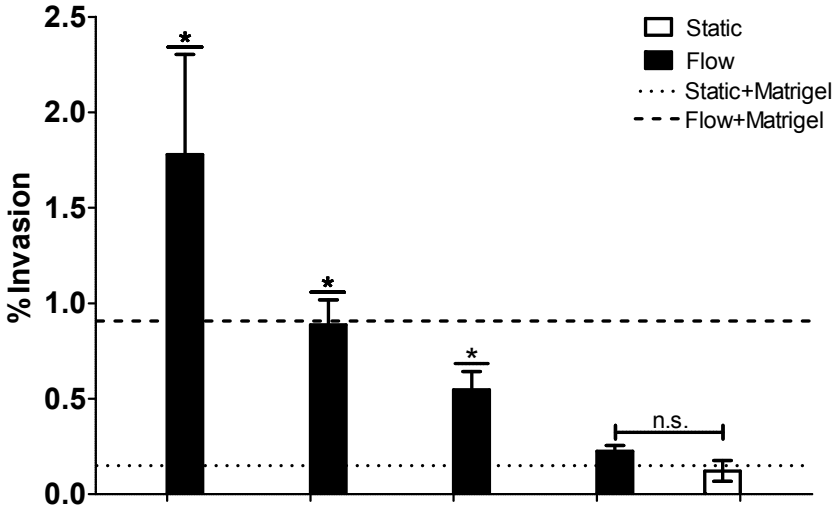


| | A | B | C | D | E |
|---|---|---|---|---|---|
| **Matrix Type** | Collagen | Collagen | Collagen | Collagen | Collagen |
| **Flow Type** | High | Medium+High | Medium | Low | No Flow |
| **Volume (µl)** | 650 | 487.5 | 325 | 162.5 | - |
| **Velocity (µm/sec)** | 0.9926 | 0.6169 | 0.2975 | 0.0644 | 0 |
| **% Invasion (flow)** | 1.771 | 0.887 | 0.548 | 0.226 | 0.122 |
| **Sample Size** | n=12 | n=6 | n=6 | n=6 | n=12 |

B.

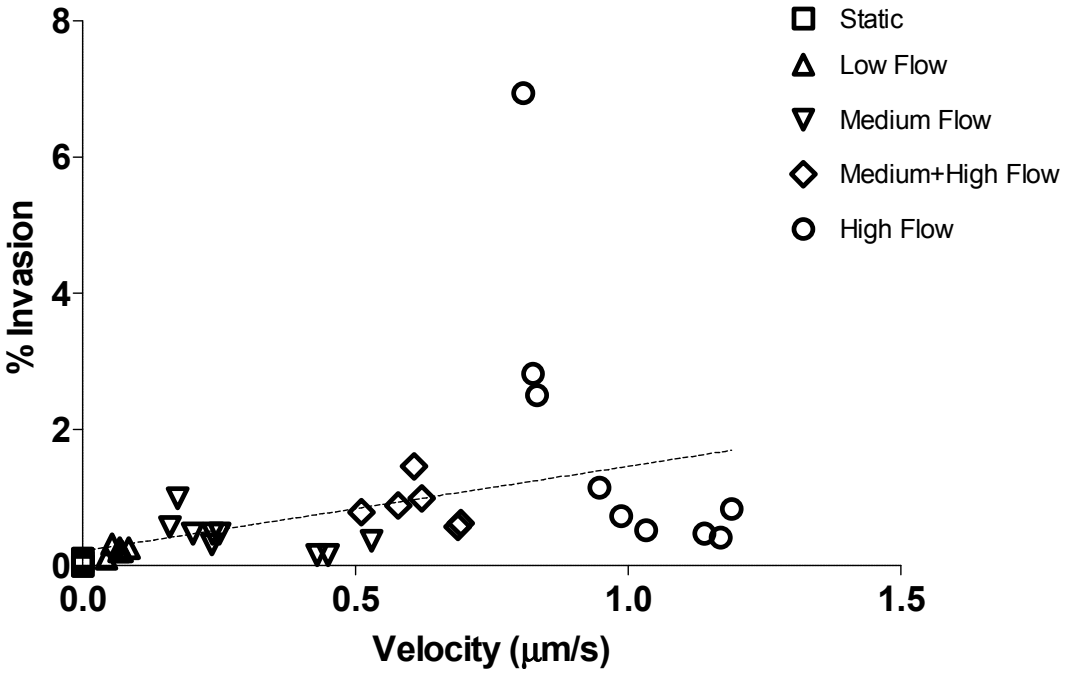

**Figure 8: Flow-induced HCC invasion is velocity-dependent.** (A) Huh7 cells exposed to varying fluid flow velocities for 6 hours. Matrix conditions A, B, C, D, and E = collagen only. Flow type dictated by volume of basal medium placed inside transwell every hour. - - - = collagen + matrigel static condition and – – – = collagen + matrigel flow condition. * = $p < 0.05$ between static vs. flow condition. n.s. = not significant between low flow and static collagen only condition. (B) Linear regression analysis results in positive relationship between fluid flow velocity and Huh7 cell invasion. ($R^2 = 0.2763$. Slope significantly differs from zero, $p = 0.0012$).

*IFF-induced HCC invasion depends on CXCR4*

The chemokine receptor CXCR4 has been shown to mediate cellular functions such as proliferation, migration, invasion, and adhesion in a variety of cancer types [235, 260, 269]. Studies have shown that HCC cells possess higher CXCR4 and CXCL12 protein levels in HCC metastases compared to normal hepatic tissues [260, 261]. This evidence further suggested CXCR4/CXCL12 could potentially promote tumor cell migration. Additionally, IFF has been shown to enhance glioma invasion through CXCR4/CXCL12-dependent autologous chemotaxis [235]. Thus we hypothesized that IFF-induced HCC cell invasion depends on the CXCR4/CXCL12 chemokine axis. To block CXCR4 activity, we incorporated the CXCR4 antagonist AMD3100 (12.6 μM) into the 3D invasion assay. AMD3100 significantly decreased IFF-induced invasion of both Huh7 and Hep3B cells, but had no statistical effect on HepG2 cells and PRHs (Figure 9A). To determine if the differences in IFF-induced invasion between Huh7, Hep3B, and HepG2 cells, and their sensitivity to AMD3100, was due to CXCR4 expression, we performed western blot analyses to measure CXCR4 levels. We confirmed the presence of CXCR4 in both 2D and 3D cultures of all three cell lines (Figure 9B). A quantitative analysis of CXCR4 levels showed that CXCR4 expression did not vary significantly between the cell lines, and IFF had no effect on CXCR4 levels in 3D conditions (Figure 9C). Overall, these findings

suggest that CXCR4 is necessary but not solely responsible for IFF invasion. Moreover, IFF does not modulate levels of CXCR4, nor does responsiveness to IFF correlate with CXCR4 protein expression in the cell lines tested.

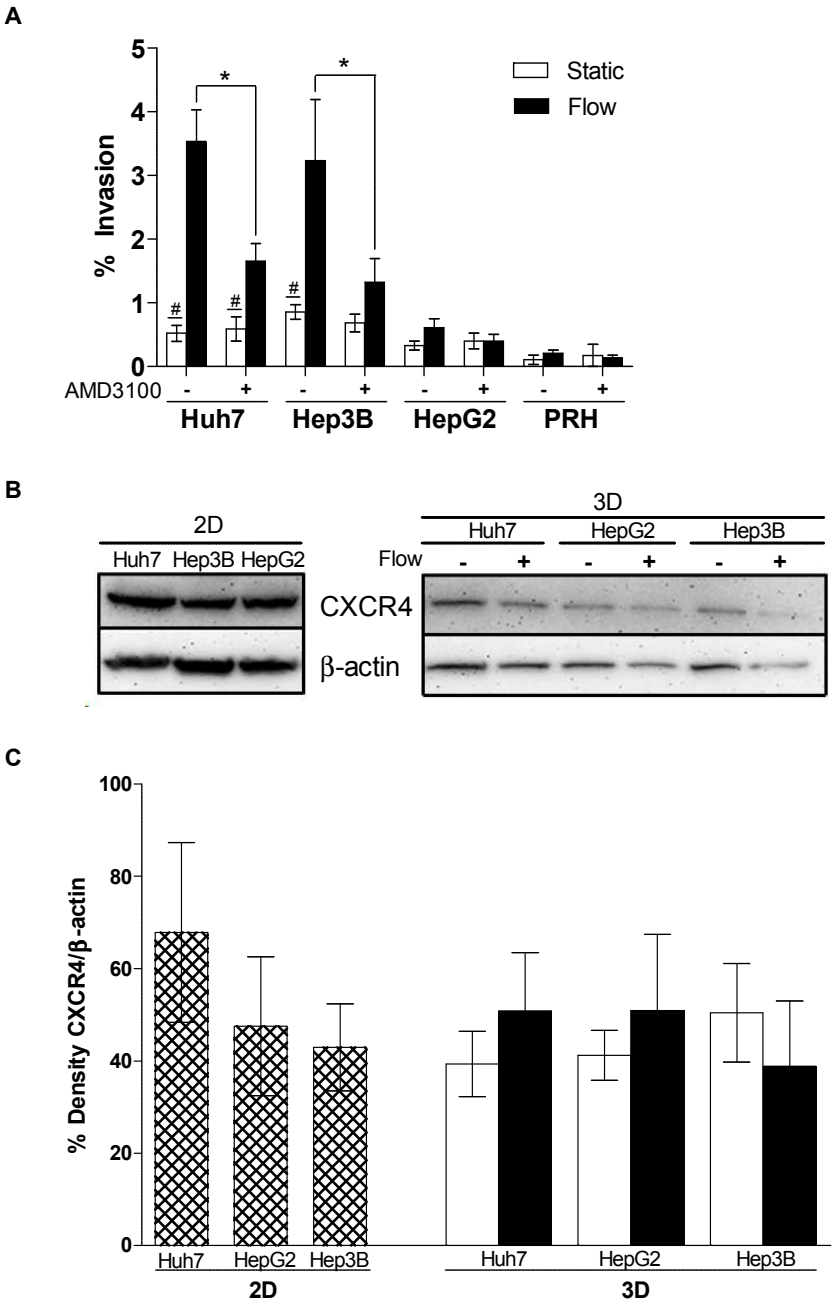

**Figure 9 : Interstitial flow-induced HCC invasion depends on CXCR4.** (A) CXCR4 antagonist AMD3100 (12.6 μM) inhibits IFF-induced invasion. Huh7 (n=18), Hep3B (n=18), HepG2 (n=12), and PRH (n=6). * = $p < 0.05$ between each respective cell line and its corresponding treatment condition. # = $p < 0.05$ between static vs. flow conditions. (B) CXCR4 is detected in HCC cell lines in both 2D and 3D lysates. CXCR4 = 43 kDa. Static 3D sample, (-) and Flow 3D Sample, (+). (C) Quantitative western blot analysis of CXCR4 compared to its respective control, β-actin. Percentage adjusted relative density compared to loading control of respective sample. Static 3D sample, (white bar); Flow 3D Sample, (black bar).

*IFF-induced Huh7 invasion requires an autologous CXCL12 gradient*

Given the functional role of CXCR4 (Figure 9), we next investigated the involvement of CXCL12 in IFF-induced invasion of Huh7 cells. The Huh7 cells showed the strongest invasion response to IFF; therefore, we proceeded with primarily this cell line in subsequent experiments. Incorporating a CXCL12 neutralizing antibody in the 3D invasion assay resulted in a significant reduction in IFF-induced Huh7 invasion (Figure 10A), suggesting that CXCL12 is necessary for IFF-induced invasion. Based on the functional response of the Huh7 cells in our serum-free invasion assay conditions, it appeared that these cells are secreting CXCL12. One of the key features of the hypothetical autologous chemotaxis mechanism is a pericellular chemoattractant gradient caused by IFF. To diminish the relative magnitude of any cell- and IFF-generated CXCL12 gradient, we added a uniform 10 nM concentration of recombinant CXCL12 to the 3D invasion assay. This resulted in decreased IFF-induced invasion compared to the untreated condition (Figure 10B). This suggests that a CXCL12 gradient is necessary for IFF-induced invasion, consistent with the previously hypothesized autologous chemotaxis mechanism [235]. We also confirmed that Huh7 cells chemotact in response to CXCL12 through a 3D chemotaxis assay (Figure 10C). Finally, to determine if CXCL12 secretion levels vary between the Huh7, Hep3B, and HepG2 cells, which could potentially explain

the differential responses to IFF, intracellular and secreted CXCL12 in 2D and 3D (static) environments was quantified by ELISA (Figure 10D). In the 2D conditions, the Hep3B cells secreted the greatest amount of CXCL12 in the medium, while HepG2 secreted no detectable amounts. The lysates of the 2D conditions exhibited low amounts of CXCL12 (~2 pg CXCL12/$10^6$ cells) for all three cell lines. Between the three cell lines in 3D conditions, all three cell lines showed relatively similar levels of CXCL12 in lysate and medium. While greater amounts of CXCL12 were measured in the lysates of the cells in the 3D condition compared to the 2D condition, there was no clear correlation between IFF-induced invasion and levels of CXCL12 secretion.

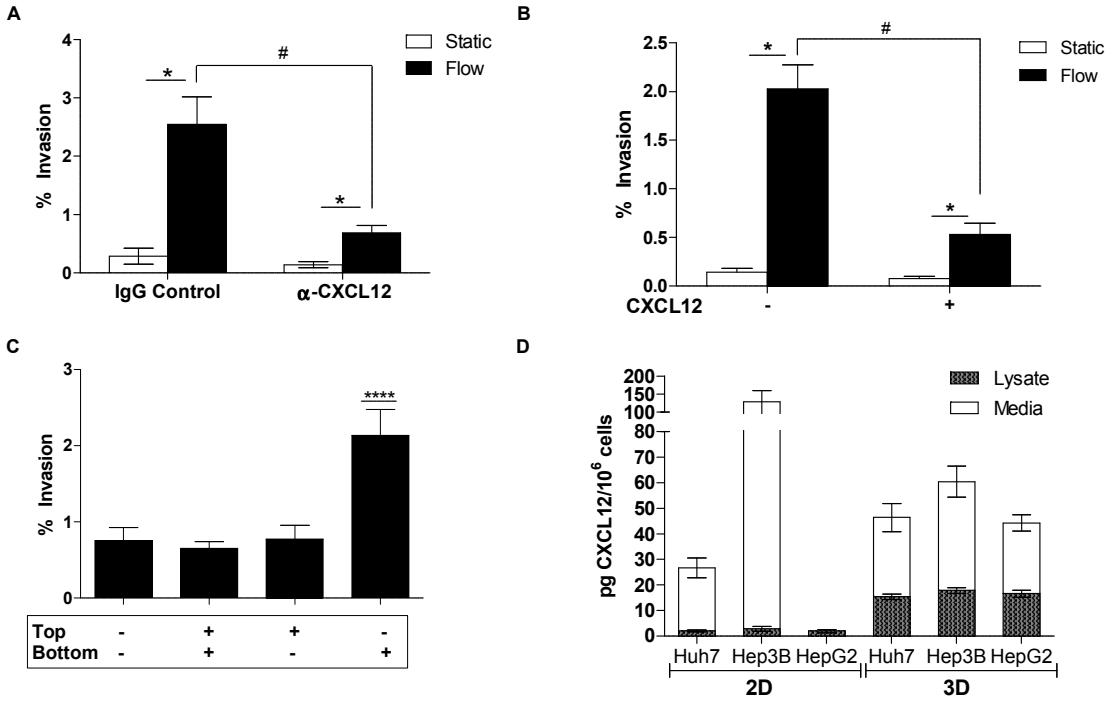


**Figure 10: Detection of CXCL12 and its functional role in HCC.** (A) Huh7 cells treated with CXCL12 neutralizing antibody and respective control (3 μg/ml) for 24 hours in a 3D invasion assay (n=9). * = $p < 0.05$ between each respective treatment condition. # = $p < 0.05$ between static vs. flow conditions of the two treatment. (B) Invasion assay (n=12) on Huh7 cells with/without CXCL12 (80 ng/ml) conditioned medium was conducted to observe changes in flow-induced cellular invasion. Test condition: + = exogenous

CXCL12 added to media; - no exogenous CXCL12 present in media. Significance between static vs. flow, * = $p < 0.05$. # = $p < 0.05$ between static vs. flow conditions of the two treatment options. (C) Chemotaxis assay conducted on Huh7 cells in static environment (n=18). Exogenous CXCL12 – 80ng/ml. Test condition: + = exogenous CXCL12 added; - = no exogenous CXCL12 present. **** = $p < 0.0001$. (D) Average CXCL12 expression in 2D and 3D lysates (static) and respective medium was measured with ELISA. Sample type: cell line (n=lysate/n=medium) – 2D: Huh7 (n=7/n=6), Hep3B (n=3), HepG2 (n=3). 3D: Huh7 (n=6), Hep3B (n=6/n=5), HepG2 (n=5/n=6).

*MEK/ERK signaling is required for IFF-induced HCC cell invasion*

Our previous results demonstrate that the CXCR4/CXCL12 signaling axis plays a critical role in IFF-induced HCC invasion, but utilization of a CXCR4 antagonist and the CXCL12 neutralizing antibody does not eliminate this flow-induced invasion entirely (Figure 9 and Figure 10). Rather these results suggest that IFF-induced invasion of HCC cells is not regulated solely by CXCR4/CXCL12 chemokine signaling, but may involve other molecular mediators. Previous studies have observed elevated levels of MEK and ERK in HCC, which have been shown to contribute to HCC cell proliferation, differentiation, tumor progression, alter cell cycle regulation and apoptosis [26, 270, 271]. Given that increased MEK1/2 and ERK1/2 activity has been observed in HCC, we investigated whether these kinases affect IFF-induced HCC invasion [26, 270]. Huh7 cells in the 3D invasion assay were treated with the MEK1/2 inhibitor U0126 (25 μM), which resulted in a significant decrease in IFF-induced invasion compared to the vehicle (DMSO) control (Figure 11A). Similarly, inhibition of ERK1/2 activity by FR180204 (10 μM) resulted in significantly decreased IFF-induced invasion of Huh7 cells (Figure 11B). The inhibitor concentrations used in these experiments were confirmed to be non-cytotoxic in 3D culture conditions. A western blot was conducted on protein from Huh7 3D samples and showed no change in total MEK1/2 levels between the static control and IFF condition

(Figure 11C). Exposure to IFF and/or AMD3100 had no effect on phosphorylated MEK1/2 (pMEK1/2) or ERK1/2 (pERK1/2) levels in Huh7 cells (Figure 11C). This lack of change in pMEK1/2 and pERK1/2 levels with IFF or AMD3100 exposure suggests that IFF is not activating MEK or ERK via CXCR4 signaling. We also verified that U0126 inhibits MEK1/2 activity by observing the loss of pERK1/2 with U0126 treatment (Figure 11C). Levels of pMEK1/2 were similar between Huh7, Hep3B, and HepG2 cells, and IFF did not show any effect on these levels compared to their respective static conditions (Figure 11D). Furthermore CXCR4 levels were measured from the lysates of Huh7 cells seeded in a collagen gel with U0126 (25 μM) and FR180204 (10 μM) inhibitor treatments, and DMSO vehicle control (Figure 11E). No change in CXCR4 levels in the Huh7 cell was observed with MEK1/2 or ERK1/2 inhibition. Similarly, there were no significant changes in secreted or intracellular CXCL12 in Huh7 cells treated with the MEK1/2 or ERK1/2 inhibitors (Figure 11F). These findings suggest that MEK/ERK signaling is involved in IFF-induced invasion, but is not upstream or downstream of CXCR4 and CXCL12. Instead, MEK/ERK may be modulating other pathways necessary for IFF-induced invasion.

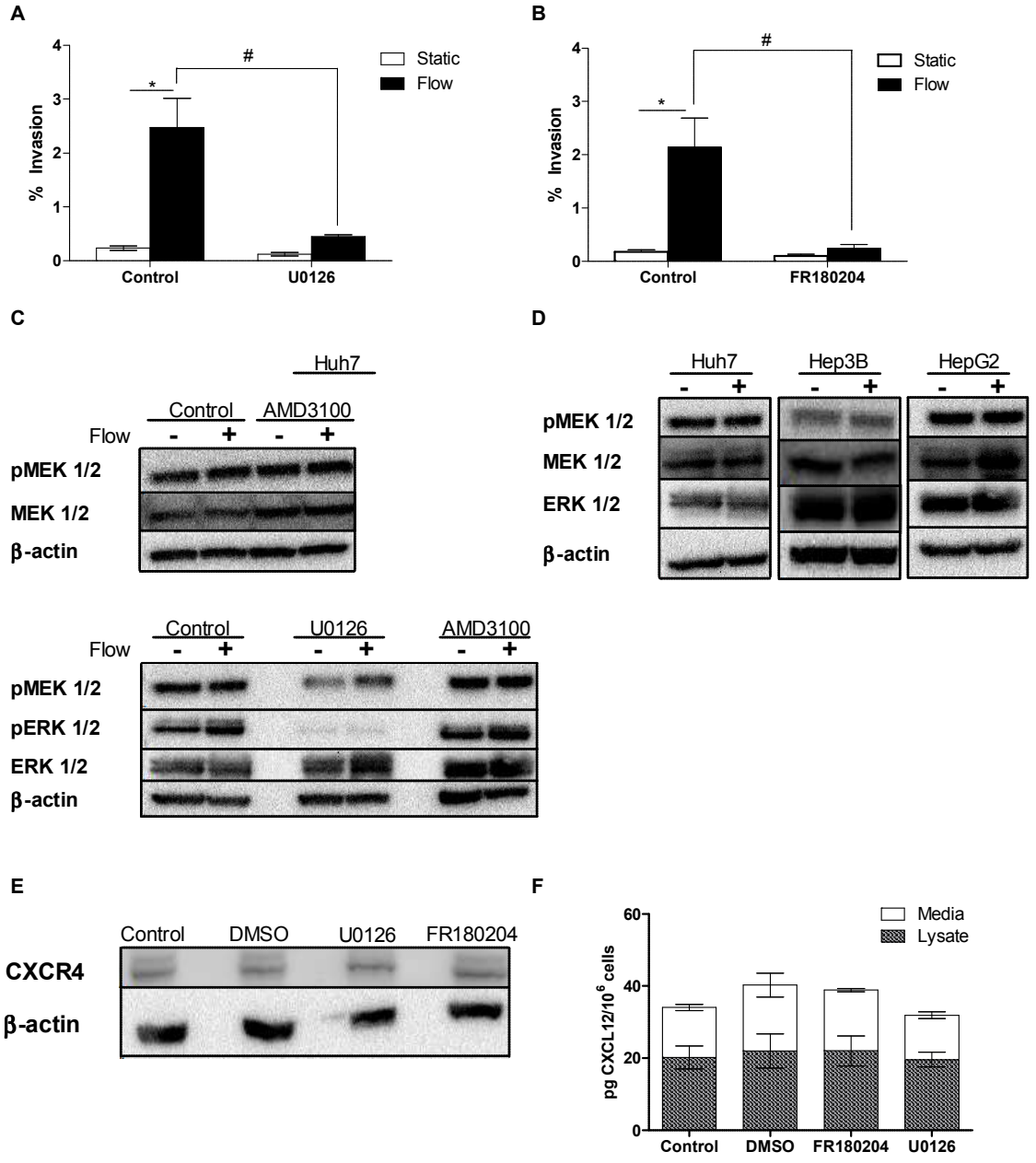


**Figure 11: MEK/ERK required for flow-induced HCC cell invasion.** (A) MEK1/2 inhibitor (U0126) at 25 μM incorporated in the 3D invasion assay with Huh7 cells (n=14). Significance between static vs. flow, * = $p < 0.05$. # = $p < 0.05$ between static vs. flow conditions of the two treatment options assessed by a two-way ANOVA. (B) ERK1/2 inhibitor (FR180204) at 10 μM incorporated in the 3D invasion assay with Huh7 cells (n=9). Significance between static vs. flow, * = $p < 0.05$. # = $p < 0.05$ between static vs. flow conditions of the two treatment options assessed by a two-way ANOVA. (C) Western blot conducted to detect the presence of total MEK1/2 protein collected from Huh7 cells under static and flow. pMEK1/2 was detected in Huh7 cells that were

incorporated in the 3D invasion assay and exposed to AMD3100. MEK1/2 and pMEK1/2 = 45kDa. pERK1/2 was detected in Huh7 cells that were incorporated in the 3D invasion assay and exposed to treatments of U0126 or AMD3100. pERK1/2 = 42/44kDa. (D) pMEK was detected in Huh7, Hep3B, and HepG2 cells. (E) Western blot conducted to detect total CXCR4 protein collected from Huh7 cells in 3D collagen gels treated with U0126, FR180204, and DMSO (vehicle control). (F) Average CXCL12 expression measured from protein of Huh7 cells seeded in 3D collage gel and treated with U0126, FR180204, and DMSO (vehicle control).

**2.4 Discussion**

IFF is slow moving fluid flow that occurs in normal tissues; however, in tumors this fluid flow is elevated, potentially driving increased cell invasion [214, 216, 235, 244, 247]. In this study we characterized the effects of IFF determined this response to fluid flow was velocity-dependent, and there was a positive relationship between IFF velocity and Huh7 cell invasion (Figure 8). Furthermore, our findings indicate that our static condition has similar invasion percentage to a low flow condition, suggesting a static condition is not very different from low physiological IFF from an invasion standpoint. Tumor interstitial pressure has been shown to create steep pressure gradient between the tumor and stroma that drives elevated IFF [144, 223]. Tumor pressure in the liver has been observed to be a reliable prognostic factor and useful tool for local recurrence for patients with tumors that were 3 cm or smaller in size [272]. Computational models have predicted IFF velocities between 0.1 – 6.0 μm/s under various conditions [181]. IFF velocity in mice with $VEGF_{165}$-expressing tumors was measured to be 0.1 - 0.5 μm/s, and even greater velocities (1.0 – 8.0 μm/s) were observed in mice with human cervical carcinoma and melanoma xenografts [145, 146]. *In vivo* IFF velocities in cervical cancer patients with pelvic lymph node metastases were measured to be between 10 – 55 μm/s [146]. The fluid velocity observed in our system was on the lower end compared to some previous *in vivo*

findings mentioned previously, however the corresponding invasion results in the short 6 hour period in our system were significantly increased. The standard invasion assay with Huh7 cells in a collagen and Matrigel matrix for 24 hours resulted in a higher overall average invasion than the Huh7 cells in the 6 hour collagen only matrix invasion assay with high fluid flow. This elevated velocity could increase cell invasion in a variety of ways, cell-secreted proteins are capable of forming gradients at interstitial flow velocities as high as 6.0 μm/s with low physiological Peclet numbers *(Pe < 1.0)*. Previous work has shown that these gradients form in a bias manner as velocity increases or the diffusion coefficient of the secreted protein decreases. The formation of such gradient can provide chemotactic ques for the cells resulting in increased migration or invasion in the direction of these gradients [181]. One of the caveats in our study is that the effects of elevated IFF in our 3D invasion assay with only collagen could alter cellular adhesion properties in the Huh7 cells. The standard 3D invasion assay contains cells encapsulated in a collage and Matrigel matrix to simulate the TME. However due to the limitations in our fluid flow assay, controlling the flow velocity required the removal of Matrigel. A significant range of IFF velocities have been observed in many models and in general higher IFF velocities have been related to poor outcomes for cancer patients. The liver is an extremely vascular tissue structure, and examining the effects of IFF on HCC cells could result in novel therapies to treat and detect HCC. Understanding and characterizing the effects of fluid flow on HCC cells will allow us to better understand various stages of HCC and how this cancer type progresses.

To date, several studies have demonstrated that IFF can drive glioma, melanoma, renal, and breast cancer cell invasion [209, 213, 214, 216, 235, 247] via one of three

proposed mechanisms: IFF-induced tension transduced by cell-matrix adhesions, glycocalyx-mediated shear stress sensing and downstream upregulation of MMP, and autologous chemotaxis. In this study, we demonstrate for the first time that IFF can induce invasion of HCC cells through the formation of autologous transcellular gradients of CXCL12. Furthermore, IFF-induced invasion of Huh7 cells requires MEK/ERK activity independent of CXCR4/CXCL12 signaling. High expression of CXCR4 and CXCL12 has been observed in various carcinomas, resulting in increased cell migration and tumor angiogenesis [269, 273]. In HCC, CXCR4 and CXCL12 have been associated with variations in the cell cycle resulting in increased risk of metastasis formation in bone, and elevated levels of the chemokine enhances migration of the tumor cells [260, 262, 263]. We showed that HCC flow-induced invasion occurs through a CXCR4-dependent mechanism (Figure 9). Tumor dissemination and poor HCC prognosis have been linked to the expression of this chemokine receptor [261]. This CXCR4-dependent mechanism is not complete without the secretion of its ligand CXCL12. CXCL12, also known as stromal cell-derived factor 1 (SDF-1), has been shown to mediate important cellular processes such as chemotaxis and leukocyte trafficking [274]. We observed that CXCR4 and CXCL12 are necessary for IFF-induced invasion and that the levels of the chemokines did not change when exposed to IFF (Figure 10). The presence of CXCR4 and CXCL12 was necessary for IFF-induced invasion in HCC cells. A potential reason as to why non-HCC cells such as the PRHs did not respond to flow-induced invasion could be due to the lack or low levels of either the CXCR4 receptor or its ligand CXCL12. Previous work identified CXCR4 messenger RNA (mRNA) and protein levels in HCC tissues and cell lines, but could not detect CXCR4 in normal hepatic tissues. Similarly, CXCL12 was detectable in HCC

patients' ascites fluid but not in normal hepatic tissue [260]. No further experiments were conducted with PRHs because they did not respond to IFF; instead, we focused our efforts to uncover the molecular mechanisms of IFF-induced HCC cell invasion. Ultimately, we were unable to identify any relationship between total protein levels of CXCR4 or CXCL12 and response to IFF; however it is important to note that autologous chemotaxis does not require increased expression of the receptor or secretion of the ligand, but requires the formation of a gradient [181]. Furthermore we observed differences in IFF-induced invasion between the three liver cancer cell lines in our study. It has been observed that Huh7 and Hep3B cells, exposed to CXCL12, respond with rapid perinuclear translocation of CXCR4 while HepG2 cells do not due to a receptor defect [261, 275]. Moreover, it was also previously shown that Huh7 cells showed a strong invasive response once exposed to CXCL12, which is quite similar to our findings (Figure 10) [261]. In conclusion, we identified the CXCR4/CXCL12 signaling axis to be a significant component in IFF-induced invasion in HCC; however, this signaling was not the only mechanism involved in IFF-induced invasion of HCC cells, as shown by the presence of some IFF-induced invasion even with inhibition of CXCR4 or CXCL12 (Figure 9A and Figure 10B).

In the past twenty years, much emphasis has been placed on the Raf-MEK-ERK signaling cascade to better understand its potential therapeutic benefits for cancer therapy. The MEK/ERK signaling cascade has been observed to be highly active in HCC and shown to regulate invasion and formation of metastasis in HCC cells [26]. Recent studies investigating the molecular pathogenesis of HCC have revealed that blocking MEK/ERK signaling in HCC cells results in multiple anticancer effects such as decreased HCC cell proliferation, growth, and increased apoptosis [271]. In HCC tissue specimens, MEK/ERK

signaling has been shown to be constitutively activated in many specimens, and inhibition of the MEK/ERK pathway in our study resulted in a significant decrease of IFF-induced invasion (Figure 11A and Figure 11B) [26]. Some studies have also suggested crosstalk between CXCR4/CXCL12 activation and MEK/ERK signaling that influences cellular invasion [27]. One study demonstrated that CXCR4/CXCL12 signaling resulted in increased phosphorylation of ERK in Huh7 cells [276]. In contrast, we demonstrated that CXCR4/CXCL12 signaling did not alter the MEK/ERK pathway in our liver cell lines (Figure 11C). This could be a result of the differences in the experimental model; our studies are performed in 3D, while the previous study used cells cultured in 2D. Furthermore, we determined that MEK/ERK signaling and chemokine signaling independently altered HCC cell invasion (Figure 11E and Figure 11F). Thus, we hypothesize that IFF-induced invasion of HCC cells depends on several different mechanisms. For example, the MEK/ERK signaling cascade has been implicated in the enhanced secretion of MMPs in HCC resulting in increased cell migration and invasiveness [277, 278]. However further investigation would be required to elucidate the role of MEK/ERK signaling in IFF-induced invasion.

In this study, we elucidated CXCR4/CXCL12-dependent autologous chemotaxis as a significant mechanism involved in IFF-induced invasion of HCC cells. Additionally we identified MEK/ERK signaling as a significant contributor to IFF-induced invasion, but one that is independent of the CXCR4/CXCL12-autologous chemotaxis mechanism. However as previously mentioned, mechanisms of IFF mechanosensing are not fully understood. The formation of autologous transcellular gradients is merely one potential mechanism that cells may use to sense and respond to IFF. Another possible mechanism

involves glycocalyx shear stress sensing, where flow-induced stresses are transduced into and transmitted as solid stresses through core proteins of the glycocalyx, leading to various intracellular signaling cascades [154, 214, 215, 229]. These studies identified that IFF mechanotransduction occurs through glycocalyx heparan sulfate proteoglycans and focal adhesion FAK-ERK signaling, resulting in increased cell motility through increased MMP activity in 3D collagen gels [202]. Focal adhesion kinase (FAK) signaling to mitogen-activated protein kinase (MAPK) has been observed to be involved in migration and differentiation in HCC [101]. It may be possible that glycocalyx-mediated IFF sensing in HCC could occur through signaling of FAK to MAPK activation resulting in increased cell motility. This may be a potential mechanism since we observed MEK/ERK signaling, an important constituent in IFF-induced invasion in HCC, but could not identify any relationship to our CXCR4/CXCL12 results. Additionally we observed CXCR4 inhibition with AMD3100 did not completely eliminate HCC-flow induced invasion (Figure 9A). CXCL12 could also act through an auxiliary receptor such as syndecan-4 (SDC-4), a transmembrane heparan sulfate proteoglycan that has been shown to regulate the migration response of HCC cells to CXCL12 gradients [276]. Alternatively, IFF could also induce invasion through mechanisms entirely independent of CXCR4/CXCL12. Previous studies have shown that IFF stimulated upstream invasion (against the direction of flow) of breast cancer cells through activation of integrins and focal adhesion reorganization and polarization [214, 245]. Given the nature of our 3D flow invasion assay and study, we only measured downstream invasion; invasion in the opposite direction would not be captured by our transwell system. Since the changes we observed resulted in increased invasion in the direction of IFF, we can also conclude that the mechanisms at play are likely separate

from any induction of upstream invasion, since we are explicitly not quantifying that component of the invasion response.

In conclusion, we demonstrated that IFF is a critical factor in HCC invasion, and potentially drives invasion through two separate signaling pathways. First, we show that HCC cells invade in response to IFF via a CXCR4/CXCL12-dependent mechanism. Our findings suggest that this occurs through autologously generated pericellular gradients due to HCC cell-secreted CXCL12 and IFF, corroborating previous studies of the autologous chemotaxis mechanism [181, 209, 213, 235]. Second, we have evidence that the MEK/ERK pathway plays a critical role in IFF-induced HCC invasion, but one that is not downstream of CXCR4/CXCL12. Our study provides a better understanding of how biomechanical forces like IFF can alter signaling pathways that drive HCC invasion, and may potentially provide a basis for investigating new therapeutic strategies for HCC. Ultimately, the goal is to reduce HCC invasion and prevent HCC from spreading intraphepatically or metastasizing to other organs. We have shown some HCC cells become invasive upon exposure to this subtle fluid flow, and identifying these specific cells that respond strongly to flow could result in new therapeutic strategies to prevent invasion. Based on our study, it is evident that biomechanical forces such as IFF can affect HCC cell invasion. However, in order to better understand the role of mechanical forces within the tumor microenvironment, the development of complex *in vitro* models is required along with a greater understanding of how cellular machinery is utilized to sense and react to these micro-environmental changes.

# CHAPTER 3: MMP-2 AND MMP-9 ACTIVITY PROMOTES INTERSTITIAL FLOW-INDUCED INVASION OF HEPATOCELLULAR CARCINOMA CELLS

## 3.1 Introduction

The poor prognosis for HCC patients is attributed to the difficulties in early detection and limited treatment options once diagnosed. Consequently the World Health Organization has ranked HCC to be the second leading cause of cancer-related deaths worldwide. The high mortality rate associated with liver cancer requires a greater fundamental and mechanistic understanding of hepatocyte transformation and tumor progression. Traditional approaches for examining tumor cell behavior has often focused on investigating the various genetic components that have been dysregulated. However, recent studies have shown the interactions between the tumor cells and surrounding microenvironment aid in HCC progression, tumor growth, and survival [44, 73, 90, 279]. These findings have shifted the focus from systemic chemotherapies to the investigation and development of drugs that target tumor-stromal interactions in order to improve the overall survival of patients with advanced HCC [43].

The dynamic interactions between tumor cells and their constantly evolving microenvironment has been observed to be a critical component for tumor progression. A significant number of studies have shown that changes in biomechanical forces within the TME such as solid stresses [257], fluid pressure [146], and fluid flow [154, 214, 215, 218] alter cancer progression [223, 258]. Previous research has demonstrated that interstitial fluid flow (IFF), one of the biomechanical forces that is altered during tumor growth, can promote cancer cell invasion [209, 245], alter stromal fibroblast behavior [216], and increase MMP secretion [218].

MMPs have been identified as key contributors to changes in the tumor microenvironment during cancer progression [130, 134]. To date, 23 human MMPs categorized by their architecture into 5 main subtypes have been identified. These zinc-dependent endopeptidases are capable of modulating various cancer signaling pathways to promote cancer cell migration, invasion, survival, and ultimately cancer progression. Of the 23 different human MMPs, we hypothesized specifically the gelatinase MMPs, MMP-9 and MMP-2, are involved in flow-induced HCC invasion. Recent literature has elucidated MMP-9 and MMP-2 in HCC to alter invasiveness of tumor cells along with variety of cell functions [280, 281]. MMP-9 secretion has been observed to be increased in HCC via the MEK/ERK, PI3K/Akt, PTEN, and NF-κB signaling pathways, resulting in increased cell migration and invasion [277, 278, 282, 283]. Inhibition of MMPs has been a therapeutic focus for various cancer types, including HCC, and has been shown to provide many anti-metastatic effects [281]. Therefore, the overall goal of this study was to elucidate the contribution of MMPs in IFF-induced HCC cell invasion. We hypothesized that IFF would increase expression of MMP-9 and MMP-2, to promote flow-induced HCC invasion. Our findings indicate IFF does not increase total protein expression of MMP-9 and MMP-2, but instead enhances MMP-9 and MMP-2 activity promoting flow-induced HCC cell invasion. For the first time we demonstrated that MMP-9 and MMP-2 are involved in flow-induced HCC invasion.

## 3.2 Methods

*Cell Culture*

Hepatoma-derived Huh7 were cultured in RPMI 1640 with L-glutamine (Cellgro, Manassas, VA) supplemented with 10% FBS (Atlanta Biologicals, Atlanta, GA) and 1% penicillin/streptomycin (Mediatech, Herndon, VA). The Huh7 cells were maintained in a humidified 37˚C environment with 5% $CO_2$.

*3D Interstitial Flow Invasion Assay*

The Huh7 cells ($5.0 \times 10^5$ cells/ml gel) were encapsulated in a gel comprised of 1.3 mg/ml rat tail tendon type I collagen (BD Biosciences, San Jose, CA) and 1 mg/ml Matrigel (BD Biosciences) and seeded into 12 mm diameter, 8 μm pore diameter culture inserts (Millipore, Bellerica, MA). Static and flow conditions were generated over the course of 24 hours by following a previously described method [209, 216, 267]. For the static condition, the level of basal medium outside of the transwell was level with the medium inside the transwell, resulting in little to no hydrostatic pressure difference. The IFF condition was created by adding more basal medium to the inside of that transwell than the outside, resulting in a hydrostatic pressure difference of approximately 1 mm Hg. This drove IFF through the collagen gel, with an average velocity of approximately 0.05 – 0.1 μm/s (based on average volumetric flow rate and the cross-sectional area of the gel). This velocity is on the lower end of velocities measured in or modeled for tumors, but much higher than the IFF velocities predicted for normal hepatic lobules [145, 146, 268]. Cells that transmigrated through the porous membrane were fixed with 4% paraformaldehyde (Sigma-Aldrich, St. Louis, MO) and stained with DAPI (2 μg/ml, MP Biomedicals, Santa

Ana, CA). Fixed and stained cells were imaged by fluorescence microscopy. Both static and flow conditions were analyzed by counting five locations on the fixed membranes. Percent invasion was calculated with the following equation:

$$\%\ Invasion = \left[\frac{(Average\ cell\ count) * (Membrane\ surface\ area)}{(Image\ area) * (Number\ of\ cells\ seeded)}\right] * 100$$

For specific experiments, pharmacological inhibitors were added to the cell/gel mixture before gel polymerization and in the media used for the experiment at their respective target concentrations. For MMP inhibition, a pan-MMP inhibitor, GM6001 (50 μM) (EMD Millipore, Billerica, MA), was utilized in the 3D invasion assay. SB-3CT (25 μM) (Selleckchem, Houston, TX) was utilized for specific MMP-2 and MMP-9 inhibition, as previously shown [284, 285]. Cell viability from the inhibitor treatments was quantified with the commercially available LIVE/DEAD cell viability assay (Molecular Probes, Eugene, OR) on Huh7 cells in 3D conditions.

*CXCL12 Chemotaxis Assay*

Huh7 cells (5.0 x $10^5$ cells/ml gel) were added to the same type of gel and cell-culture inserts used for the 3D flow invasion assay. To determine if CXCL12 could stimulate invasion while inhibiting MMP-9 and MMP-2 the cells were exposed to a gradient of recombinant human CXCL12 (80 ng/ml) with or without SB-3CT (25 μM) added to the gel and/or medium. Cells were placed in their respective treatment conditions for 24 hours at 37˚C with 5% $CO_2$. Cells that migrated through the membrane of the cell-

culture insert were fixed and stained. Invasion was quantified following the same method described for the 3D flow invasion assay.

*Enzyme-linked immunosorbent assay (ELISA)*

Cell lysates and basal medium were collected from Huh7 cells that were utilized for our 3D invasion assay. First cells were digested out of the gels with collagenase D (0.5625 U/ml, Roche Life Science, Indianapolis, IN) for 45 minutes and then centrifuged for 10 minutes at 1,000 RPM. Cells were lysed with RIPA buffer containing protease inhibitors. Basal medium from their respective static or flow conditions was pooled together and concentrated using Amicon Ultra-15 centrifugal filter units (EMD Millipore, Billerica, MA). MMP-9, MMP-2, TIMP-1, and TIMP-2 levels were quantified using a commercially available DuoSet ELISA kit (R&D Systems, Minneapolis, MN). Standard curves were generated using known concentrations of the supplied recombinant human protein and data were fit with a four parameter logistic curve in MATLAB (MathWorks, Natick, MA).

*Gelatin Zymography of MMP-2 and MMP-9 Activity*

Gelatinase activity was measured by performing electrophoresis of protease samples in denaturing and non-reducing conditions. For 3D samples, cells were first digested out of the gels with collagenase D (0.5625 U/ml, Roche Life Science, Indianapolis, IN) for 45 minutes and then centrifuged for 10 minutes at 1,000 RPM. Cells were lysed with RIPA buffer without any protease inhibitors. A commercial protein quantification assay (Pierce BCA Protein Assay Kit, Thermo Fisher Scientific, Waltham,

MA) was utilized to quantify protein in order to better normalize the samples for the zymogram. Samples were prepared in at a 1:1 ratio of 2X SDS loading buffer to lysate without any boiling. Lysates were ran in non-reducing conditions on Novex 10% tris-glycine zymogram gelatin gels (Thermo Fisher Scientific, Waltham, MA) with 1X tris-glycine SDS run buffer. Once completed, the gels were placed in 1X renaturing buffer (Thermo Fisher Scientific, Waltham, MA) for 30 minutes, followed by 1X developing buffer (Thermo Fisher Scientific, Waltham, MA) over night at 37ºC. Zymogram gels were stained with SimplyBlue Safestain (Thermo Fisher Scientific, Waltham, MA) for 1 hour at room temperature. Zymogram imaging was conducted with a FluorChem M imaging system (Proteinsimple, San Jose, California) and quantified with ImageJ 1.51 (National Institutes of Health (NIH), Bethesda, Maryland). MMP activity levels were normalized to the respective matrix conditions and densitometry was used to determine fold change resulting from exposure to flow.

*Statistical Analysis*

All data are presented as mean ± SEM. All results for invasion and chemotaxis assays are based on a minimum of two independent experiments with sample size $n \geq 3$ for each experiment. Statistical significance between two groups was determined by conducting a Student's t-test. For three or more groups, one or two-factor ANOVA with a Bonferroni or Tukey's multiple comparison test was utilized. GraphPad Prism 5 (San Diego, CA) was used to perform statistical analyses.

## 3.3 Results

*MMPs contribute to flow-induced HCC invasion*

MMPs have been recognized as significant contributors to tumorigenesis, and they serve as major non-cellular modulators of the TME in various carcinomas. These proteolytic enzymes are most often observed to contribute to the remodeling of the ECM, in turn promoting migration and invasion in most cancer types [57, 130, 198, 277, 283]. Therefore, we hypothesized that MMPs could enhance IFF-induced HCC invasion. To block MMP activity, GM6001 (50 μM) a broad spectrum MMP inhibitor, was incorporated into the 3D invasion assay. The inhibition of MMPs with GM6001 resulted in a 3.2 fold decrease in flow-induced invasion (Figure 12A). Furthermore to verify the concentration of GM6001 was not inflicting any cytotoxic effects on the Huh7 cells, a commercial cell viability assay was conducted on Huh7 cells and no significant cell death was observed (Figure 12B). Our results indicate that MMPs could play a key role in flow-induced HCC invasion.

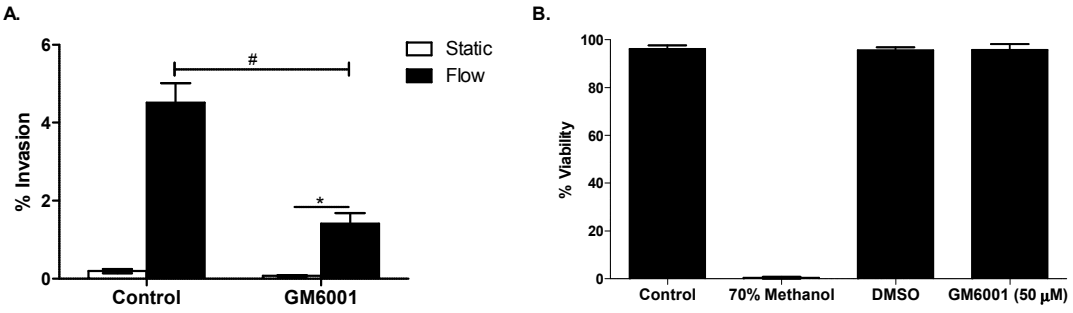


**Figure 12: MMPs involved in flow-induced invasion.** (A) GM6001 (50 μM), a broad spectrum MMP inhibitor reduces IFF-induced invasion in Huh7 cells. (n=12). * = $p < 0.05$ between each respective treatment condition. # = $p < 0.05$ between static vs. flow conditions of the two treatments assessed by two-way ANOVA. (B) LIVE/DEAD cell viability assay conducted on Huh7 cells in a 3D conditions to determine cytotoxic effect of inhibitors and their chose concentrations. (n = 3).

*The gelatinase MMPs regulate flow-induced HCC invasion*

To specifically block MMP-9 and MMP-2 activity, SB-3CT (25 μM), a selective gelatinase inhibitor, was incorporated into the 3D invasion assay [284, 285]. This resulted in nearly a complete cessation of flow-induced invasion in the Huh7 cells (Figure 13A). Verification of cell viability of Huh7 cells treated with SB-3CT (25 μM) was conducted with a commercial LIVE/DEAD cell viability assay and confirmed no significant cell death from the inhibitor treatment (Figure 13B). Overall these findings implicate MMP-9 and MMP-2 specifically as their inhibition results significant decrease in flow-induced invasion.

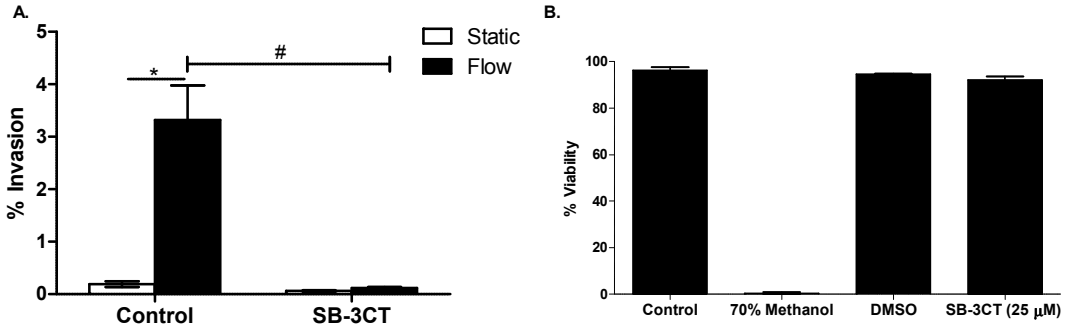


**Figure 13: MMP-9 and MMP-2 inhibition significantly reduces IFF-induced Huh7 invasion.** (A) SB-3CT (25 μM), specific inhibitor for the gelatinase MMPs, MMP-9 and MMP-2, significantly reduces IFF-induced invasion in Huh7 cells. (n=6). * = $p < 0.05$ between each respective treatment condition. # = $p < 0.05$ between static vs. flow conditions of the two treatments assessed by two-way ANOVA. (B) LIVE/DEAD cell viability assay conducted on Huh7 cells in a 3D conditions to determine if there is a cytotoxic effect of the inhibitors at experimental concentrations. (n=3).

*CXCL12-mediated chemotaxis is not affected by MMP-9 and MMP-2 inhibition*

Our previous findings of autologous chemotaxis as mechanism for IFF-induced HCC invasion suggests that Huh7 cells secrete the chemokine CXCL12, and subsequent

transport by IFF generates a pericellular chemokine gradient [286]. Functional testing with a CXCL12 neutralizing antibody and oversaturation of the CXCR4 receptors with exogenous CXCL12 highlight the significance of this gradient component in the autologous chemotaxis mechanism [286] (Figure 10). To determine if MMP-9 and MMP-2 contribute to the autologous chemotaxis mechanism, we conducted a chemotaxis assay incorporating SB-3CT. In the presence of a CXCL12 gradient (80 ng/ml), Huh7 cells were nearly 1.5 fold more invasive (Figure 14). In the absence of CXCL12 with inhibition of MMP-9 and MMP-2, Huh7 cells were less migratory. Simultaneously blocking MMP-9 and MMP-2 with the presence of a CXCL12 gradient suggest that the Huh7 are capable of chemotaxis under MMP-9/2 inhibition. Therefore, suggesting inhibition of MMP-9 and MMP-2 is not tied to our earlier findings of chemokine-dependent autologous chemotaxis.

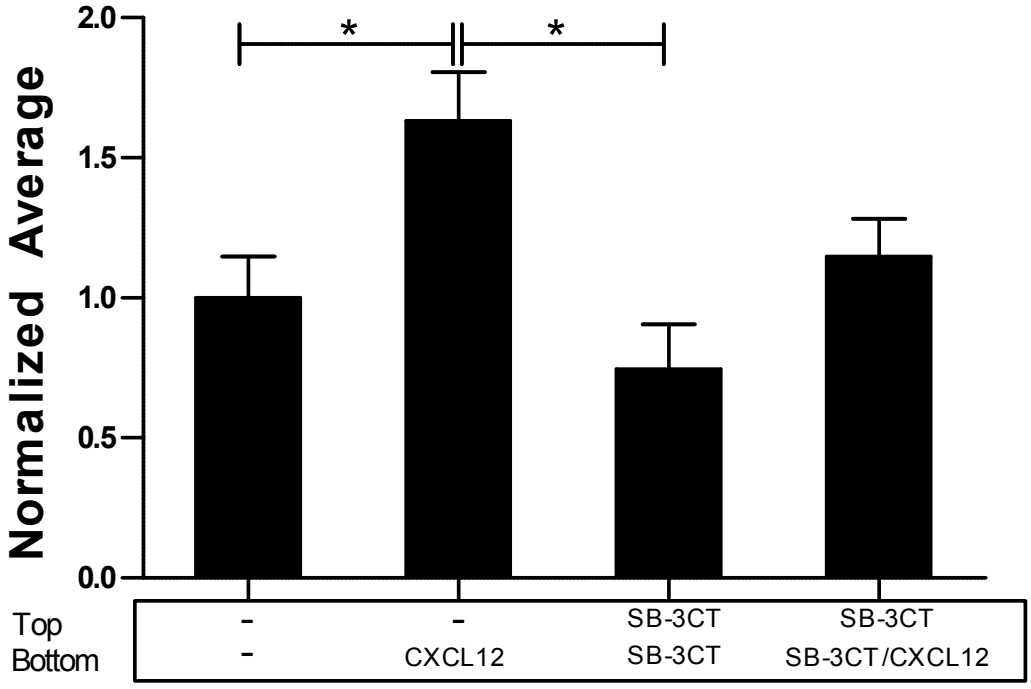


**Figure 14: Huh7 cells chemotact in response to CXCL12 irrespective of inhibition of MMP-9 and MMP-2.** Chemotaxis assay conducted on Huh7 cells in static environment

(n=15). Exogenous CXCL12 – 80 ng/ml. SB-3CT (25 μM). Top or Bottom = location of CXCL12 or SB-3CT added to Boyden chamber. Test condition: - = no exogenous CXCL12 present; CXCL12 = exogenous CXCL12 added; SB-3CT = SB-3CT added; and SB-3CT/CXCL12 = both exogenous CXCL12 and SB-3CT added. Invasion results normalized to control condition with no exogenous CXCL12 or SB-3CT. * = $p < 0.05$ between respective conditions.

*IFF does not modulate MMP-9 and MMP-2 protein levels*

IFF has been shown to upregulate MMP protein levels by shear stress sensing via the glycocalyx in various cell types such as metastatic renal carcinoma cells, fibroblasts, vascular smooth muscle cells, myofibroblasts, and dermal fibroblasts co-cultured with tumor cells [172, 184, 216-218]. Here we hypothesized that IFF-induced HCC invasion was a result of increased MMP expression and secretion resulting in degradation of the ECM to promote invasion. Therefore we quantified the expression and secretion of MMP-9 and MMP-2 with via ELISA. Cell lysates and basal medium (concentrated) from our 3D invasion assay were collected to quantify the amount of secreted MMP-2 and MMP-9 representing intracellular and cell-associated MMP levels. Our results indicate that IFF does not alter the intracellular/cell-associated expression or secretion of either MMP-9 or MMP-2 (Figure 15). Notably, the overall amount of MMP-2 is nearly 100X greater than MMP-9 in the cell lysates and basal medium (Figure 15B).

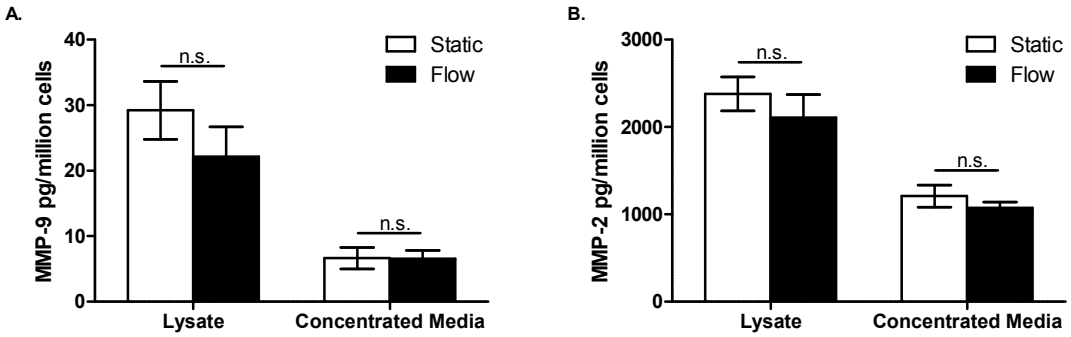


**Figure 15: IFF does not alter MMP-9 or MMP-2 expression or secretion Huh7 cells.** (A) Average MMP-9 expression in 3D cell lysates and basal medium (concentrated) collected from 3D invasion assay (lysate and medium, n=3). n.s. = no significant difference. (B) Average MMP-2 expression in 3D cell lysates and basal medium (concentrated) collected from 3D invasion assay (lysate and medium, n=3). n.s. = no significant difference.

*IFF increases MMP-9 and MMP-2 activity*

A variety of MMPs and their inhibitors are often expressed in the TME, however their respective activation or inhibition is quite complex. The local balance of these MMPs with their respective inhibitors is a determining factor in net MMP activity and may ultimately affect tumor progression. The expression of these MMPs have been observed in a variety of carcinomas, but more important is their activation. Recently mechanical forces in the TME have been shown to be regulatory factors in MMP activity by promoting proteolytic degradation of the ECM [287, 288]. Therefore, we investigated the effects of IFF on MMP-9 and MMP-2 activity by gelatin zymography. Cell lysates and media (supernatants) were collected from Huh7 cells exposed to IFF. Zymogram results indicate that cell lysates from Huh7 cells exposed to IFF have greater MMP-9 and MMP-2 activity compared to their static counterparts (**Figure 16**A). A noticeable increase in both the latent (pro form) and active form of both MMPs is observed for cells exposed to IFF; nearly a 1.4 fold increase in MMP-9 and 2.3 fold increase in MMP-2 activity (**Figure 16**C).

Conversely, IFF did not increase MMP-2 or MMP-9 activity from the concentrated media samples. However a noticeable difference was observed in the presence of pro-MMP-2 compared to its active form, but there was no difference between static vs. flow conditions (**Figure 16**B and D). Overall these results indicate that IFF does not increase expression of MMP-9 and MMP-2, but does enhances MMP-9 and MMP-2 activity in cell lysates, which in turn may increase invasion of cells exposed to IFF.

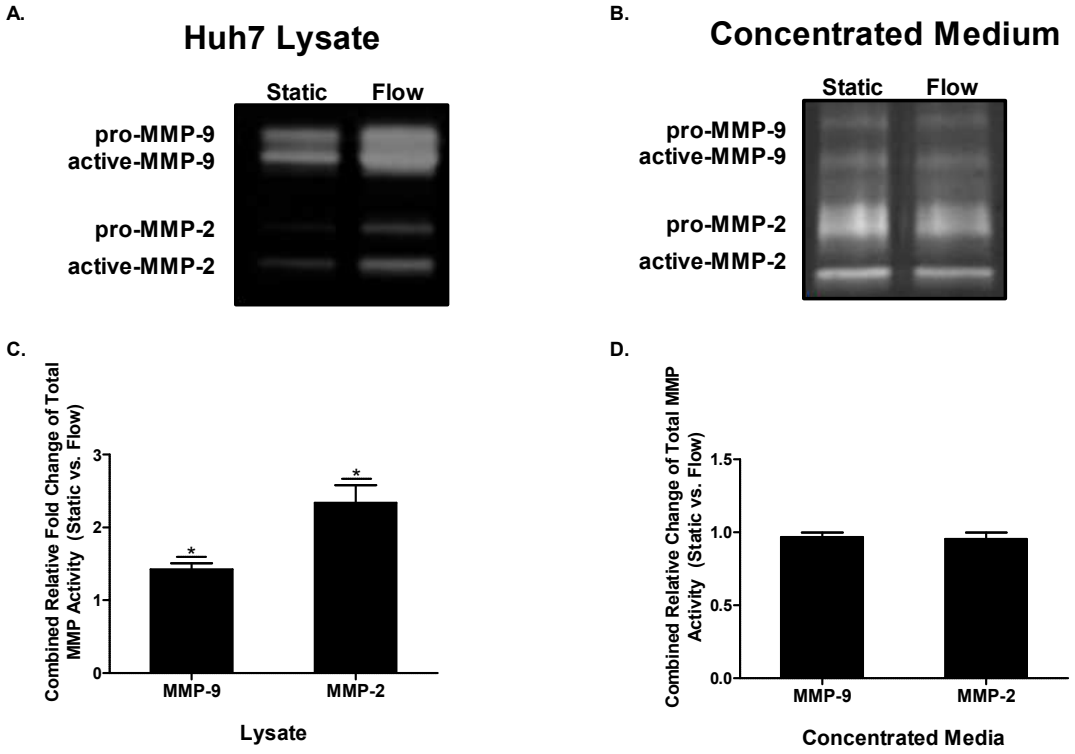


**Figure 16: Exposure to IFF results in greater MMP activity in Huh7 cells.** (A) Representative gelatin zymogram of MMP-9 and MMP-2 activity in Huh7 cells exposed to IFF (n = 6). Pro-MMP-9 = 92 kDa, active-MMP-9 = 87 kDa, pro-MMP-2 = 72 kDa, and active-MMP-2 = 66 kDa. (B) Representative gelatin zymogram of MMP-9 and MMP-2 activity from concentrated basal medium (n = 2). Pro-MMP-9 = 92 kDa, active-MMP-9 = 87 kDa, pro-MMP-2 = 72 kDa, and active-MMP-2 = 66 kDa. (C) Densitometry of zymogram results of the cell lysate samples (n = 6). Combined average relative fold change of total MMP activity (static vs. flow). Sum of pixel density of flow condition (pro-MMP + active-MMP) divided by the sum of pixel density of respective static condition (pro-

MMP + active-MMP). Averaged for each zymogram. * = $p < 0.05$, one sample T test. (D) Densitometry of zymogram results of concentrated basal medium samples (n = 2). Combined average relative fold change of total MMP activity (static vs. flow). Sum of pixel density of flow condition (pro-MMP + active-MMP) divided by the sum of pixel density of respective static condition (pro-MMP + active-MMP). Averaged for each zymogram.

*IFF does not alter TIMP levels to promote flow-induced HCC invasion*

Tumor and stromal cells secrete MMPs promoting tumor cell invasion from the increased enzymatic activity. Proteolytic activity of MMPs is inhibited by tissue inhibitors of metalloproteinases (TIMPs) at a 1:1 ratio of TIMP to active MMP. This balance of MMPs to TIMPs is important in regulating remodeling of the ECM architecture. Therefore, we examined the TIMP-1 and TIMP-2 levels in Huh7 cells exposed to IFF. We determined that TIMP-1 levels from the cell lysate and concentrated medium did not change in cells exposed to IFF (Figure 17A). There was no significant difference in TIMP-2 levels between the two conditions in either the cell lysate or concentrated medium (Figure 17B). However, it was noted that there was a significant difference in TIMP-2 levels between the concentrated medium and cell lysate for Huh7 cells exposed to IFF (Figure 17B). These findings suggest that the IFF-induced increase in MMP-2 and MMP-9 activity is not due to modulation of TIMP-1 and TIMP-2 levels in response to IFF.

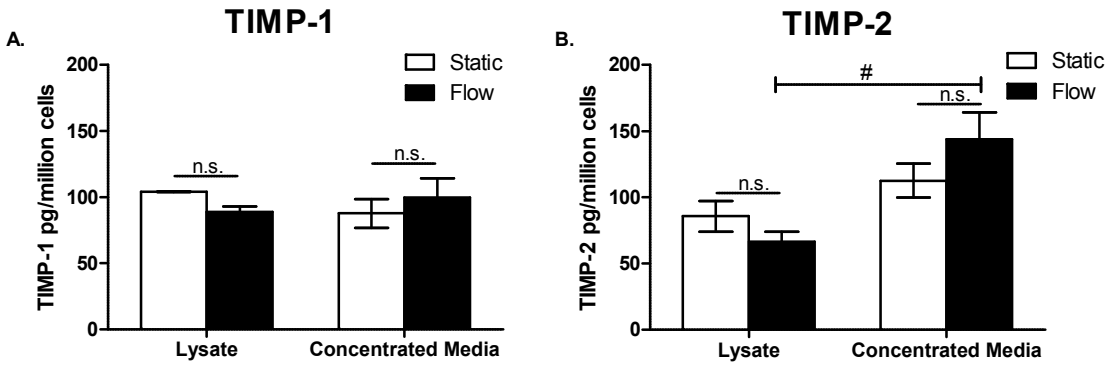


**Figure 17: TIMP-1 and TIMP-2 expression in Huh7 cells and respective medium.** (A) Average TIMP-1 expression in 3D cell lysates and basal medium (concentrated) collected from 3D invasion assay (lysate and medium, n=2). n.s. = no significant difference. (B) Average TIMP-2 expression in 3D cell lysates and basal medium (concentrated) collected from 3D invasion assay (lysate and medium, n=3). n.s. = no significant difference. # = $p < 0.05$ between lysate and concentrated basal medium from the flow condition assessed by two-way ANOVA.

### 3.4 Discussion

In this study we uncovered that IFF is capable of increasing MMP-9 and MMP-2 activity in Huh7 cells. These findings suggest that MMP-9 and MMP-2 are necessary and play an integral role in IFF-induced HCC invasion, but are not directly involved in the previously elucidated autologous chemotaxis mechanism [286], as Huh7 cells treated with a selective MMP-9 and MMP-2 inhibitor are still invasive in the presence of an exogenous CXCL12 gradient. Furthermore, these findings also indicate the expression levels of either MMP-9 or MMP-2 cannot be correlated to flow-induced invasion, rather the MMP activity is enhanced when cells are exposed to IFF. Finally, natural inhibitors of activated MMPs, both TIMP-1 and TIMP-2 levels are not altered due to IFF. These findings suggest that IFF disturbs the balance of MMPs and TIMPs, as TIMP-1 nor TIMP-2 are increased to mitigate the imbalance of ECM enzymes. These results ultimately highlight the importance of MMP-9 and MMP-2 in HCC flow-induced invasion and provides the basis for another

potential mechanism that may regulate IFF-induced invasion or effect a cells ability to invade.

MMPs were not of much interest to researchers until the 1960s when they were observed to be upregulated in inflammatory diseases like rheumatoid arthritis and cancer. MMPs have been observed to play a critical role in cancer; primarily they are known for their roles in ECM remodeling [289]. In pathological cases like fibrosis, the balance of MMPs to their natural inhibitors, TIMPs, is crucial in regulating matrix production and degradation. These zinc-dependent endopeptidases play a critical role in the TME and promote HCC tumorigenesis by modulating various cancer signaling pathways [130]. Recently, mechanical forces in the TME have been shown to be regulatory factors in MMP activity by promoting proteolytic degradation of the ECM [287, 288]. Shear stress generated by IFF has been shown to directly upregulate MMPs in glioma cells promoting cell motility and ultimately tumor progression [218]. IFF has been shown to induce differentiation in fibroblast and increase MMP secretion, which indirectly promotes tumor cell migration via matrix priming [216, 221].

Our current results indicate that IFF does not increase MMP-9 or MMP-2 expression in HCC cells, but rather increases activity of these MMPs (Figure 15). These findings differ from some of the current literature that has shown exposure to fluid flow shear stresses on glioma cells resulted in decreased MMP-2 expression and in rat aortic smooth muscle cells suppressed MMP-2 activity, but upregulated MMP-1, reducing migration [172, 218, 290]. Tarbell and colleagues have proposed a mechanism with heparan sulfate proteoglycan-mediated FAK activation is responsible for flow-induced mechanotransduction. In this mechanism, MMP expression is increased via IFF that is

sensed by the components of the glycocalyx and transduced into a biochemical signal in turn activating the FAK-ERK-c-Jun signaling axis to promote vascular cell motility [198, 202]. While our findings do not match up with some of Tarbell and colleagues work, it is important to note the significant differences in experimental set up, length of fluid flow exposure, and observation of MMP activity. The Darcy flow experimental apparatus possesses constant hydrostatic pressure to drive fluid flow, generating shear stress on the cells which is substantially different than the 3D flow invasion assay our experiments utilized. The use of Boyden chambers is a commonality that is observed for the 3D *in vitro* conditions in both this and Tarbell's experimental set-up; however, the incubation periods for the cell/gel suspensions and length/magnitude of flow exposure vary tremendously. The Boyden chambers are decoupled from the Darcy flow apparatus and incubated in a static environment with medium containing a chemoattractant for 48 hour and eventually cell migration and protein expression are quantified [218]. This is substantially different from the 3D invasion assay set up utilized in this study as cell invasion, protein expression, and activity were quantified immediately after 24 hours exposure to IFF to determine specifically the effects of IFF. Gel compaction and cell viability were not of concern as they were in the Tarbell study due to the magnitude of shear stresses that were applied. Thus explaining the differences in our findings and suggesting proteolytic activity of MMPs is specific and in response to IFF.

Recent HCC studies have implicated specifically MMP-9 and MMP-2 to alter invasiveness of tumor cells along with variety of cell functions [280, 281]. A noteworthy difference that was observed in this study was the difference in MMP levels in the Huh7 cells; nearly 100X more MMP-2 compared to MMP-9. This elevated level of MMP-2 is

also observed in humans with fibrosis, which could correspond to the high levels we observed since most HCCs develop in underlying cases of chronic liver injury [291]. Many studies have shown that stromal cells are the major source of MMPs, which could explain why we did not observe increased levels of MMP in our single cell system [130]. Our major finding in this study was the difference in MMP-9 and MMP-2 activity in cells exposed to IFF (Figure 16). Notably, we observed increased pro and active forms of both MMPs in Huh7 cells exposed to IFF. This increased activity is not due to the presence of more MMP nor TIMP expression. The increased MMP-9 and MMP-2 activity could be due to the localization of MMPs on the cell surface in response to IFF. Future studies are required to examine the effects of the SB-3CT inhibitor on MMP-2 and MMP-9 activity levels via gelatin zymography; this would further confirm the role of these two MMPs in flow-induced invasion and validate the specificity of the inhibitor. Alternatively, MMP-2/9 have the potential to promote HCC cell invasion from the release of growth factors, cytokines, and angiogenic factors from proteolytic processing of ECM proteins [292-294]. Additionally, extracellular proteolysis can activate or inactivate cell surface receptors such as cytokines, chemokines, and growth factors. The processing of these cell surface proteins can cause intracellular signal transduction triggering irreversible changes to tumor cell behavior by altering cell growth, survival, migration, and invasion; ultimately resulting in disease progression [130, 294, 295]. Utilizing antibodies for specific cell surface receptors with IF/ICC techniques and fluorescent microscopy, future studies would quantify changes to these surface receptors in wildtype and MMP knockdown HCC cells. Standard ELISA assays could accurately quantify the release of various growth factors and cytokines into the ECM post-proteolysis. Localization or compartmentalization of MMPs triggers an

imbalance in MMP: TIMP ratio, and the presence of IFF could generate a gradient of soluble factors that activate the MMPs. Additionally TIMP-2 possesses unique characteristics as it is observed to be both an MMP inhibitor and activator of MMP-2 at low to moderate levels. We observed such levels of TIMP-2 in the concentrated medium which could explain the significantly high MMP-2 levels. Notably, Qazi and Tarbell, observed increased MMP-1 and MMP-2 activity in highly metastatic renal carcinoma cells and the upregulation of these MMPs and cell adhesion molecules was mediated by the glycocalyx components which ultimately regulated flow-enhanced migration [217]. Further investigation into components that regulate cell adhesion such as integrins and E-cadherin are essential to determine the effect of IFF on cell invasion and MMP-9/-2 activity.

In this study we determined MMP-2/9 to play a critical role in flow-induced HCC invasion as the activity of the gelatinases increased with IFF exposure. However the outstanding question that remains is how IFF is increasing MMP-2/9 activity in the Huh7 cells. One likely candidate would be the transmembrane MMP, MT1-MMP, which has been shown to activate various pro-MMPs via pro-MMP-2/13 activation, which results in the cleavage of various ECM proteins [296, 297]. MT1-MMP also plays a crucial role in maintaining ECM turnover of various collagens, fibronectin, laminin, and even proteoglycan; however, it plays a crucial role in the progression of various cancer types, including HCC [298-300]. In HCC, MT1-MMP has been observed to play a critical role in intrahepatic spread by promoting cell survival while playing a prominent role in matrix degradation to increase invasion [301]. MT1-MMP is one potential lead worth investigating in the 3D fluid flow assay considering the significantly elevated levels of

MMP-2 that were detected in this study. Based on our initial findings of MMP-2 levels, I hypothesize that MT1-MMP would be upregulated in HCC cells exposed of IFF via MMP-2, further enhancing HCC invasion. Profiling and quantifying RNA expression of MT1-MMP along with western blotting to determine expression levels under fluid flow would provide a foundational understanding regarding this membrane MMP. Alternatively, it is well known that ECM proteolysis can result in the release of bioactive compounds that can activate the latent gelatinases. Thrombin and activated protein C have been observed to be activators for pro-MMP-2, while plasmin, trypsin, and activated MMP-2/3/13 can activate pro-MMP-9 [294, 295]. Therefore, future studies would quantify the levels of these compounds in the presence of IFF to determine if bioavailability and bioactivity is altered in the presence of fluid flow resulting in increased MMP-2/9 activity.

Previously, we demonstrated CXCR4/CXCL12 mediated autologous chemotaxis as a mechanism for flow-induced invasion. One of the major components of this mechanism is the presence of a CXCL12 gradient that is detected by the HCC cells. Utilizing a chemotaxis assay, we observed Huh7 cells were still invasive even when MMP-9 and MMP-2 signaling was inhibited. These findings show that MMP-9 and MMP-2 were not involved in the elucidated autologous chemotaxis mechanism, but played a separate role in flow-induced invasion. Future studies are required to investigate the various signaling pathways that may be involved in this increased MMP-9 and MMP-2 activity. MMP secretion has been observed to be increased in HCC via the MEK/ERK, PI3K/Akt, PTEN, and NF-κB signaling pathways, resulting in increased cell migration and invasion [277, 278, 282, 283]. These studies could be conducted with the 3D flow assay and with western blot, we could determine signaling pathways that are involved. Identifying a

relationship with any of these signaling pathways and increased MMP-9/2 activity in response to IFF could result in an effective therapeutic strategy to limit HCC cell invasion and metastasis.

# CHAPTER 4: THE SYNERGISTIC RELATIONSHIP BETWEEN INTERSTITIAL FLUID FLOW AND MATRIX STIFFNESS ON HEPATOCELLULAR CARCINOMA INVASION

## 4.1 Introduction

Uncontrollable tumor progression and intrahepatic metastasis serve as the main causes of death in HCC patients. Notably patients with HCC often have an underlying chronic liver disease which plays a pivotal role in the development of HCC. In the presence of HBV, HCV, non-alcoholic fatty liver disease (NAFLD), or the more severe form of NAFLD, non-alcoholic steatohepatitis (NASH), chronic liver injury and inflammation is present and over time these events result in fibrosis and cirrhosis of the liver, often progressing to HCC [7, 9, 47]. More than 80% of HCCs occur in patients who suffer from chronic fibrosis or cirrhosis where inflammation and the hepatic wound-healing response contributes to hepatocarcinogenesis [302]. Chronic liver injury promotes changes in the hepatic architecture most notably with the formation of fibrotic scars and subsequently increasing matrix stiffness [303-305].

The remodeling of the ECM has been highlighted as a critical component in tumorigenesis and the spread of these tumor cells to distant tissues. The accumulation of type I collagen and fibronectin together plays an integral part in the mechanical strength of the interstitial matrix [306]. In a variety of cancer types, it has been observed that the increase in matrix stiffness is a result of tumor growth, which can disturb the mechanical forces and biochemical signaling that occurs in the microenvironment, effectively promoting disease progression [304, 307-310]. Similar results have been observed in HCC from the increase in matrix stiffness and clinically this increase in stiffness has served as a predictor for HCC development [79, 101, 257, 277, 303, 311, 312]. While increased matrix

stiffness serves as a good indicator of cancer progression and growth, more importantly the synergistic changes in mechanical forces and signaling pathways and there interactions in this microenvironment stimulate invasion. With such a unique disease profile and risk factors, many studies have examined the effects of stiffness in a static form on HCC progression. To date, there are no studies that examine the effect of IFF on HCC cells in a stiff matrix microenvironment. We previously highlighted some key signaling pathways (MEK/ERK), proteolytic enzymes (MMP-9/MMP-2), and elucidated a mechanism (autologous chemotaxis via CXCR4/CXCL12) involved in HCC flow-induced invasion. We hypothesize that HCC cells in a fibrotic microenvironment exposed to IFF will result in increased CXCL12 secretion, enabling autologous chemotaxis to promote greater flow-induced invasion. In this chapter we will highlight the synergistic relationship of increased matrix stiffness and flow-induced invasion.

## 4.2 Methods

*Cell Culture*

Hepatoma-derived Huh7 were cultured in RPMI 1640 with L-glutamine (Cellgro, Manassas, VA) supplemented with 10% FBS (Atlanta Biologicals, Atlanta, GA) and 1% penicillin/streptomycin (Mediatech, Herndon, VA). The Huh7 cells were maintained in a humidified 37˚C environment with 5% $CO_2$.

*Non-enzymatic Glycation of Collagen*

In order to examine the effects of matrix stiffness and IFF on HCC cells, the first objective was to develop a method to increase the stiffness of the collagen/Matrigel matrix

for the 3D invasion assay that would not hinder the HCC cells ability to invade. Non-enzymatic pre-glycation was utilized as a method to increase the stiffness of the collagen/Matrigel matrix [313, 314]. First the rat tail tendon type I collagen (BD Biosciences, San Jose, CA) was pre-glycated with 250 mM D-ribose (Acros Organics, Geel, Belgium) diluted in 0.1% acetic acid for 5 days at 4ºC. After the 5 day incubation in 250mM D-ribose the pre-glycated collagen with Matrigel was utilized for the 3D invasion assay.

*Rheological Analysis of Collagen Gels*

Rheometry was utilized to validate that non-enzymatic glycation of collagen increased the stiffness of collagen gels. The rheological analysis was conducted on the Discovery Hybrid Rheometer 3 (DHR-3) (TA Instruments, New Castle, DE) using a 25 mm parallel plate geometry. To validate the pre-glycation method, three collagen conditions were compared: normal stock collagen, pre-glycated collagen with 250 mM D-ribose in 0.1% acetic acid incubated for 5 days at 4ºC, and collagen with 250mM D-ribose in 0.1% acetic acid added the same day. The three collagen/Matrigel acellular gels were prepared in the same manner and concentration as they were prepared in the 3D interstitial flow invasion assay and incubated on the platens at 37ºC for 30 minutes to polymerize before rheological analysis. A solvent trap was utilized during polymerization of the gels to minimize any dehydration. Upon polymerization, the solvent trap was removed before any rheological analysis. An initial set of amplitude sweeps with an angular frequency of 1, 10, and 100 rad/s were conducted in order to determine linear viscoelastic region of the gels to assess proper testing. Oscillation frequency sweeps from 0.1 – 100 rad/s were

performed at 1% strain determined from the initial amplitude sweeps. The shear storage modulus (G') of each gel condition was calculated using the resulting stress and strain data and the following equation:

$$G' = \cos(\delta)\left(\frac{\tau}{\gamma}\right)$$

$$\delta = phase\ angle;\ \tau = shear\ stress;\ \gamma = shear\ strain$$

Stiffness of the three collagen gel conditions were reflected by changes in G'. Four experiments were conducted to validate the pre-glycation method with corresponding 3D interstitial flow invasion assays to examine the effects of stiffness and fluid flow. Shear storage moduli results are presented with +/- standard deviation and average shear storage moduli values are reported based on the average values over a frequency range of 0.25 – 39.8 rad/s.

*3D Interstitial Flow Invasion Assay*

The Huh7 cells (5.0 x $10^5$ cells/ml gel) were encapsulated in a gel comprised of 1.3 mg/ml rat tail tendon type I collagen (BD Biosciences, San Jose, CA) and 1 mg/ml Matrigel (BD Biosciences) and seeded into 12 mm diameter, 8 μm pore diameter culture inserts (Millipore, Bellerica, MA) for normal matrix conditions. To expose the Huh7 cells to a stiff matrix, rat tail tendon type I collagen was pre-glycated for 5 days at 4ºC with 250mM d-ribose in 0.1% acetic acid and was utilized with Matrigel at the respective concentrations mentioned previously. The pre-glycated gel with the Huh7 were seeded into the 12 mm diameter, 8 μm pore diameter culture inserts. To validate and confirm the pre-glycation method with 5 day collagen and ribose incubation increased stiffness, a third gel condition with collagen treated with 250 mM D-ribose in 0.1% acetic acid added the same day was

incorporated (denoted in results as 'same day' condition). Once the three gel conditions polymerized, encapsulating the cells in either a normal or stiff matrix, the 8 μm pore diameter culture inserts were placed in basal medium for a 40 minute incubation 37ºC to allow residual D-ribose to diffuse out, ameliorating the effects of un-glycated sugar on HuH7 cell invasion. This incubation was done to both the pre-glycated matrix and normal matrix to ensure consistent experimental conditions. Static and flow conditions were generated over the course of 24 hours by following a previously described method [209, 216, 267]. For the static condition, the level of basal medium outside of the transwell was level with the medium inside the transwell, resulting in little to no hydrostatic pressure difference. The IFF condition was created by adding more basal medium to the inside of that transwell than the outside, resulting in a hydrostatic pressure difference of approximately 1 mm Hg. Cells that transmigrated through the porous membrane were fixed with 4% paraformaldehyde (Sigma-Aldrich, St. Louis, MO) and stained with DAPI (2 μg/ml, MP Biomedicals, Santa Ana, CA). Fixed and stained cells were imaged by fluorescence microscopy. Both static and flow conditions were analyzed by counting five locations on the fixed membranes. Percent invasion was calculated with the following equation:

$$\%\ Invasion = \left[\frac{(Average\ cell\ count) * (Membrane\ surface\ area)}{(Image\ area) * (Number\ of\ cells\ seeded)}\right] * 100$$

For specific experiments, pharmacological inhibitors were added to the cell/gel mixture before gel polymerization and in the media used for the experiment at their respective target concentrations. AMD3100 (12.6 μM) (R&D Systems, Minneapolis, MN) was utilized for

CXCR4 inhibition. SB-3CT (25 μM) (Selleckchem, Houston, TX) was utilized for MMP-2/MMP-9 inhibition.

*Western Blot*

Western blot was used to measure changes in total and phosphorylated protein levels in response to IFF and specific inhibitors. Cells were lysed with RIPA buffer containing Halt protease and phosphatase inhibitor cocktail (Thermo Scientific, Waltham, MA). For 3D samples, cells were first digested out of the gels with collagenase D (0.5625 U/ml, Roche Life Science, Indianapolis, IN) for 45 minutes and then centrifuged for 10 minutes at 1,000 RPM. The following primary antibodies were used to detect the proteins of interest: anti-CXCR4 (1:1,000, Abcam, Cambridge, England), anti-MMP-2 (1:1000, Abcam, Cambridge, England), anti-MMP-9 (1:1000, Abcam, Cambridge, England), and β-actin (13E5) (1:2,000, Cell Signaling Technology, Beverly, MA). The following secondary antibody was used: goat anti-rabbit IgG-HRP (1:10,000, Abcam, Cambridge, England), and anti-rabbit IgG (1:2,000, Cell Signaling Technology, Beverly, MA). Chemiluminescence imaging was conducted with a FluorChem M imaging system (Proteinsimple, San Jose, California) and quantified with ImageJ 1.51 (National Institutes of Health (NIH), Bethesda, Maryland). Target protein levels were normalized to β-actin.

*Enzyme-linked immunosorbent assay (ELISA)*

Protein from 3D cell lysates and medium were collected from Huh7 cells in static varying matrix stiffness conditions after a 24 hour incubation at 37˚C and 5% $CO_2$. Protease inhibitors were added to all cell lysates and media. CXCL12 levels were

quantified using a commercially available DuoSet ELISA kit (R&D Systems, Minneapolis, MN). Standard curves were generated using known concentrations of recombinant human CXCL12 and data were fit with a four parameter logistic curve in MATLAB (MathWorks, Natick, MA).

*Gelatin Zymography of MMP-2 and MMP-9 Activity*

Gelatinase MMP activity was measured by performing electrophoresis of protease samples in denaturing and non-reducing conditions. For 3D samples, cells were first digested out of the gels with collagenase D (0.5625 U/ml, Roche Life Science, Indianapolis, IN) for 45 minutes and then centrifuged for 10 minutes at 1,000 RPM. Cells were lysed with RIPA buffer without any protease inhibitors. A commercial protein quantification assay (Pierce BCA Protein Assay Kit, Thermo Fisher Scientific, Waltham, MA) was utilized to quantify protein in order to better normalize the samples for the zymogram. Samples were prepared in at a 1:1 ratio of 2X SDS loading buffer to lysate without any boiling. Lysates were ran in non-reducing conditions on Novex 10% tris-glycine zymogram gelatin gels (Thermo Fisher Scientific, Waltham, MA) with 1X tris-glycine SDS run buffer. Once completed, the gels were placed in 1X renaturing buffer (Thermo Fisher Scientific, Waltham, MA) for 30 minutes, followed by 1X developing buffer (Thermo Fisher Scientific, Waltham, MA) over night at 37ºC. Zymogram gels were stained with SimplyBlue Safestain (Thermo Fisher Scientific, Waltham, MA) for 1 hour at room temperature. Zymogram imaging was conducted with a FluorChem M imaging system (Proteinsimple, San Jose, California) and quantified with ImageJ 1.51 (National Institutes of Health (NIH), Bethesda, Maryland). MMP activity levels were normalized to

the respective matrix conditions and densitometry was used to determine fold change resulting from exposure to flow.

*Statistical Analysis*

All data are presented as mean ± SEM. All results for invasion assays are based on a minimum of two independent experiments with sample size $n \geq 3$ for each experiment. Statistical significance between two groups was determined by conducting a Student's t-test. For three or more groups, one or two-factor analysis of variance (ANOVA) with a Bonferroni or Tukey's multiple comparison test was utilized. GraphPad Prism 5 (San Diego, CA) was used to perform statistical analyses.

**4.3 Results**

*Pre-glycation of collagen increases the stiffness of collagen gels*

In this study, we utilized non-enzymatic glycation as a method to increase the stiffness of our polymerized gels, which encapsulate the HCC cells in the 3D flow assay. Glycation and increased proteoglycan levels are two methods for non-enzymatic collagen cross-linking [315-317]. Glycation, utilizing sugars like D-ribose, promotes collagen cross-linking and ultimately results in a stiff matrix compared to a non-glycated one. Pre- and post-glycation have both been observed to increase hydrogel stiffness, however pre-glycation results in a greater accumulation of Amadori intermediates to aid in the formation of advanced glycation end products (AGEs) which have been shown to increase mechanical properties of hydrogels [313, 314]. Upon pre-glycating our collagen for 5 days at 4˚C with 250 mM D-ribose, we prepared normal, ribose added same day, and preglycated

collagen gels at the same concentration as gels used in the 3D invasion assay. After polymerization, rheological analysis for the shear storage modulus was completed by running frequency sweeps on the 3 gels. The pre-glycated gels possessed an average shear storage moduli that was more than four times greater than the normal gels (Figure 18A). Average shear storage modulus and standard deviation were calculated from the linear region of the frequency sweeps (0.25 – 39.8 rad/s) for each gel (Figure 18B). The pre-glycated gels possessed statistically significant greater shear moduli compared to the normal or same day conditions. Further statistical analysis also confirmed that there was no statistical difference between the ribose added same day to the collagen or the normal collagen hydrogel, which signifies the glycation process is essential and requires the 5 day incubation to allow for increased stiffness. The rheological analysis confirmed that pre-glycation of collagen with 250 mM D-ribose is an acceptable method for increasing the stiffness of the gels utilized in the 3D invasion assay [318].

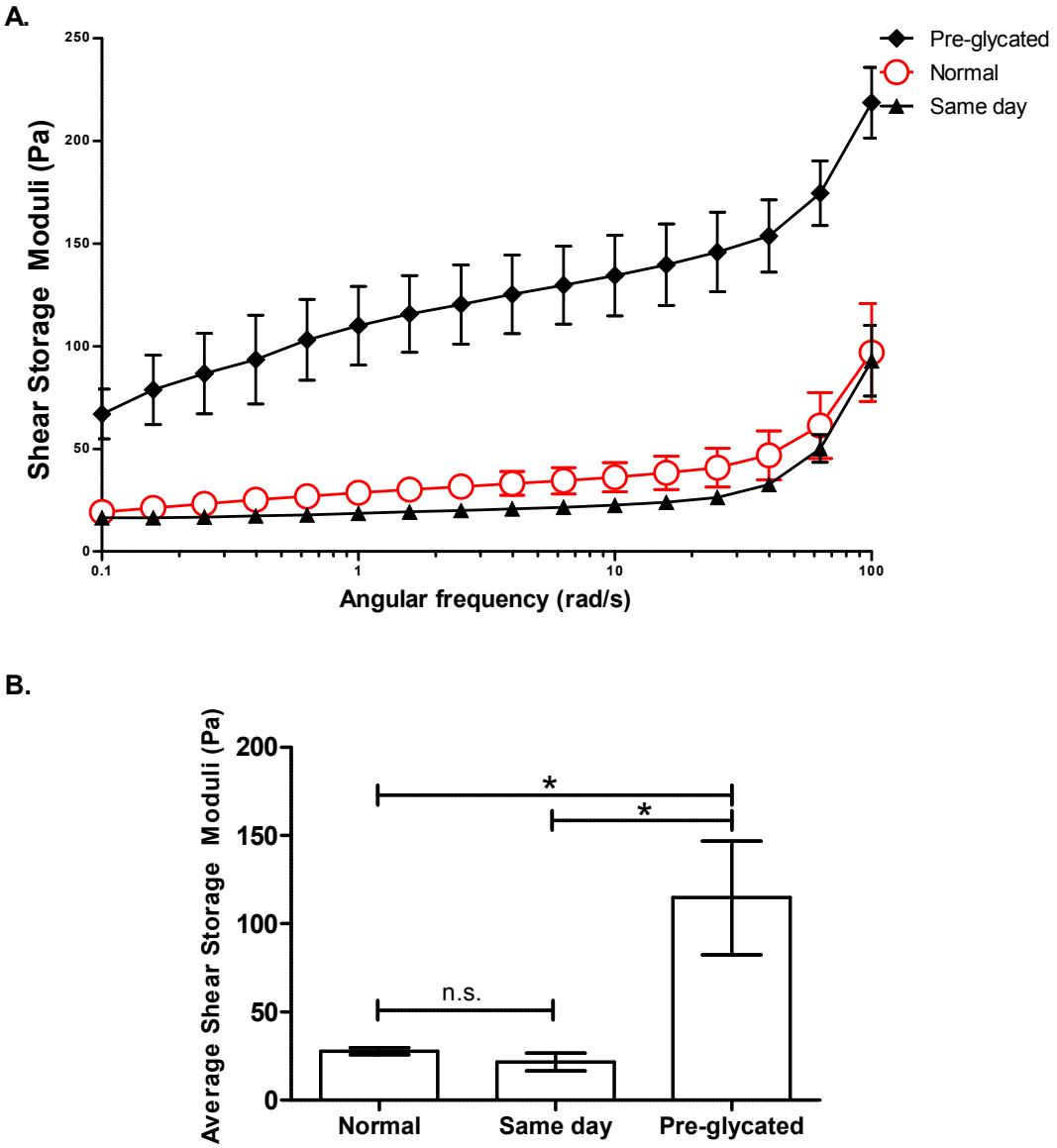


| Matrix Condition | Average Shear Storage Moduli (Pa) |
|---|---|
| Normal (n=4) | 27.76 |
| Same Day (n=3) | 21.59 |
| Pre-glycated (n=4) | 114.72 |

**Figure 18: Pre-glycation as a method for increasing hydrogel stiffness.** (A) Shear storage moduli of varying collagen treatments from rheological analysis. Error bars represent standard error of mean. (B) Average shear storage moduli of linear region from the frequency sweeps for the varying gel conditions. Error bars represent SEM. Statistical significance between gel conditions determined by one-way analysis of variance with Bonferroni's multiple comparison test. * = $p < 0.05$. n.s. = no significant difference.

*Multiplicative increase in flow-induced HCC invasion in a stiff matrix*

Once we were able to validate our method to increase the stiffness of our collagen/matrigel matrix, the next step involved observing the effects of both flow and stiffness on HCC cell invasion. Huh7 cells in the pre-glycated matrix exposed to flow invaded significantly higher than the cells in the normal or same day condition (Figure 19A). Furthermore, it was important to note that the Huh7 cells in the matrix with ribose added the same day and the normal matrix had comparable flow-induced invasion percentages, confirming that the ribose itself was not responsible for the increase cell invasion (Figure 19A). Corresponding stiffness values were identified from the respective collagen conditions via rheometry (Figure 19B). The increased stiffness and exposure to fluid flow ultimately resulted in a nonlinear increase in cellular invasion providing us with compelling evidence of a synergistic relationship between these two forces. The synergistic relationship between IFF and matrix stiffness on HCC invasion was confirmed by conducting a two way ANOVA with a Bonferroni posttest. The statistical analysis determined the interaction between a stiff matrix and IFF-induced invasion was significantly different and there is only a 0.56% chance of randomly observing such an interaction. A synergistic relationship is observed when an effect arising between two factors results in an effect that is observed to be greater than the sum of their respective individual effects. Thus, our results indicated the combination of matrix stiffness and IFF resulted on HCC cell invasion was greater than the sum of these individual factors.

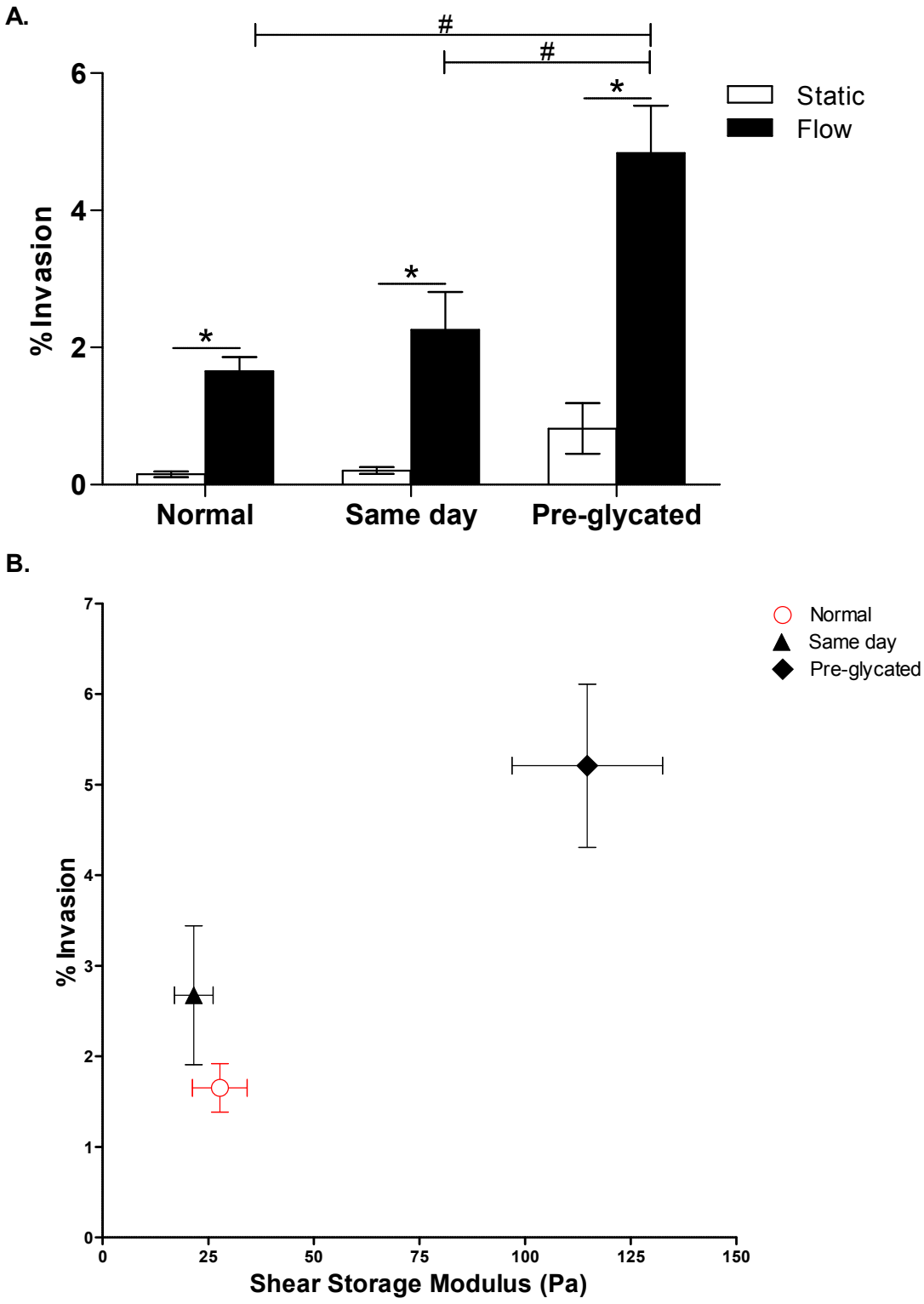


**Figure 19: Increased matrix stiffness results in a multiplicative increase of flow-induced HCC cell invasion.** (A) Percentage of Huh7 cells that invaded in response to fluid flow in a normal or stiff matrix. Increased stiffness denoted in the pre-glycated matrix

condition. Control matrix to validate stiffness and the ribose had no external effect on invasion was represented by the same day matrix condition. Normal and Pre-glycated matrix, n=12 (static and flow); Same day matrix, n=9 (static and flow). Error bars represent standard error of mean. * = $p < 0.05$ between static vs. flow of respective matrix condition. # = $p < 0.05$ between static vs. flow condition of the three matrix conditions assessed by a two-way analysis of variance and Bonferroni's multiple comparison test. (B) Representation of average percentage of Huh7 cells that invaded vs. shear storage moduli of corresponding matrix condition. Normal and Pre-glycated matrix, n=9 (static and flow); Same day matrix, n=6 (static and flow). Error bars represent standard error of mean (horizontal error bars = shear storage modulus standard error of mean; vertical error bars = % invasion standard error of mean).

*The synergistic effect of matrix stiffness on IFF-induced cell invasion is not mediated through CXCR4 or CXCL12*

Our previous work elucidated autologous chemotaxis via CXCR4/CXCL12 as one mechanism for flow-induced HCC cell invasion. Therefore, we investigated the components in autologous chemotaxis, CXCR4 and CXCL12, in a stiff matrix. First we observed if CXCR4 expression in a Huh7 cells within a stiff matrix changed. The Huh7 cells were encapsulated in the varying matrix stiffness conditions without the presence of flow for 24 hours and digested out of their respective gels and lysed. Western blot results revealed no significant change in expression of CXCR4 irrespective of the matrix the Huh7 cells were in (Figure 20A). Based on initial gel densitometry analysis of the western blot, there was a decrease in CXCR4 expression in Huh7 cells encapsulated in a stiff matrix (Figure 20A) compared to cells in a normal matrix. Additionally, after utilizing AMD3100, a pharmacological inhibitor for CXCR4, in a 3D interstitial flow assay with pre-glycated matrix, there was much lower functional response to the inhibitor compared to Huh7 cells in a normal matrix (Figure 20B).

There was only a 1.3 fold decrease in flow-induced invasion in Huh7 cells in the pre-glycated matrix, and this effect caused by matrix stiffness is still measurable even after

inhibition of CXCR4 suggesting that matrix stiffness is not affecting IFF-induced invasion by modulating receptor levels or binding to CXCL12 (Figure 20B). However, it is important to realize that autologous chemotaxis does not require the increase in expression of the receptor to be an effective mechanism of flow-induced invasion. Therefore, the next step was to investigate the expression and secretion of the ligand in a stiff matrix. Again Huh7 cells were encapsulated in a 3D static gels in various matrix conditions for 24 hours. Upon digestion of their matrix, cells were lysed and media collected from each respective condition. A commercial CXCL12 ELISA kit was utilized to quantify ligand production and secretion from the Huh7 cells. Ultimately there was no significant change in CXCL12 production or secretion in either of the matrix conditions (Figure 20C). In conclusion, our results indicate that matrix stiffness itself has a distinct effect on Huh7 invasion independent of CXCR4/CXCL12 signaling.

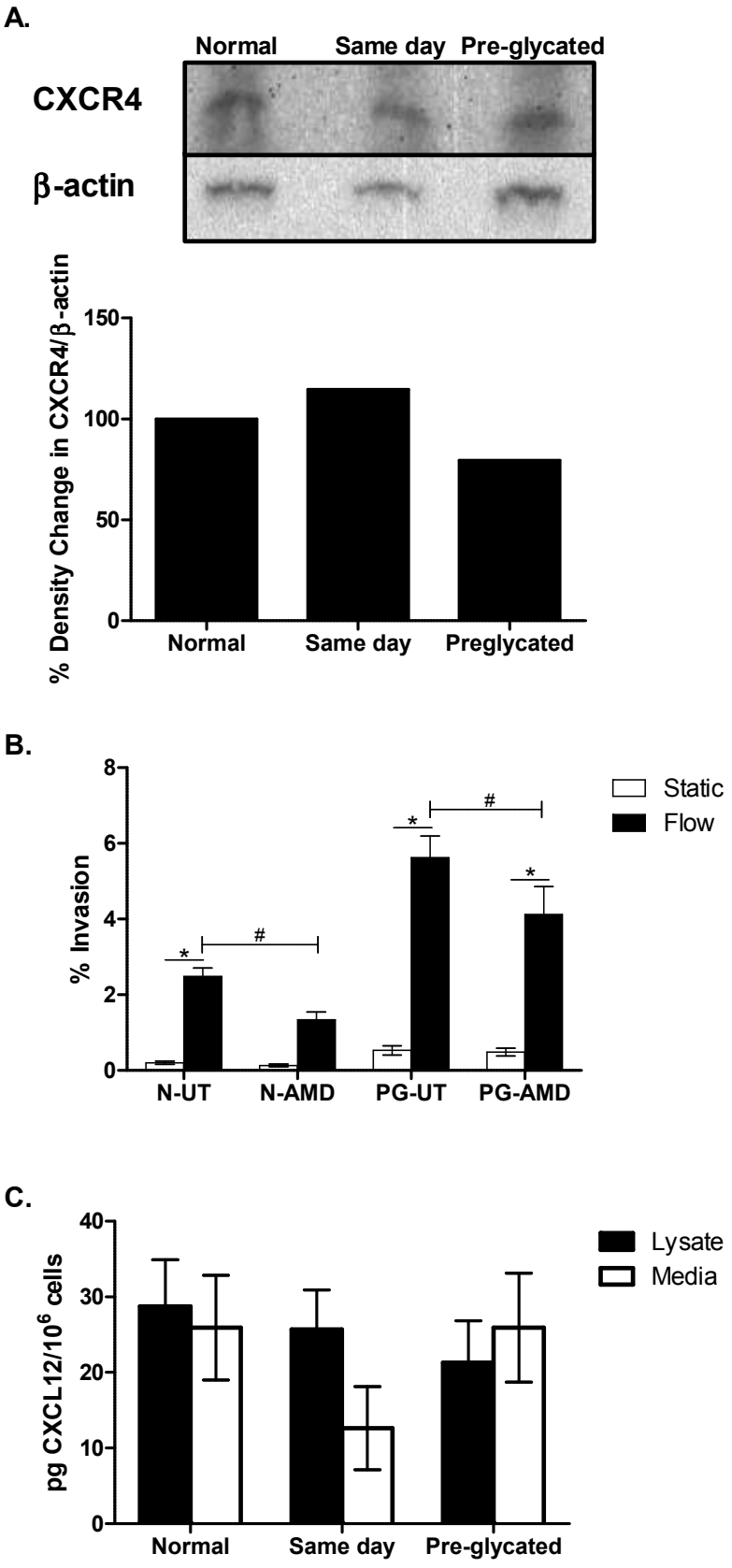
A.
Normal
Same day
Pre-glycated
CXCR4
β-actin
% Density Change in CXCR4/β-actin
150
100
50
0
Normal
Same day
Preglycated
B.
% Invasion
8
6
4
2
0
Static
Flow
*
#
*
#
*
N-UT
N-AMD
PG-UT
PG-AMD
C.
pg CXCL12/10^6 cells
40
30
20
10
0
Lysate
Media
Normal
Same day
Pre-glycated

**Figure 20: HCC cells in the presence of a stiff matrix does not alter components elucidated in the CXCR4/CXCL12 autologous chemotaxis mechanism.** (A) CXCR4 detection in Huh7 cells in 3D static gels with varying stiffness and quantitative western blot analysis. CXCR4 = 43 kDa. Percentage relative density compared to loading control for each lysate and normalized to the normal matrix condition. (B) CXCR4 antagonist AMD3100 (12.6 μM) inhibits IFF-induced invasion less effectively in Huh7 cells in pre-glycated matrix (n = 9). N-UT = normal matrix untreated, N-AMD = normal matrix with AMD3100, PG-UT = pre-glycated matrix untreated, PG-AMD = pre-glycated matrix with AMD3100. Error bars represent standard error of mean. * = $p < 0.05$ between static vs. flow of respective matrix condition. # = $p < 0.05$ between flow conditions of the treatment groups in respective matrix condition assessed by a two-way analysis of variance and Bonferroni's multiple comparison test. (C) Average CXCL12 expression in Huh7 cells in 3D static with varying matrix conditions with ELISA. Sample type: (n = cell lysate/n = medium) – (n=4).

*Evaluation of MMP-2 and MMP-9 in Huh7 cells in a stiff matrix exposed to interstitial fluid flow*

The previous chapter highlights the significance of proteolytic enzymes like MMPs in HCC cell invasion. Additionally many studies have highlighted the critical role MMPs play in the TME aiding in disease progression and metastatic spread [130, 134, 136] . Their role is just as important in liver fibrosis, as MMPs and their inhibitors, TIMPs, create a positive feedback loop of collagen deposition due to their imbalance [50]. Based on our findings in Chapter 3, we identified that MMP-2 and MMP-9 are likely involved in IFF-induced invasion of HCC cells. Therefore we tested the selective inhibitor for MMP-9 and MMP-2, SB-3CT (25 μM), in varying matrix conditions. We observed a significant decrease in flow-induced HCC cell invasion in both normal and pre-glycated matrix conditions treated with the inhibitor SB-3CT (**Figure 21**A). These inhibitor results provided some early evidence that stiffness could enhance invasion in response to IFF via MMP-9 and MMP-2. Next we investigated the expression of MMP-9 and MMP-2 in varying matrix conditions to determine if any significant changes could be attributed to stiffness. However, no significant change in MMP-9 or MMP-2 expression was observed

in relation to matrix stiffness (Figure 21B). MMP-9 and MMP-2 are also known as gelatinases, and they are often activated from various mechanical stimuli and soluble factors in the liver microenvironment [136-138, 291]. The expression of these activated MMPs by hepatoma cells is observed to significantly promote stromal invasion [319]. Gelatin zymography was utilized to examine MMP-9 and MMP-2 activity in the presence of flow with varying matrix conditions. IFF independently increased both latent and active forms of both MMP-9 and MMP-2, irrespective of matrix condition (Figure 21C). However stiffness alone did not result in in greater MMP-9 or MMP-2 activity, confirmed by densitometry (Figure 21D). In conclusion these findings highlight the significance in the synergistic relationship between HCC flow-induced invasion in the presence of increased matrix stiffness, and MMPs play a critical role in the flow-sensing aspect for the increased invasion.

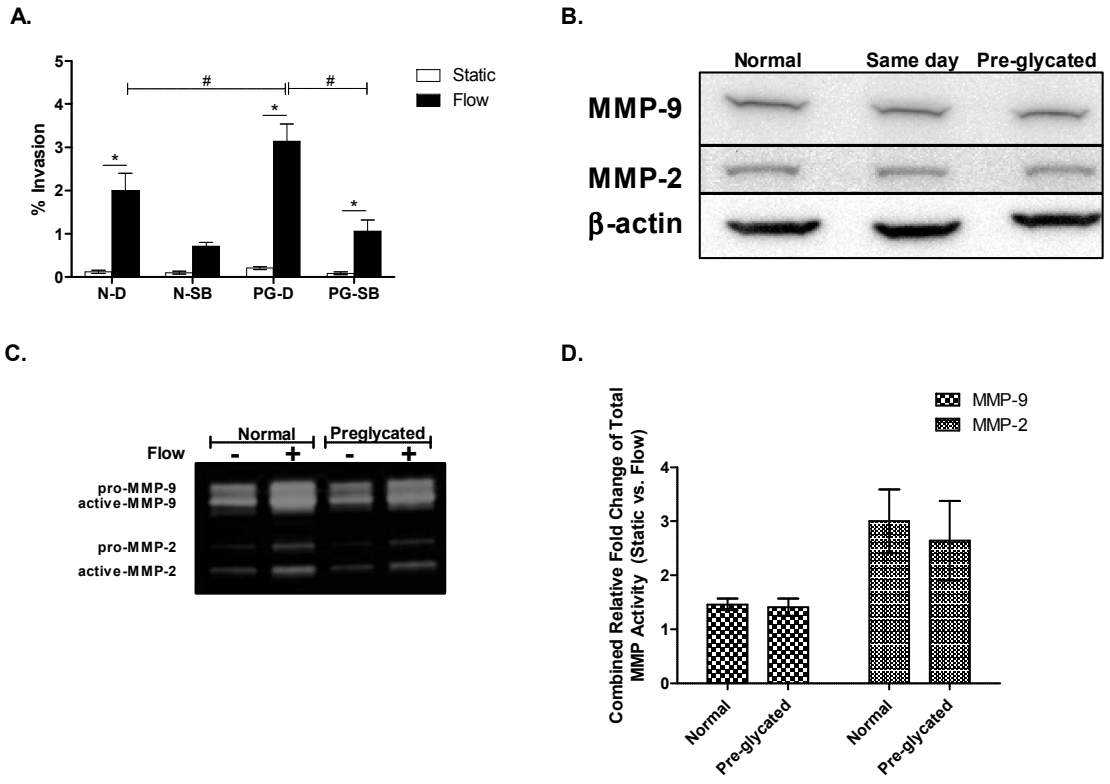


**Figure 21: Examining the effects of increased stiffness and fluid flow on MMP-9 and MMP-2.** (A) SB-3CT (25 μM), a selective inhibitor for MMP-9 and MMP-2 inhibits IFF-induced HCC invasion independent of matrix condition. (n = 12). N-D = normal matrix with DMSO control, N-SB = normal matrix with SB-3CT, PG-D = pre-glycated matrix with DMSO, PG-SB = pre-glycated matrix with SB-3CT.* = $p < 0.05$ between static vs. flow of respective matrix condition. # = $p < 0.05$ between flow conditions of the treatment groups in respective matrix condition assessed by a two-way analysis of variance and Bonferroni's multiple comparison test. (B) MMP-9 and MMP-2 expression in Huh7 cells encapsulated in 3D static gels with varying matrix stiffness. MMP-9 = 92 kDa and MMP-2 = 72 kDa. (C) Representative gelatin zymogram of MMP-9 and MMP-2 activity in Huh7 cells exposed to IFF in stiff matrix conditions. (n = 3). Static 3D sample, (-) and Flow 3D Sample, (+). Pro-MMP-9 = 92 kDa, active-MMP-9 = 87 kDa, pro-MMP-2 = 72 kDa, and active-MMP-2 = 66 kDa. (D) Densitometry of zymogram results. Combined average relative fold change of total MMP activity (static vs. flow conditions) for respective matrix condition. Sum of pixel density of flow condition (pro-MMP + active-MMP) divided by the sum of pixel density of respective static condition (pro-MMP + active-MMP). Averaged for each zymogram for respective matrix condition. (n = 3).

## 4.4 Discussion

For the first time, we investigated the interaction between interstitial flow and increased matrix stiffness and their combined effects on HCC cell invasion. Fibrosis and cirrhosis of the liver have been investigated extensively; ECM deposition is a hallmark for these events and results in increased matrix stiffness. The increase in tumor and surrounding tissue stiffness has been observed in many different malignant tumors [320]. Additionally the mechanisms and soluble factors involved in tumor-associated fibrosis are also involved in fibrosis from chronic liver injury [321, 322].

In order to investigate the effects of matrix stiffness with the presence of IFF on HCC cells, we were tasked with first developing a method to increase matrix stiffness, without hindering the flow properties or exposing the HCC cells to cytotoxic chemicals/cross-linkers. A potential method that could be utilized is simply increasing the concentration of the collagen to obtain increased stiffness. However, there are a few significant drawbacks to this method such the resulting gel would possess increased ligand binding sites and increased cross-linking would result in the decrease of pore size from what is normally observed. A more viable alternative is non-enzymatic glycation of the collagen gel which has been shown to control the stiffness of the gels without affecting collagen fibril mesh size or significantly increasing ligand binding sites while maintaining high cell viability [313, 314, 323]. ECM stiffness increases over decades for individuals with chronic liver injury triggering ECM deposition, thus the pre-glycation method was an ideal for increasing the stiffness of our hydrogels without altering the flow properties.

There have been many studies that have investigated ECM stiffness of liver tissue under varying pathological conditions; magnetic resonance elastography of normal liver

tissue has measured values of Young's modulus (E) of 300-600 Pa, while fibrotic and cirrhotic livers (depending on progression) can range from 1,500-20,000 Pa [324, 325]. It is crucial to point out that our measurements are of collagen (normal vs. preglycated) matrices and most measurements for diseased livers are conducted on rat or human liver tissue. However recent rheology measurements conducted on decellularized liver tissue (normal vs. fibrotic) observed approximate storage moduli of ~40 Pa for normal decellularized liver tissue and 100-125 Pa for fibrotic decellularized liver tissue [318]. These results are comparable to our rheology measurements from normal and preglycated acellular gels, suggesting cells in our model system are experiencing comparable matrix stiffness values to what they would see *in vivo* (Figure 18).

After identifying a feasible method that would allow us to generate an *in vitro* environment simulating a stiff matrix and IFF, the next objective was to expose Huh7 cells to these mechanical forces. Huh7 cells in a stiff 3D matrix (G' ~ 115 Pa) and exposed to IFF were observed to be 3-fold more invasive than cells exposed to IFF in a softer environment (G' ~ 27 Pa) (Figure 19A). Similarly, the cells in a stiff static gel were also much more invasive compared to the cells in a normal matrix, but stiffness alone was not responsible for the multiplicative increase in invasion in the presence of IFF (Figure 19A). Stiffness and IFF had a multiplicative effect on invasion and together these results highlight the need for more studies that investigate multiple mechanical forces and their potential role in disease progression. An outstanding question that remains in this study is determining if the effect of preglycating the collagen matrix on invasion is due solely to the increased stiffness. Particularly, preglycation of the collagen results in the formation of AGE cross-links which alter the chemical composition of the matrix [326, 327].

Mechanosensitive cells, like endothelial cells, possess receptors for advanced glycation end products (RAGE) which are capable of interacting with the AGE cross-links in the glycated collagen matrix. The AGE/RAGE interaction consequently results in changes in cell behavior and their ability to sense shear stress, cyclic stretch, and barrier function [328-330]. Kemeny and colleagues investigated the diminished FAK activation due to the interactions with the glycated matrix and saw decreased Rho-GTPase signaling which in turn inhibited cytoskeletal changes in endothelial cells [328]. The same group further investigated the response of endothelial cells in a glycated matrix to cyclic strain and observed diminished integrin binding, activation, or lack of clustering of these mechanosensors, which inhibits FAK activation [329]. Furthermore, preliminary findings have stated that cells exposed to IFF can sense fluid drag-induced matrix tension and respond via increased integrin and FAK activation [214]. For this reason it is particularly important to determine the effects of pre-glycation on invasion due to increased stiffness and not due to the chemistry of the glycated matrix or the impairment in mechanotransduction of IFF in the HCC cells.

Under those circumstances, examining the chemistry of the glycated matrix by investigating the AGE/RAGE interaction in our system would be an ideal starting point by inhibiting RAGE from binding to AGE with a RAGE antagonist such as FPS-ZM1. However, it is important to note that RAGE inhibitors are not completely specific in blocking the RAGE/AGE interaction and are capable of altering various cellular functions [331]. Additionally, the use of specific antibodies for blocking RAGE is an alternative measure to inhibit the RAGE/AGE interaction, but this would only be a viable and feasible option for short term functional testing as long term use of blocking antibodies would

become ineffective and the receptor would localize back to the surface of the cell [331]. Investigating the RAGE/AGE interaction would be a straight forward way of examining the effects of flow-induced invasion in a pre-glycated matrix are impairing mechanotransduction of IFF, but until specific RAGE inhibitors and blocking antibodies are developed that do not possess the negative affects discussed previously, an alternative method of examining these mechanical stimuli is required.

Glycation has been observed to enhance collagen crosslinking and change fibril assembly of type I collagen, as a result causes alterations in integrin binding site accessibility which in turn can prevent clustering and activation of integrins [332, 333]. For the purpose of determining the effects on invasion are solely due to stiffness, independent of the chemistry of glycated collagen; the use of mixed synthetic and natural hydrogels would provide control of the mechanical properties. Hydrogel matrices composed of collagen with varying concentrations of poly(ethylene glycol) di-(succinic acid N-hydroxysuccinimidyl ester) have been utilized to investigate HCC cell malignancy while providing control of matrix stiffness and limited changes to matrix permeability and chemical cues [334]. Examining HCC cells in a stiff matrix for integrin clustering, FAK activation, and tracking migration rates would allow for identifying the role stiffness on invasion. Regulating any of the signaling components with specific antibodies or inhibitors in flow conditions would verify the contribution of stiffness on invasion.

Next we investigated if stiffness-induced signaling had any effect on the mechanisms of IFF-induced HCC invasion that we have previously described in Chapter 2 with CXCR4/CXCL12 and Chapter 3 with MMP-2/9. These results indicated that neither CXCR4 nor CXCL12 are changed in the presence of a stiff matrix (Figure 20). Rather

there was a decreased response to AMD3100 for Huh7 cells exposed to IFF in a stiff matrix compared to cells in a normal matrix (Figure 20A). Correspondingly, our results indicated that stiffness did not alter CXCL12 secretion by Huh7 cells (Figure 20C). With this in mind, it must be noted that *in vivo* activated HSCs in a fibrotic environment are known to secrete CXCL12, resulting in HCC cell migration and metastasis [260, 335, 336]. Additionally we examined no change in expression level of MMP-2 and MMP-9 in the various matrix conditions in HCC cells encapsulated in a 3D static gel (Figure 21B). Similarly there was no difference in MMP-2/9 activity levels in HCC cells exposed to IFF in either the normal matrix condition or the stiff matrix (Figure 21C). Ultimately it appears that autologous chemotaxis applies to flow-induced HCC invasion while stiffness contributes to the invasion via another sensory mechanism such as glycocalyx shear stress sensing or integrin clustering. These results show that MMPs are more likely to be implicated in flow-induced invasion as opposed to directly contributing to the invasion from stiffness.

Our findings further suggest that HCC cells are mechanosensitive to their environments and adapt their responses to biomechanical changes. The findings in this chapter suggest that another mechanism could be involved in flow-induced invasion, as we observed the effects of stiffness to be independent of autologous chemotaxis. We know that IFF can create drag forces on matrix fibers found on the extracellular matrix generating high shear stresses on these fibers which can be transmitted to engaged integrin receptors [154]. In addition, integrins have been observed to be clustered on stiff substrates, thus IFF could potentially generate significantly high tension forces on these integrins resulting in increased migration and activation of various downstream signaling such as FAK

activation [337, 338]. With this in mind, it is important to note that the glycocalyx is capable of sensing shear stress resulting in changes to focal adhesion kinase (FAK), and extracellular signal-related kinase (ERK) [202, 203]. However non-enzymatic glycation of type I collagen has been observed to diminish collagen-proteoglycan binding and weaken cell adhesion [339]. Therefore, this current modified assay would not be an ideal method to examine glycocalyx shear stress sensing as a mechanism for IFF-induced invasion in a stiff matrix. Provided that, I hypothesize increased integrin clustering presence in HCC cells embedded in a stiff matrix and with the presence of IFF results in increased focal adhesion turn over and activation promoting invasion. Changes in integrin expression and clustering can be determined with fluorescence-activated cell sorting analysis to further conclude the effects of matrix stiffness on these mechanosensors. Furthermore, additional work could aid in determining if IFF alters localization of integrin clustering or activation via IF/ICC in HCC cells in a stiff matrix condition. It is important to note that upstream migration has been observed in cells exposed to fluid flow with resultant tension forces, but our experimental set up does not examine migration upstream and notably the described study was not conducted in the context of a stiff matrix [245]. Functional testing by inhibiting various families of integrins would allow us to determine which subclass is more responsive to IFF, but careful consideration of the experimental conditions would be required as inhibiting total cell adhesion could result in an experimental condition that would not be valid or desired. Next observing downstream signaling components such as focal adhesion kinase and its crosstalk with Rho GTPase would be ideal. I hypothesized due to increased integrin clustering, matrix tension will be significantly increased on cells in a stiff matrix exposed to IFF in turn resulting in

phosphorylation of FAK and increased Rho GTPase activity. By modulating these signaling components, this would provide a better understanding of their role in flow-induced invasion. Examining the mechanosensory components in a stiff matrix could result in further elucidation of another mechanism for IFF-induced HCC invasion to corroborate the findings in this chapter.

Matrix stiffness has been shown to modulate HCC cell proliferation, chemotherapeutic response, and even migration [340]. Migration through dense 3D ECM is only possible when the cell generates enough traction forces which are then transmitted through the cell-ECM adhesion components to displace itself from the matrix [341]. Increased matrix stiffness is directly implicated in enhancing cellular contractility by changes in intracellular tension that is experienced by the cell from forces caused by contracting in respect to the elastic resistance by the stiff ECM [237]. For example, contractile forces have been shown to be increased in breast cancer cells in stiff 3D collagen matrices enhancing cell invasion [342]. Actin-myosin contraction inhibition has been shown to directly stop cell migration through a 3D matrix; this contraction and cytoskeletal change is regulated by Rho/ROCK signaling pathway. ROCK signaling critically for cell migration in response to matrix stiffness, as it is capable of enhancing actin-myosin contractility and downstream substrates such as LIM-kinase and myosin light chain 2 which also aid in cytoskeletal reorganization and promote migration [343-345]. Rho/ROCK are particularly important clinically HCC; overexpression of RhoA in patients with HCC are likely to have greater chances of tumor reoccurrence and lower overall disease free survival [346]. Interestingly, a recent study has demonstrated that contact guidance by collagen alignment is particularly important via Rho/ROCK pathway for cell

migration and this matrix reorganization is more dependent on the initial contractility [347]. Furthermore, IFF increases contractile forces which in turn can alter cytoskeletal organization to promote tumor cell invasion. In addition, Rho-mediated fibroblast contractility has been shown to enhance tumor cell invasion with IFF [216]. Therefore, examining the Rho-ROCK signaling pathway and determining any cytoskeletal changes from IFF exposure in a stiff matrix environment could elucidate a different mechanism corroborating the findings in this chapter. ROCK is known to be a direct effect of RhoA, inhibiting ROCK with Y27632 would provide a method to determine the functional involvement of the Rho-ROCK signaling pathway. Further investigation of the components of Rho-ROCK signaling, such as actin reorganization, focal adhesion formation, and myosin activity would be assessed with the inhibitor to verify the signaling generated by the IFF and/or a stiff matrix. Examining the effects of IFF on cell contractility via ROCK activity can be further verified by utilizing a kinase activity assay. For the first time we have investigated and identified the synergistic relationship between matrix stiffness and IFF on HCC cell invasion. The preliminary findings in this chapter highlight the significant role IFF has on tumor cell invasion, but also exposes the dearth of knowledge and lack of mechanistic understanding we have regarding this subtle fluid flow.

# CHAPTER 5: CONCLUSIONS AND FUTURE WORK

## 5.1 Major Findings and Signficance

*Introduction*

The findings from this dissertation establish a foundation for studying the effects of IFF on HCC cell invasion. This research provides a multi-mechanistic understanding of flow-induced HCC invasion by identifying key signaling pathways that cause HCC cells to be more invasive when exposed to this subtle fluid flow. The approach taken in this research examines the direct effect of IFF on HCC cells in a 3D microenvironment unlike many of the current and previous work that has been published. HCC often develops in the presence of chronic liver injury which promotes changes to the hepatic architecture resulting in altered biomechanical forces such as increased matrix stiffness in the liver microenvironment. This study establishes the development and validation of a 3D *in vitro* method to examine the synergistic effects of matrix stiffness and IFF on HCC cell invasion (Chapter 4). For the first time this work carefully examines the effects of IFF on HCC invasion and shows how different mechanisms can govern HCC cell response to fluid flow. The major findings of this study are **(A) the IFF-induced invasion response of HCC cells occurs through multiple mechanisms and (B) there is a synergistic relationship between flow-induced HCC invasion in the presence of a stiff matrix.**

(A) HCC cells are capable of invading in response to IFF through multiple mechanisms.

- Autologous chemotaxis as a mechanism for HCC invasion occurs through the CXCR4/CXCL12 signaling axis. This work carefully identifies that there is no

change in the expression or secretion of these chemokines, but rather IFF is capable of generating a biased chemoattractant gradient in the direction of fluid flow.

- MEK/ERK signaling is required for IFF-induced HCC cell invasion but does not occur upstream or downstream of the elucidated CXCR4/CXCL12 autologous chemotaxis.
- IFF enhances MMP-9 and MMP-2 activity, independent of chemokine-dependent autologous chemotaxis. This flow-induced enhancement of MMP-2/-9 activity occurs without any changes in MMP or TIMP expression.

(B) The second major finding from this study highlights the synergy in flow-induced invasion in the presence of a stiff matrix

- Matrix stiffness and IFF synergistically promotes HCC invasion independent of the previously elucidated CXCR4/CXCL12 autologous chemotaxis mechanism.
- IFF independently increased MMP-9 and MMP-2 activity irrespective of the matrix condition.

*Prior understanding of IFF-induced mechanisms*

Prior to the findings in this study, it was hypothesized that IFF increased cellular invasion through autologous gradient formation of chemokines that promote migration; this mechanism was coined, ‘autologous chemotaxis’. Previous studies showed breast cancer cell lines exhibited increased invasion in the direction of IFF through a CCR7 dependent mechanism while glioma cells were more invasive through a CXCR4-dependent

autologous chemotaxis mechanism [209, 235]. The findings in this study show that HCC cells are capable of sensing transcellular gradients of CXCL12 corroborating with the findings observed in flow-induced glioma invasion. However, autologous chemotaxis is not the only mechanism observed in flow-induced invasion, which was observed in our findings as inhibition of the CXCR4 receptor did not completely diminish flow-induced invasion.

The mechanisms of IFF mechanosensing have not been fully identified and the formation of autologous transcellular gradients is only one mechanism that HCC cells may use to sense and respond to IFF. The findings in this study identified the involvement of MEK/ERK signaling to be critical in flow-induced HCC invasion. However the presence of elevated MEK/ERK signaling did not function through the CXCR4/CXCL12 signaling axis, suggesting the possibility of other mechanisms being simultaneously involved. Another mechanism that has been identified in IFF sensing is glycocalyx shear stress sensing, where flow-induced stresses are transduced into and transmitted as solid stresses through core proteins of the glycocalyx, leading to various intracellular signaling cascades [154, 214, 215, 229]. Glycocalyx shear stress sensing could be argued as a potential mechanism for explaining the MEK/ERK involvement identified in this study as ERK1/2 was upregulated when exposed to fluid flow shear stresses in smooth muscle cells [202]. However, it is important to note the significant difference in experimental set up of fluid flow exposure compared to our gravity driven fluid-flow assay, as our hydrostatic pressure is not maintained at a constant amount for extensive periods of time. Additionally experimental set up utilized in this body of work examines strictly the effects of fluid flow on the various signaling pathways immediately after the HCC cells are exposed to fluid

flow. Tarbell and colleagues also showed ERK1/2 was activated in a non-tumor cell line after exposure to shear stress generated by fluid flow, which was different from the findings in this research as there was no observable difference in ERK1/2 with flow, but it was required for chemotaxis.

Additionally, this study identified an increase in MMP-2/9 activity in Huh7 cells exposed to IFF, but not an increase in MMP-2/9 expression. These findings do not align with some of the current literature that has shown exposure to fluid flow shear stresses on U087 and CNS-1 glioma cells resulted in downregulated MMP-2 expression and in rat aortic smooth muscle cells suppressed MMP-2 activity, but upregulated MMP-1 reducing migration [172, 218, 290]. The findings in this dissertation possess many differences from the findings in Tarbell and colleagues work, it is important to note the significant difference in experimental set up, length of fluid flow exposure, and observation of MMP activity. First, the experimental set up for application of fluid flow is substantially different in the Tarbell studies as their Darcy Flow Experimental Apparatus generates constant hydrostatic pressure to drive fluid flow exposing cells to shear stress. Upon completion of the exposure to shear stress in the Tarbell experimental set up, the Boyden chambers are incubated in a static environment with basal medium containing a chemoattractant where finally invasion and protein expression/activity are quantified [218]. The Darcy Flow Experimental Apparatus set-up is substantially different from the 3D invasion assay set up utilized in this dissertation where protein expression and activity were quantified immediately after 24 hours of exposure to IFF; ultimately allowing us to isolate and determine specifically the effects of IFF. Therefore the findings in this study could be due to difference in the flow model and time point for measuring protein activity suggesting proteolytic activity of

MMPs is specific and in response to IFF. The MMP-2/9 activity results also appeared to function separately from the autologous chemotaxis mechanism previously identified, further strengthening the argument that cells are capable of sensing and responding to IFF through multiple mechanisms.

*Synergy of matrix stiffness and IFF on HCC cell invasion*

The synergy of IFF and matrix stiffness resulted in a multiplicative increase in flow-induced HCC invasion. However these findings had minimal mechanistic relation to the molecular pathways elucidated in prior chapters. The findings in this study showed IFF increased MMP-9 and MMP-2 activity, independent of stiffness. These results also indicated that the MMP-2/9 activity was independent from autologous chemotaxis via CXCR4/CXCL12 signaling. Downregulation of total MMP-2 expression has been observed in glioma cells upon exposure to shear stress generated by IFF, while the active-MMP-2 was upregulated, this only slightly contradicts the results in this study as it was observed IFF increase MMP-2 activity for both the pro and active forms. The effect of IFF on HCC cells in a stiff matrix could result in increased matrix tension and contractile forces which could be amplified by mechanosensors such as integrins. Matrix shear stress sensing and the presence of glycocalyx have been shown to regulate integrin clustering on the cell surface in the presence of a stiff matrix. The drag forces experienced would be much higher and disturbing the balance of contractile force signaling pathways such as GTPase RhoA would result in cytoskeletal changes and even increased ERK and MMP regulation. Furthermore, studies have shown that ECM rigidity can influence HCC cell migration behavior. These cells have been shown to interchange between mesenchymal and

amoeboid migration in response to the microenvironment. Mesenchymal mode of cell migration in the HCC cells in a stiff and stably cross-linked matrix possessed enhanced MMP-2 activity and integrin β1 expression [348].

*Conclusion*

In conclusion, this study provides evidence supporting multiple mechanisms regulate flow-induced HCC invasion. This body of work uncovers autologous chemotaxis via CXCR4/CXCL12 signaling as one mechanism for flow-induced HCC invasion and suggests MEK/ERK signaling and MMP-2/9 activity to be involved independent of chemokine signaling in flow-induced invasion. Additionally, from this body of work we learn that IFF-induced invasion in the context of a stiff matrix results in a multiplicative increase in invasion, thus the combination of these TME changes play a significant role in HCC progression. The findings in this research contribute directly to the field of tumor mechanobiology by establishing a basic fundamental and mechanistic understanding of how HCC cells respond to mechanical forces in the tumor microenvironment. This research establishes the foundation for future studies investigating how mechanical forces can alter molecular factors in the tumor microenvironment to help promote tumor progression.

## 5.2 Future Work

The findings from this research raise many new questions in regards to flow-induced HCC invasion and how IFF may alter HCC spread. Future work will emphasize two major areas to further advance the findings in this study: (1) Improving the 3D IFF

assay to further investigate autologous chemotaxis and (2) examining the other elucidated mechanisms of flow-induced invasion.

### *5.2.1 Improving the 3D IFF assay to further investigate autologous chemotaxis*

The motivation for improving the 3D IFF assay would allow for deeper investigation into the autologous chemotaxis mechanism and ultimately provide a better understanding of cells interacting with the tumor microenvironment cohesively promote flow-induced invasion. Two main areas of the 3D *in vitro* fluid flow assay require further investigation to better mimic physiological conditions; (1A) quantification of IFF velocity *in vivo* and simulating those IFF velocities in the 3D *in vitro* assay, and (1B) incorporation of hepatic stellate cells with HCC tumor cells in 3D fluid flow assay. The future work proposed is significantly important in investigating and furthering our understanding of autologous chemotaxis as a mechanism for flow-induced HCC invasion in a more physiological perspective.

#### *Quantification of in vivo IFF velocity and the replication of IFF in vitro*

First there is an initial need to determine accurate IFF velocities from *in vivo* human or rat HCCs to better simulate this fluid flow in our study. One weakness in this study is the assumption of physiological IFF velocity in the liver; the basis for this study is conducted in the low velocity spectrum of IFF which is determined by computational modeling and simulations correlating IFP to IFF velocity. Many computational and modeling studies have simulated IFF or IFP in various physiological states; however, there is a clear need to measure IFF velocity in both animal and human tumor models in the liver.

The quantification and replication of accurate velocities are particularly important in studying autologous gradient formation. One major criteria for this mechanism is the formation of extracellular gradients by fluid flow that cells are capable of detecting. Models of interstitial flow and autocrine morphogen secretion of a single cell demonstrate that convective forces alone can establish transcellular autologous gradients which are biologically relevant at IFF velocities ranging from 0.12 - 6.0 μm/s, even if the Peclet number suggests that diffusion is the dominant mechanism of mass transport. If the secreted factor is a chemoattractant, these autologous gradients can drive directed cell migration via a mechanism called autologous chemotaxis [209, 235]. Furthermore, HCC often develops in the context of chronic liver injury resulting in changes to many biomechanical forces in the TME. Examining fluid flow velocity in HCCs in the presence of fibrotic hepatic architecture could result in significantly different velocities altering convective mass transport. With this in mind, *in vivo* IFF velocities have been observed to be significantly higher, ranging between 5 μm/s – 50 μm/s, which are much higher than the velocity observed in our 3D fluid flow assay [146, 147].

Examining and replicating *in vivo* IFF velocities and flow profiles would ultimately answer the following questions to help further our understanding of autologous chemotaxis:

1) Are IFF velocities different in HCCs that arise in the context of chronic liver injury compared to primary HCCs?
2) How do higher or *in vivo* IFF velocities alter mass transport or gradient formation? Downstream formation?

3) How does IFF velocity affect receptor/ligand affinity and recycling of surface receptor?

Having accurate IFF velocity values in a variety of HCC tumor stages would result in accurate *in vitro* testing conditions for understanding HCC invasion. Furthermore, most HCC cases arise in the context of chronic liver injury, understanding the role of the morphological and architectural changes on IFF in a diseased liver would provide a range of physiologically relevant IFF velocities and fluid flow patterns utilized for future *in vitro* studies. I hypothesize IFF velocity in a late stage HCC tumor is significantly higher than earlier stage HCCs. Measuring IFF velocity can be accomplished by utilizing dynamic contrast-enhanced MRI (DCE-MRI) with gadolinium diethylene-triamine penta-acetic acid (Gd-DTPA contrast agents as described in the Hompland study [146]. Utilization of DCE-MRI with Gd-DTPA contrast agents would allow for a non-invasive method of measuring IFF velocity. An alternative non-invasive options such as Doppler optical coherence tomography could be utilized in highly vascularized tumors as this method is capable of measuring flow velocity without contrast agents [349]. Utilization of computational fluid dynamics software such as COMSOL, it would be possible to determine the potential of gradients to form under relevant IFF velocities based on the hepatic architecture. Examining the receptor and ligand components elucidated in Chapter 2 along with their binding affinity would tell us how the HCC cells are invading due to the autologous chemotaxis mechanism, or if they are utilizing another flow-sensing mechanism. One of the early findings in Chapter 2 identified a correlative increase in HCC cell invasion with respect to increased fluid flow velocity. Profiling IFF velocity could lead to clinical applications or strategies to prevent intrahepatic spread.

*HCC tumor cells co-cultured with hepatic stellate cells (HSCs) in the 3D fluid flow assay*

The development of *in vitro* experimental systems that incorporate cellular components to better simulate pathological conditions observed *in vivo,* ultimately help advance our understanding of cellular events that occur and aid in uncovering the potential mechanisms involved. In this body of work, the experimental set up examined directly the effect of IFF on the HCC tumor cells, however much evidence has indicated HCC cells and HSCs work in a bidirectional fashion as 'partners in crime for liver metastases' as described by Kang and colleagues [350]. In fact the development of HCC is often in the presence of underlying chronic liver injury such as fibrosis, and quiescent HSCs are activated by this repeated liver injury and various activators [75]. The incorporation of HSCs into the 3D fluid flow assay with HCC cells is not to simply add complexity to the *in vitro* assay, but rather examine their crosstalk on the autologous chemotaxis mechanism. With attention on HSCs as major contributors to HCC progression, these cells are capable in contributing to autologous chemotaxis via CXCR4/CXCL12, but also play a significant role in cellular contractility in stiff ECMs. Upon activation, HSCs experience a phenotypic transformation where they increase proliferation, secretion of ECM proteins, production various cytokines, chemokines, and growth factors [46, 51, 52, 77, 78].

With this in mind, the development of a valid co-culture of HSCs and HCC tumor cells will allow us to examine the elucidated CXCR4/CXCL12 autologous chemotaxis mechanism further in-depth. Recent findings show SDF-1 (CXCL12) is released by activated HSCs within liver tumors resulting in liver metastasis of colon cancer cells which possess CXCR4 [351]. This brings into question whether IFF can activate latent HSCs resulting in CXCL12 secretion. Consequently, stromal cells have been observed to be

express active TGF-β, which interacts with CXCR4. Additionally TGF-β upregulates CXCR4 expression in HCC cells to ultimately sensitize them to the ligand CXCL12, resulting in increased tumor cell migration and survival [352]. For this reason, future work co-culturing HSCs with tumor cells in the 3D fluid flow assay has the potential to elucidate alternative flow-induced mechanisms. Additionally this co-culture system would allow for further investigation of cell-to-cell and cell-to-ECM interactions allowing further investigation into the flow-induced invasion mechanisms elucidated earlier or hypothesized (contractility).

Incorporating HSCs with the HCC tumor cells will require future testing and validation of the viability and quiescent state of the cells. Verification of the HSCs' inactive state can be determined with various microscopy techniques. HSCs in a quiescent state will possess vitamin A lipid depositions and a stellate morphology. Activated HSCs will no longer possess this stellate morphology, but rather an elongated cell body with visible reduction in vitamin A lipid depositions and express α-SMA. One drawback to this method of microscopy is the thickness of the gel these cells are encapsulated in, therefore confocal microscopy could be utilized to examine the state of these cells. Therefore, this new co-cultured 3D fluid flow assay could provide further insight into autologous chemotaxis via CXCR4/CXCL12 as a mechanism for flow-induced HCC invasion or help identify alternative mechanisms for flow-induced HCC invasion.

### *5.2.2 Examining alternative mechanisms of flow-induced invasion*

One of the major findings in this body of work is the autologous chemotaxis mechanism for flow-induced HCC invasion described in Chapter 2. However one major

consensus can be made from this body of work is that flow-induced HCC invasion is regulated by multiple mechanisms, which is apparent with our MMP-2/9 findings. Future work will address the existing mechanisms for flow-induced invasion described in Chapter 1 and elucidate various signaling pathways that are involved in this response to fluid flow. The motivation for this work has two major purposes: (1) elucidate the various components in signaling pathways involved in the other mechanisms that regulate flow-induced invasion and (2) determine if specific HCC cell types and their propensity to utilize a specific mechanism for flow-induced invasion or are all of the elucidated mechanisms simultaneously. The purpose of uncovering all the mechanisms that regulate flow-induced HCC invasion would highlight the significance of biomechanical forces in tumor progression and show that these forces must be taken into consideration for therapeutic strategies. For this reason, elucidating the factors that determine which mechanisms the cells' use or specific cells prefer at certain stages of the disease could result in a therapy targeting the mechanisms in use for flow-induced invasion.

The alternative mechanisms described in Chapter 1 for flow-induced invasion investigated and described shear stress sensing through the glycocalyx and matrix tension and integrin activation by IFF. Shear stress sensing via the glycocalyx has been extensively studied by Tarbell and colleagues; furthermore, one of the seminal findings in this work is the increase in MMP-2/9 activity but not an increase in gelatinase expression. Under those circumstances, investigating the matrix tension and integrin activation mechanism could be a logical avenue worth pursuing first. I hypothesize that IFF exposure results in increased matrix tension and traction forces which triggers ECM proteolysis via MMP-2/9 as a result releasing growth factors such as TGF-β and PDGF to increase cell invasion via

EMT. Alternatively, ECM proteolysis via MMP-2/9 activity could alternatively degrade various cell surface receptors and diminish cell-matrix adhesions. The basis for this mechanism is based on our initial findings of increased MMP-2/9 activity in HCC cells exposed to IFF. A pivotal study by Zaman and colleagues showed that migration of tumor cells in 3D conditions is governed by ECM stiffness, cell-matrix adhesion, proteolysis [341]. Therefore the first major task that is required to elucidate this mechanism further is to determine if matrix tension or contractility are increased in HCC cells exposed to fluid flow. Examining RhoA activity would confirm changes in contractile actin myosin filaments in response to IFF. Alternatively, staining for FAK or integrin activation could serve as additional measures to confirm increased contractile forces are possible due to increased cell-matrix adhesions. Next it has been shown that mechanical forces or external stimuli can cause proteolysis and specifically the degradation of ECM proteins can alter focal adhesion, cytoskeletal architecture, and even integrin-mediated anchorage [353]. Our current results state, IFF results in increased MMP-2/9 activity, therefore functional testing of the gelatinases and examining cell-matrix adhesions would tell us if proteolysis is directly affecting cellular adhesion. If MMP-2/9 proteolysis is diminishing cell-ECM adhesion, the cell would not adhere to the collagen matrices they are embedded in and exposed to fluid flow. Diminished cell-matrix adhesion via proteolysis would cause the cells to simply end up in the bottom of the 12 well plate and not attached to the bottom of the Boyden chamber. Flow cytometry could be utilized to quantify the cells that did not adhere to the matrix. In the event that cell-matrix adhesion was not completely diminished, quantification of growth factors such as TGF-β and PDGF via ELISA would be conducted first to test the hypothesis of invasion in response to IFF is facilitated by EMT. These two

growth factors are found in the ECM in normal healthy livers as well as HCCs, and they are both capable of promoting EMT in HCC cells observed to facilitate increased invasion [354]. EMT can be confirmed with follow up experiments identifying EMT markers such as E-cadherin and functional inhibition of EMT should result in decreased invasion. Furthermore, elucidation of this mechanism would not identify if autologous chemotaxis was not completely involved. Therefore, since it is already known that TGF-β can sensitize CXCR4 and promote CXCL12 binding enhancing migration. Knocking down CXCR4 would diminish the cells ability to detect a gradient of CXCL12, simultaneously promoting EMT and measuring cell invasion would determine the mechanism cells prefer to utilize for flow induced invasion. Alternatively, exposing cells to IFF and isolating the cells that migrated through the matrix and to the bottom of the Boyden chamber could be probed for EMT markers to determine what mechanism a population of cells utilized. Changing matrix conditions and repeating the previous experiments could yield in a different mechanistic preference for flow-induced invasion.

In conclusion, this body of work uncovered that HCC cells utilize multiple mechanisms for flow-induced invasion. The elucidation of autologous chemotaxis provided insight into one mechanism for flow-induced HCC invasion. However the later findings in this body of work revealed how little is known about IFF and the mechanisms that regulate flow-induced invasion and the various components that are involved. The current findings and future work could potentially provide a better understanding of which mechanism(s) these cells have a propensity to utilize under relevant physiological conditions. Profiling of these cells or HCC stage, could provide better insight into clinical applications and strategies for treating HCC spread.

# LIST OF REFERENCES


1. Reticker-Flynn, N.E., et al., *A combinatorial extracellular matrix platform identifies cell-extracellular matrix interactions that correlate with metastasis.* Nat Commun, 2012. **3**: p. 1122.

2. Siegel, R.L., K.D. Miller, and A. Jemal, *Cancer statistics, 2016.* CA Cancer J Clin, 2016. **66**(1): p. 7-30.

3. Howlader, N., et al., *SEER Cancer Statistics Review, 1975–2011*. 2013, National Cancer Institute. Bethesda, MD, http://seer. cancer. gov/csr/1975_2011/, based on November.

4. Mazzanti, R., U. Arena, and R. Tassi, *Hepatocellular carcinoma: Where are we?* World J Exp Med, 2016. **6**(1): p. 21-36.

5. Colombo, M., *Natural history of hepatocellular carcinoma.* Cancer Imaging, 2005. **5**(1): p. 85-88.

6. Pascual, S., I. Herrera, and J. Irurzun, *New advances in hepatocellular carcinoma.* World Journal of Hepatology, 2016. **8**(9): p. 421-438.

7. Mazzanti, R., L. Gramantieri, and L. Bolondi, *Hepatocellular carcinoma: epidemiology and clinical aspects.* Mol Aspects Med, 2008. **29**(1-2): p. 130-43.

8. Sangiovanni, A., et al., *The natural history of compensated cirrhosis due to hepatitis C virus: A 17-year cohort study of 214 patients.* Hepatology, 2006. **43**(6): p. 1303-10.

9. Reeves, H.L., M.Y. Zaki, and C.P. Day, *Hepatocellular Carcinoma in Obesity, Type 2 Diabetes, and NAFLD.* Dig Dis Sci, 2016. **61**(5): p. 1234-45.

10. Bouchard, M.J. and S. Navas-Martin, *Hepatitis B and C virus hepatocarcinogenesis: Lessons learned and future challenges.* Cancer Letters, 2011. **305**(2): p. 123-143.

11. Gearhart, T.L. and M.J. Bouchard, *The Hepatitis B Virus X Protein Modulates Hepatocyte Proliferation Pathways To Stimulate Viral Replication.* Journal of Virology, 2010. **84**(6): p. 2675-2686.

12. Chen, S.L. and T.R. Morgan, *The Natural History of Hepatitis C Virus (HCV) Infection.* International Journal of Medical Sciences, 2006. **3**(2): p. 47-52.

13. Hoek, J.B. and J.G. Pastorino, *Ethanol, oxidative stress, and cytokine-induced liver cell injury.* Alcohol, 2002. **27**(1): p. 63-8.

14. McClain, C.J., et al., *Monocyte activation in alcoholic liver disease.* Alcohol, 2002. **27**(1): p. 53-61.

15. Hoshida, Y., et al., *Integrative Transcriptome Analysis Reveals Common Molecular Subclasses of Human Hepatocellular Carcinoma.* Cancer Res, 2009. **69**(18): p. 7385-92.

16. Ersahin, T., M. Ozturk, and R. Cetin-Atalay, *Molecular Biology of Liver Cancer*, in *Reviews in Cell Biology and Molecular Medicine*. 2015, Wiley-VCH Verlag GmbH & Co. KGaA. p. 206-243.

17. Leicht, D.T., et al., *Raf kinases: function, regulation and role in human cancer.* Biochim Biophys Acta, 2007. **1773**(8): p. 1196-212.

18. Hwang, Y.H., et al., *Over-expression of c-raf-1 proto-oncogene in liver cirrhosis and hepatocellular carcinoma.* Hepatol Res, 2004. **29**(2): p. 113-121.

19. Murakami, S., *Hepatitis B virus X protein: a multifunctional viral regulator.* J Gastroenterol, 2001. **36**(10): p. 651-60.

20. Tarn, C., et al., *Hepatitis B virus X protein differentially activates RAS-RAF-MAPK and JNK pathways in X-transforming versus non-transforming AML12 hepatocytes.* J Biol Chem, 2001. **276**(37): p. 34671-80.

21. Natoli, G., et al., *Induction of the DNA-binding activity of c-jun/c-fos heterodimers by the hepatitis B virus transactivator pX.* Mol Cell Biol, 1994. **14**(2): p. 989-98.

22. Benn, J. and R.J. Schneider, *Hepatitis B virus HBx protein activates Ras-GTP complex formation and establishes a Ras, Raf, MAP kinase signaling cascade.* Proc Natl Acad Sci U S A, 1994. **91**(22): p. 10350-4.

23. Aravalli, R.N. and C.J. Steer, *Hepatocellular Carcinoma: Cellular and Molecular Mechanisms and Novel Therapeutic Strategies*. 2014: Springer.

24. Avila, M.A., et al., *New therapies for hepatocellular carcinoma.* Oncogene, 2006. **25**(27): p. 3866-84.

25. Llovet, J.M. and J. Bruix, *Molecular targeted therapies in hepatocellular carcinoma.* Hepatology, 2008. **48**(4): p. 1312-27.

26. Huynh, H., et al., *Over-expression of the mitogen-activated protein kinase (MAPK) kinase (MEK)-MAPK in hepatocellular carcinoma: its role in tumor progression and apoptosis.* BMC Gastroenterol, 2003. **3**: p. 19.

27. Leelawat, K., et al., *Roles of the MEK1/2 and AKT pathways in CXCL12/CXCR4 induced cholangiocarcinoma cell invasion.* World J Gastroenterol, 2007. **13**(10): p. 1561-8.

28. Chen, Y.L., P.Y. Law, and H.H. Loh, *Inhibition of PI3K/Akt signaling: an emerging paradigm for targeted cancer therapy.* Curr Med Chem Anticancer Agents, 2005. **5**(6): p. 575-89.

29. Fang, T., L. Feng, and J. Xia, *Heterogeneity of Hepatocellular Carcinoma*, in *Application of Clinical Bioinformatics*, X. Wang, et al., Editors. 2016, Springer Netherlands: Dordrecht. p. 371-398.

30. Alexia, C., et al., *An evaluation of the role of insulin-like growth factors (IGF) and of type-I IGF receptor signalling in hepatocarcinogenesis and in the resistance of hepatocarcinoma cells against drug-induced apoptosis.* Biochem Pharmacol, 2004. **68**(6): p. 1003-15.

31. Desbois-Mouthon, C., et al., *Insulin and IGF-1 stimulate the beta-catenin pathway through two signalling cascades involving GSK-3beta inhibition and Ras activation.* Oncogene, 2001. **20**(2): p. 252-9.

32. Chen, J.S., et al., *Involvement of PI3K/PTEN/AKT/mTOR pathway in invasion and metastasis in hepatocellular carcinoma: Association with MMP-9.* Hepatol Res, 2009. **39**(2): p. 177-86.

33. Grabinski, N., et al., *Combined targeting of AKT and mTOR synergistically inhibits proliferation of hepatocellular carcinoma cells.* Mol Cancer, 2012. **11**: p. 85.

34. Zhou, Q., V.W. Lui, and W. Yeo, *Targeting the PI3K/Akt/mTOR pathway in hepatocellular carcinoma.* Future Oncol, 2011. **7**(10): p. 1149-67.

35. Roberts, L.R. and G.J. Gores, *Hepatocellular carcinoma: molecular pathways and new therapeutic targets.* Semin Liver Dis, 2005. **25**(2): p. 212-25.

36. de La Coste, A., et al., *Somatic mutations of the beta-catenin gene are frequent in mouse and human hepatocellular carcinomas.* Proc Natl Acad Sci U S A, 1998. **95**(15): p. 8847-51.

37. Aravalli, R.N. and C.J. Steer, *Molecular Mechanisms of HCC*, in *Hepatocellular Carcinoma: Cellular and Molecular Mechanisms and Novel Therapeutic Strategies*. 2014, Springer International Publishing: Cham. p. 33-46.

38. Anson, M., et al., *Oncogenic beta-catenin triggers an inflammatory response that determines the aggressiveness of hepatocellular carcinoma in mice.* J Clin Invest, 2012. **122**(2): p. 586-99.

39. Wong, C.M., S.T. Fan, and I.O. Ng, *beta-Catenin mutation and overexpression in hepatocellular carcinoma: clinicopathologic and prognostic significance.* Cancer, 2001. **92**(1): p. 136-45.

40. Giles, R.H., J.H. van Es, and H. Clevers, *Caught up in a Wnt storm: Wnt signaling in cancer.* Biochim Biophys Acta, 2003. **1653**(1): p. 1-24.

41. Gu, W., X. Li, and J. Wang, *miR-139 regulates the proliferation and invasion of hepatocellular carcinoma through the WNT/TCF-4 pathway.* Oncol Rep, 2014. **31**(1): p. 397-404.

42. Eggert, T. and T.F. Greten, *Tumor regulation of the tissue environment in the liver.* Pharmacol Ther, 2017.

43. Yang, J.D., I. Nakamura, and L.R. Roberts, *The tumor microenvironment in hepatocellular carcinoma: current status and therapeutic targets.* Semin Cancer Biol, 2011. **21**(1): p. 35-43.

44. Joyce, J.A., *Therapeutic targeting of the tumor microenvironment.* Cancer Cell, 2005. **7**(6): p. 513-20.

45. Joyce, J.A. and D.T. Fearon, *T cell exclusion, immune privilege, and the tumor microenvironment.* Science, 2015. **348**(6230): p. 74-80.

46. Campbell, J.S., et al., *Platelet-derived growth factor C induces liver fibrosis, steatosis, and hepatocellular carcinoma.* Proc Natl Acad Sci U S A, 2005. **102**(9): p. 3389-94.

47. El–Serag, H.B. and K.L. Rudolph, *Hepatocellular Carcinoma: Epidemiology and Molecular Carcinogenesis.* Gastroenterology, 2007. **132**(7): p. 2557-2576.

48. Luedde, T. and R.F. Schwabe, *NF-[kappa]B in the liver[mdash]linking injury, fibrosis and hepatocellular carcinoma.* Nat Rev Gastroenterol Hepatol, 2011. **8**(2): p. 108-118.

49. Wells, R.G., *The role of matrix stiffness in regulating cell behavior.* Hepatology, 2008. **47**(4): p. 1394-400.

50. Hernandez-Gea, V. and S.L. Friedman, *Pathogenesis of liver fibrosis.* Annu Rev Pathol, 2011. **6**: p. 425-56.

51. Friedman, S.L., et al., *Hepatic lipocytes: the principal collagen-producing cells of normal rat liver.* Proc Natl Acad Sci U S A, 1985. **82**(24): p. 8681-5.

52. Bataller, R. and D.A. Brenner, *Liver fibrosis.* J Clin Invest, 2005. **115**(2): p. 209-18.

53. Friedman, S.L., *Liver fibrosis -- from bench to bedside.* J Hepatol, 2003. **38 Suppl 1**: p. S38-53.

54. Szabo, G., P. Mandrekar, and A. Dolganiuc, *Innate immune response and hepatic inflammation.* Semin Liver Dis, 2007. **27**(4): p. 339-50.

55. Reynaert, H., et al., *Hepatic stellate cells: role in microcirculation and pathophysiology of portal hypertension.* Gut, 2002. **50**(4): p. 571-81.

56. Friedman, S.L., *Evolving challenges in hepatic fibrosis.* Nat Rev Gastroenterol Hepatol, 2010. **7**(8): p. 425-36.

57. Knittel, T., et al., *Expression patterns of matrix metalloproteinases and their inhibitors in parenchymal and non-parenchymal cells of rat liver: regulation by TNF-alpha and TGF-beta1.* J Hepatol, 1999. **30**(1): p. 48-60.

58. !!! INVALID CITATION !!! {Geerts, 2001 #714;Lotersztajn, 2005 #713;Friedman, 2008 #679;Friedman, 2010 #720}.

59. Marra, F., *Hepatic stellate cells and the regulation of liver inflammation.* J Hepatol, 1999. **31**(6): p. 1120-30.

60. Milani, S., et al., *Procollagen expression by nonparenchymal rat liver cells in experimental biliary fibrosis.* Gastroenterology, 1990. **98**(1): p. 175-84.

61. Geerts, A., *History, heterogeneity, developmental biology, and functions of quiescent hepatic stellate cells.* Semin Liver Dis, 2001. **21**(3): p. 311-35.

62. Maher, J.J., *Interactions between hepatic stellate cells and the immune system.* Semin Liver Dis, 2001. **21**(3): p. 417-26.

63. Schuppan, D., et al., *Matrix as a modulator of hepatic fibrogenesis.* Semin Liver Dis, 2001. **21**(3): p. 351-72.

64. Lotersztajn, S., et al., *Hepatic fibrosis: molecular mechanisms and drug targets.* Annu Rev Pharmacol Toxicol, 2005. **45**: p. 605-28.

65. Vinas, O., et al., *Human hepatic stellate cells show features of antigen-presenting cells and stimulate lymphocyte proliferation.* Hepatology, 2003. **38**(4): p. 919-29.

66. Wells, R.G., *Cellular Sources of Extracellular Matrix in Hepatic Fibrosis.* Clinics in liver disease, 2008. **12**(4): p. 759-viii.

67. Discher, D.E., P. Janmey, and Y.-l. Wang, *Tissue Cells Feel and Respond to the Stiffness of Their Substrate.* Science, 2005. **310**(5751): p. 1139-1143.

68. Olaso, E., et al., *DDR2 receptor promotes MMP-2–mediated proliferation and invasion by hepatic stellate cells.* Journal of Clinical Investigation, 2001. **108**(9): p. 1369-1378.

69. Wallace, M.C. and S.L. Friedman, *Hepatic fibrosis and the microenvironment: fertile soil for hepatocellular carcinoma development.* Gene Expr, 2014. **16**(2): p. 77-84.

70. Fransvea, E., et al., *Blocking transforming growth factor-beta up-regulates E-cadherin and reduces migration and invasion of hepatocellular carcinoma cells.* Hepatology, 2008. **47**(5): p. 1557-66.

71. Fransvea, E., et al., *Targeting transforming growth factor (TGF)-betaRI inhibits activation of beta1 integrin and blocks vascular invasion in hepatocellular carcinoma.* Hepatology, 2009. **49**(3): p. 839-50.

72. Bhowmick, N.A., E.G. Neilson, and H.L. Moses, *Stromal fibroblasts in cancer initiation and progression.* Nature, 2004. **432**(7015): p. 332-7.

73. Pietras, K. and A. Ostman, *Hallmarks of cancer: interactions with the tumor stroma.* Exp Cell Res, 2010. **316**(8): p. 1324-31.

74. Ostman, A. and M. Augsten, *Cancer-associated fibroblasts and tumor growth--bystanders turning into key players.* Curr Opin Genet Dev, 2009. **19**(1): p. 67-73.

75. Wynn, T.A., *Cellular and molecular mechanisms of fibrosis.* J Pathol, 2008. **214**(2): p. 199-210.

76. Pellicoro, A., et al., *Liver fibrosis and repair: immune regulation of wound healing in a solid organ.* Nat Rev Immunol, 2014. **14**(3): p. 181-194.

77. Friedman, S.L., *Hepatic stellate cells: protean, multifunctional, and enigmatic cells of the liver.* Physiol Rev, 2008. **88**(1): p. 125-72.

78. Eghbali-Fatourechi, G., et al., *Type I procollagen production and cell proliferation is mediated by transforming growth factor-beta in a model of hepatic fibrosis.* Endocrinology, 1996. **137**(5): p. 1894-903.

79. Amann, T., et al., *Activated hepatic stellate cells promote tumorigenicity of hepatocellular carcinoma.* Cancer Sci, 2009. **100**(4): p. 646-53.

80. Dubuisson, L., et al., *Expression and cellular localization of fibrillin-1 in normal and pathological human liver.* J Hepatol, 2001. **34**(4): p. 514-22.

81. Zhao, W., et al., *Hepatic stellate cells promote tumor progression by enhancement of immunosuppressive cells in an orthotopic liver tumor mouse model.* Lab Invest, 2014. **94**(2): p. 182-91.

82. Ji, J., et al., *Hepatic stellate cell and monocyte interaction contributes to poor prognosis in hepatocellular carcinoma.* Hepatology, 2015. **62**(2): p. 481-95.

83. Thomson, A.W. and P.A. Knolle, *Antigen-presenting cell function in the tolerogenic liver environment.* Nat Rev Immunol, 2010. **10**(11): p. 753-766.

84. Ryschich, E., et al., *Molecular fingerprinting and autocrine growth regulation of endothelial cells in a murine model of hepatocellular carcinoma.* Cancer Res, 2006. **66**(1): p. 198-211.

85. Amin, D.N., et al., *Tumor Endothelial Cells Express Epidermal Growth Factor Receptor (EGFR) but not ErbB3 and Are Responsive to EGF and to EGFR Kinase Inhibitors.* Cancer Research, 2006. **66**(4): p. 2173-2180.

86. Rolny, C., et al., *Platelet-derived growth factor receptor-beta promotes early endothelial cell differentiation.* Blood, 2006. **108**(6): p. 1877-86.

87. Yu, Q., *The dynamic roles of angiopoietins in tumor angiogenesis.* Future Oncol, 2005. **1**(4): p. 475-84.

88. Davis, G.E. and D.R. Senger, *Endothelial extracellular matrix: biosynthesis, remodeling, and functions during vascular morphogenesis and neovessel stabilization.* Circ Res, 2005. **97**(11): p. 1093-107.

89. Dudley, A.C., *Tumor endothelial cells.* Cold Spring Harb Perspect Med, 2012. **2**(3): p. a006536.

90. Leonardi, G.C., et al., *The tumor microenvironment in hepatocellular carcinoma (review).* Int J Oncol, 2012. **40**(6): p. 1733-47.

91. Konerding, M.A., et al., *Evidence for characteristic vascular patterns in solid tumours: quantitative studies using corrosion casts.* Br J Cancer, 1999. **80**(5-6): p. 724-32.

92. Benetti, A., et al., *Transforming growth factor-beta1 and CD105 promote the migration of hepatocellular carcinoma-derived endothelium.* Cancer Res, 2008. **68**(20): p. 8626-34.

93. Baluk, P., H. Hashizume, and D.M. McDonald, *Cellular abnormalities of blood vessels as targets in cancer.* Curr Opin Genet Dev, 2005. **15**(1): p. 102-11.

94. Li, X.M., et al., *Serum vascular endothelial growth factor is a predictor of invasion and metastasis in hepatocellular carcinoma.* J Exp Clin Cancer Res, 1999. **18**(4): p. 511-7.

95. Hashizume, H., et al., *Openings between defective endothelial cells explain tumor vessel leakiness.* Am J Pathol, 2000. **156**(4): p. 1363-80.

96. Yamaguchi, R., et al., *Expression of vascular endothelial growth factor in human hepatocellular carcinoma.* Hepatology, 1998. **28**(1): p. 68-77.

97. Poon, R.T., et al., *Prognostic significance of serum vascular endothelial growth factor and endostatin in patients with hepatocellular carcinoma.* Br J Surg, 2004. **91**(10): p. 1354-60.

98. Cressman, D.E., et al., *Liver failure and defective hepatocyte regeneration in interleukin-6-deficient mice.* Science, 1996. **274**(5291): p. 1379-83.

99. Lin, W.W. and M. Karin, *A cytokine-mediated link between innate immunity, inflammation, and cancer.* J Clin Invest, 2007. **117**(5): p. 1175-83.

100. Parks, W.C., C.L. Wilson, and Y.S. Lopez-Boado, *Matrix metalloproteinases as modulators of inflammation and innate immunity.* Nat Rev Immunol, 2004. **4**(8): p. 617-29.

101. Carloni, V., et al., *The integrin, alpha6beta1, is necessary for the matrix-dependent activation of FAK and MAP kinase and the migration of human hepatocarcinoma cells.* Hepatology, 2001. **34**(1): p. 42-9.

102. Tahmasebi Birgani, M. and V. Carloni, *Tumor Microenvironment, a Paradigm in Hepatocellular Carcinoma Progression and Therapy.* Int J Mol Sci, 2017. **18**(2).

103. He, G. and M. Karin, *NF-[kappa]B and STAT3 - key players in liver inflammation and cancer.* Cell Res, 2011. **21**(1): p. 159-168.

104. Sun, B. and M. Karin, *Obesity, inflammation, and liver cancer.* Journal of Hepatology, 2012. **56**(3): p. 704-713.

105. Wong, V.W., et al., *High serum interleukin-6 level predicts future hepatocellular carcinoma development in patients with chronic hepatitis B.* Int J Cancer, 2009. **124**(12): p. 2766-70.

106. Fausto, N., J.S. Campbell, and K.J. Riehle, *Liver regeneration.* Hepatology, 2006. **43**(S1): p. S45-S53.

107. Karin, M., *Nuclear factor-[kappa]B in cancer development and progression.* Nature, 2006. **441**(7092): p. 431-436.

108. Huang, Y.S., et al., *Serum levels of cytokines in hepatitis C-related liver disease: a longitudinal study.* Zhonghua Yi Xue Za Zhi (Taipei), 1999. **62**(6): p. 327-33.

109. Nakazaki, H., *Preoperative and postoperative cytokines in patients with cancer.* Cancer, 1992. **70**(3): p. 709-13.

110. Budhu, A. and X.W. Wang, *The role of cytokines in hepatocellular carcinoma.* J Leukoc Biol, 2006. **80**(6): p. 1197-213.

111. Pietras, K., et al., *Functions of paracrine PDGF signaling in the proangiogenic tumor stroma revealed by pharmacological targeting.* PLoS Med, 2008. **5**(1): p. e19.

112. Murata, M., et al., *Hepatitis B virus X protein shifts human hepatic transforming growth factor (TGF)-beta signaling from tumor suppression to oncogenesis in early chronic hepatitis B.* Hepatology, 2009. **49**(4): p. 1203-17.

113. Yang, J.C., et al., *Enhanced expression of vascular endothelial growth factor-A in ground glass hepatocytes and its implication in hepatitis B virus hepatocarcinogenesis.* Hepatology, 2009. **49**(6): p. 1962-71.

114. Neaud, V., et al., *Human hepatic myofibroblasts increase invasiveness of hepatocellular carcinoma cells: evidence for a role of hepatocyte growth factor.* Hepatology, 1997. **26**(6): p. 1458-66.

115. Presta, M., et al., *Fibroblast growth factor/fibroblast growth factor receptor system in angiogenesis.* Cytokine Growth Factor Rev, 2005. **16**(2): p. 159-78.

116. Gomis, R.R., et al., *C/EBPbeta at the core of the TGFbeta cytostatic response and its evasion in metastatic breast cancer cells.* Cancer Cell, 2006. **10**(3): p. 203-14.

117. Massague, J., *TGFbeta in Cancer.* Cell, 2008. **134**(2): p. 215-30.

118. Bedossa, P., et al., *Transforming growth factor-beta 1 (TGF-beta 1) and TGF-beta 1 receptors in normal, cirrhotic, and neoplastic human livers.* Hepatology, 1995. **21**(3): p. 760-6.

119. Matsuzaki, K., et al., *Chronic inflammation associated with hepatitis C virus infection perturbs hepatic transforming growth factor beta signaling, promoting cirrhosis and hepatocellular carcinoma.* Hepatology, 2007. **46**(1): p. 48-57.

120. Ooi, L.P., et al., *Evidence that "myofibroblast-like" cells are the cellular source of capsular collagen in hepatocellular carcinoma.* J Hepatol, 1997. **26**(4): p. 798-807.

121. Ji, J., et al., *Let-7g targets collagen type I alpha2 and inhibits cell migration in hepatocellular carcinoma.* J Hepatol, 2010. **52**(5): p. 690-7.

122. Miner, J.H., *Laminins and their roles in mammals.* Microsc Res Tech, 2008. **71**(5): p. 349-56.

123. Giannelli, G., et al., *Laminin-5 chains are expressed differentially in metastatic and nonmetastatic hepatocellular carcinoma.* Clin Cancer Res, 2003. **9**(10 Pt 1): p. 3684-91.

124. Hynes, R.O., *Integrins: versatility, modulation, and signaling in cell adhesion.* Cell, 1992. **69**(1): p. 11-25.

125. Wu, Y., et al., *Proapoptotic function of integrin beta(3) in human hepatocellular carcinoma cells.* Clin Cancer Res, 2009. **15**(1): p. 60-9.

126. Mizuno, H., et al., *Changes in adhesive and migratory characteristics of hepatocellular carcinoma (HCC) cells induced by expression of alpha3beta1 integrin.* Biochim Biophys Acta, 2008. **1780**(3): p. 564-70.

127. Fu, Y., et al., *Overexpression of integrin beta1 inhibits proliferation of hepatocellular carcinoma cell SMMC-7721 through preventing Skp2-dependent degradation of p27 via PI3K pathway.* J Cell Biochem, 2007. **102**(3): p. 704-18.

128. Ogasawara, S., et al., *Expressions of basic fibroblast growth factor and its receptors and their relationship to proliferation of human hepatocellular carcinoma cell lines.* Hepatology, 1996. **24**(1): p. 198-205.

129. Gross, J. and C.M. Lapiere, *COLLAGENOLYTIC ACTIVITY IN AMPHIBIAN TISSUES: A TISSUE CULTURE ASSAY.* Proc Natl Acad Sci U S A, 1962. **48**(6): p. 1014-22.

130. Kessenbrock, K., V. Plaks, and Z. Werb, *Matrix metalloproteinases: regulators of the tumor microenvironment.* Cell, 2010. **141**(1): p. 52-67.

131. Bourboulia, D. and W.G. Stetler-Stevenson, *Matrix MetalloProteinases (MMPs) andTissue Inhibitors of MetalloProteinases (TIMPs): positive and negative regulators intumor cell adhesion.* Semin Cancer Biol, 2010. **20**(3): p. 161-8.

132. Liotta, L.A., et al., *Metastatic potential correlates with enzymatic degradation of basement membrane collagen.* Nature, 1980. **284**(5751): p. 67-68.

133. Van Wart, H.E. and H. Birkedal-Hansen, *The cysteine switch: a principle of regulation of metalloproteinase activity with potential applicability to the entire matrix metalloproteinase gene family.* Proc Natl Acad Sci U S A, 1990. **87**(14): p. 5578-82.

134. Sternlicht, M.D. and Z. Werb, *How matrix metalloproteinases regulate cell behavior.* Annu Rev Cell Dev Biol, 2001. **17**: p. 463-516.

135. Sun, M.H., et al., *Expressions of inducible nitric oxide synthase and matrix metalloproteinase-9 and their effects on angiogenesis and progression of hepatocellular carcinoma.* World J Gastroenterol, 2005. **11**(38): p. 5931-7.

136. Roomi, M.W., et al., *Patterns of MMP-2 and MMP-9 expression in human cancer cell lines.* Oncol Rep, 2009. **21**(5): p. 1323-33.

137. Arii, S., et al., *Overexpression of matrix metalloproteinase 9 gene in hepatocellular carcinoma with invasive potential.* Hepatology, 1996. **24**(2): p. 316-22.

138. Yu, Q. and I. Stamenkovic, *Localization of matrix metalloproteinase 9 to the cell surface provides a mechanism for CD44-mediated tumor invasion.* Genes Dev, 1999. **13**(1): p. 35-48.

139. Kohga, K., et al., *Expression of CD133 confers malignant potential by regulating metalloproteinases in human hepatocellular carcinoma.* Journal of Hepatology. **52**(6): p. 872-879.

140. Xia, D., et al., *Overexpression of TIMP-1 mediated by recombinant adenovirus in hepatocellular carcinoma cells inhibits proliferation and invasion in vitro.* Hepatobiliary Pancreat Dis Int, 2006. **5**(3): p. 409-15.

141. Levick, J.R., *Flow through interstitium and other fibrous matrices.* Q J Exp Physiol, 1987. **72**(4): p. 409-37.

142. Ng, C.P. and M.A. Swartz, *Fibroblast alignment under interstitial fluid flow using a novel 3-D tissue culture model.* Am J Physiol Heart Circ Physiol, 2003. **284**(5): p. H1771-H1777.

143. Hamdan, M., et al. *A permeability function for Brinkman's equation*. in *WSEAS International Conference. Proceedings. Mathematics and Computers in Science and Engineering*. 2009. WSEAS.

144. Chary, S.R. and R.K. Jain, *Direct measurement of interstitial convection and diffusion of albumin in normal and neoplastic tissues by fluorescence photobleaching.* Proc Natl Acad Sci U S A, 1989. **86**(14): p. 5385-9.

145. Dafni, H., et al., *Overexpression of vascular endothelial growth factor 165 drives peritumor interstitial convection and induces lymphatic drain: magnetic resonance imaging, confocal microscopy, and histological tracking of triple-labeled albumin.* Cancer Res, 2002. **62**(22): p. 6731-9.

146. Hompland, T., et al., *Interstitial fluid pressure and associated lymph node metastasis revealed in tumors by dynamic contrast-enhanced MRI.* Cancer Res, 2012. **72**(19): p. 4899-908.

147. Jain, R.K., R.T. Tong, and L.L. Munn, *Effect of vascular normalization by antiangiogenic therapy on interstitial hypertension, peritumor edema, and lymphatic metastasis: insights from a mathematical model.* Cancer Res, 2007. **67**(6): p. 2729-35.

148. Starling, E.H., *The influence of mechanical factors on lymph production.* J Physiol, 1894. **16**(3-4): p. 224-67.

149. Taylor, A.E., *Capillary fluid filtration. Starling forces and lymph flow.* Circ Res, 1981. **49**(3): p. 557-75.

150. Heldin, C.-H., et al., *High interstitial fluid pressure—an obstacle in cancer therapy.* Nat Rev Cancer, 2004. **4**(10): p. 806-813.

151. Rackow, E.C., I.A. Fein, and J. Leppo, *Colloid osmotic pressure as a prognostic indicator of pulmonary edema and mortality in the critically ill.* Chest, 1977. **72**(6): p. 709-713.

152. Stohrer, M., et al., *Oncotic pressure in solid tumors is elevated.* Cancer Res, 2000. **60**(15): p. 4251-5.

153. Kvietys, P.R., in *The Gastrointestinal Circulation*. 2010: San Rafael (CA).

154. Pedersen, J.A., F. Boschetti, and M.A. Swartz, *Effects of extracellular fiber architecture on cell membrane shear stress in a 3D fibrous matrix.* J Biomech, 2007. **40**(7): p. 1484-92.

155. Whitaker, S., *Flow in porous media I: A theoretical derivation of Darcy's law.* Transport in porous media, 1986. **1**(1): p. 3-25.

156. Swartz, M.A. and M.E. Fleury, *Interstitial flow and its effects in soft tissues.* Annu Rev Biomed Eng, 2007. **9**: p. 229-56.

157. Gentleman, E., et al., *Short collagen fibers provide control of contraction and permeability in fibroblast-seeded collagen gels.* Tissue Eng, 2004. **10**(3-4): p. 421-7.

158. Ng, C.P. and S.H. Pun, *A Perfusable 3D cell–matrix tissue culture chamber for in situ evaluation of nanoparticle vehicle penetration and transport.* Biotechnol Bioeng, 2008. **99**(6): p. 1490-1501.

159. de Marsily, G., *Quantitative hydrogeology: groundwater hydrology for engineers*. 1986: Academic Press.

160. Ajubi, N.E., et al., *Pulsating fluid flow increases prostaglandin production by cultured chicken osteocytes—a cytoskeleton-dependent process.* Biochem Biophys Res Commun, 1996. **225**(1): p. 62-8.

161. Buschmann, M.D., et al., *Stimulation of Aggrecan Synthesis in Cartilage Explants by Cyclic Loading Is Localized to Regions of High Interstitial Fluid Flow1.* Arch Biochem Biophys, 1999. **366**(1): p. 1-7.

162. Galbraith, C.G., R. Skalak, and S. Chien, *Shear stress induces spatial reorganization of the endothelial cell cytoskeleton.* Cell Motil Cytoskeleton, 1998. **40**(4): p. 317-30.

163. Johnson, D.L., T.N. McAllister, and J.A. Frangos, *Fluid flow stimulates rapid and continuous release of nitric oxide in osteoblasts.* Am J Physiol, 1996. **271**(1): p. E205-8.

164. Kapur, S., D.J. Baylink, and K.H. Lau, *Fluid flow shear stress stimulates human osteoblast proliferation and differentiation through multiple interacting and competing signal transduction pathways.* Bone, 2003. **32**(3): p. 241-51.

165. Leu, A.J., et al., *Flow velocity in the superficial lymphatic network of the mouse tail.* Am J Physiol, 1994. **267**(4): p. H1507-13.

166. McAllister, T.N., T. Du, and J.A. Frangos, *Fluid shear stress stimulates prostaglandin and nitric oxide release in bone marrow-derived preosteoclast-like cells.* Biochem Biophys Res Commun, 2000. **270**(2): p. 643-8.

167. Reich, K.M., C.V. Gay, and J.A. Frangos, *Fluid shear stress as a mediator of osteoblast cyclic adenosine monophosphate production.* J Cell Physiol, 1990. **143**(1): p. 100-104.

168. Semino, C.E., R.D. Kamm, and D.A. Lauffenburger, *Autocrine EGF receptor activation mediates endothelial cell migration and vascular morphogenesis induced by VEGF under interstitial flow.* Exp Cell Res, 2006. **312**(3): p. 289-298.

169. Topper, J.N. and M.A. Gimbrone, Jr., *Blood flow and vascular gene expression: fluid shear stress as a modulator of endothelial phenotype.* Mol Med Today, 1999. **5**(1): p. 40-6.

170. Rutkowski, J.M. and M.A. Swartz, *A driving force for change: interstitial flow as a morphoregulator.* Trends Cell Biol, 2007. **17**(1): p. 44-50.

171. Arisaka, T., et al., *Effects of shear stress on glycosaminoglycan synthesis in vascular endothelial cells.* Ann N Y Acad Sci, 1995. **748**(1): p. 543-54.

172. Shi, Z.D., et al., *Interstitial flow promotes vascular fibroblast, myofibroblast, and smooth muscle cell motility in 3-D collagen I via upregulation of MMP-1.* Am J Physiol Heart Circ Physiol, 2009. **297**(4): p. H1225-H1234.

173. Blatnik, J.S., G.W. Schmid-Schonbein, and L.A. Sung, *The influence of fluid shear stress on the remodeling of the embryonic primary capillary plexus.* Biomech Model Mechanobiol, 2005. **4**(4): p. 211-20.

174. Butler, T.P., F.H. Grantham, and P.M. Gullino, *Bulk transfer of fluid in the interstitial compartment of mammary tumors.* Cancer Res, 1975. **35**(11): p. 3084-8.

175. Dewey, C.F., Jr., et al., *The dynamic response of vascular endothelial cells to fluid shear stress.* J Biomech Eng, 1981. **103**(3): p. 177-85.

176. Sheikh, S., et al., *Exposure to fluid shear stress modulates the ability of endothelial cells to recruit neutrophils in response to tumor necrosis factor-α: a basis for local variations in vascular sensitivity to inflammation.* Blood, 2003. **102**(8): p. 2828-2834.

177. Swartz, M.A., et al., *Mechanical stress is communicated between different cell types to elicit matrix remodeling.* Proc Natl Acad Sci U S A, 2001. **98**(11): p. 6180-5.

178. Tzima, E., et al., *A mechanosensory complex that mediates the endothelial cell response to fluid shear stress.* Nature, 2005. **437**(7057): p. 426-31.

179. Baxter, L.T. and R.K. Jain, *Transport of fluid and macromolecules in tumors. I. Role of interstitial pressure and convection.* Microvasc Res, 1989. **37**(1): p. 77-104.

180. Thibodeaux, L.J. and J.D. Boyle, *Bedform-generated convective transport in bottom sediment.* 1987.

181. Fleury, M.E., K.C. Boardman, and M.A. Swartz, *Autologous morphogen gradients by subtle interstitial flow and matrix interactions.* Biophys J, 2006. **91**(1): p. 113-21.

182. Boardman, K.C. and M.A. Swartz, *Interstitial flow as a guide for lymphangiogenesis.* Circ Res, 2003. **92**(7): p. 801-8.

183. Ng, C.P., C.L. Helm, and M.A. Swartz, *Interstitial flow differentially stimulates blood and lymphatic endothelial cell morphogenesis in vitro.* Microvasc Res, 2004. **68**(3): p. 258-64.

184. Shi, Z.D. and J.M. Tarbell, *Fluid flow mechanotransduction in vascular smooth muscle cells and fibroblasts.* Ann Biomed Eng, 2011. **39**(6): p. 1608-1619.

185. Wang, S. and J.M. Tarbell, *Effect of fluid flow on smooth muscle cells in a 3-dimensional collagen gel model.* Arterioscler Thromb Vasc Biol, 2000. **20**(10): p. 2220-5.

186. Shieh, A.C., *Biomechanical forces shape the tumor microenvironment.* Ann Biomed Eng, 2011. **39**(5): p. 1379-1389.

187. Takeuchi, H., et al., *CCL21 chemokine regulates chemokine receptor CCR7 bearing malignant melanoma cells.* Clin Cancer Res, 2004. **10**(7): p. 2351-8.

188. Brighton, C.T. and W.P. McCluskey, *Cellular response and mechanisms of action of electrically induced osteogenesis.* Bone and Mineral Research/4. Amsterdam, The Netherlands: Elsevier Science Publishers BV, 1986: p. 213-254.

189. Fukada, E. and I. Yasuda, *On the piezoelectric effect of bone.* J. Phys. Soc. Japan, 1957. **12**(10): p. 1158-1162.

190. Hillsley, M.V. and J.A. Frangos, *Bone tissue engineering: the role of interstitial fluid flow.* Biotechnol Bioeng, 1994. **43**(7): p. 573-81.

191. Kufahl, R.H. and S. Saha, *A theoretical model for stress-generated fluid flow in the canaliculi-lacunae network in bone tissue.* J Biomech, 1990. **23**(2): p. 171-80.

192. Meinel, L., et al., *Bone tissue engineering using human mesenchymal stem cells: effects of scaffold material and medium flow.* Ann Biomed Eng, 2004. **32**(1): p. 112-22.

193. Montgomery, R.J., et al., *Interstitial fluid flow in cortical bone.* Microvasc Res, 1988. **35**(3): p. 295-307.

194. Tan, S.D., et al., *Osteocytes subjected to fluid flow inhibit osteoclast formation and bone resorption.* Bone, 2007. **41**(5): p. 745-51.

195. Turner, C.H., M.R. Forwood, and M.W. Otter, *Mechanotransduction in bone: do bone cells act as sensors of fluid flow?* FASEB J, 1994. **8**(11): p. 875-8.

196. Weinbaum, S., S.C. Cowin, and Y. Zeng, *A model for the excitation of osteocytes by mechanical loading-induced bone fluid shear stresses.* J Biomech, 1994. **27**(3): p. 339-60.

197. Civelek, M., et al., *Smooth muscle cells contract in response to fluid flow via a Ca2+-independent signaling mechanism.* J Appl Physiol, 2002. **93**(6): p. 1907-17.

198. Shi, Z.D., et al., *Interstitial flow induces MMP-1 expression and vascular SMC migration in collagen I gels via an ERK1/2-dependent and c-Jun-mediated mechanism.* Am J Physiol Heart Circ Physiol, 2010. **298**(1): p. H127-H135.

199. Ainslie, K.M., et al., *Vascular smooth muscle cell glycocalyx influences shear stress-mediated contractile response.* J Appl Physiol (1985), 2005. **98**(1): p. 242-9.

200. Yao, Y., A. Rabodzey, and C.F. Dewey, Jr., *Glycocalyx modulates the motility and proliferative response of vascular endothelium to fluid shear stress.* Am J Physiol Heart Circ Physiol, 2007. **293**(2): p. H1023-30.

201. Florian, J.A., et al., *Heparan sulfate proteoglycan is a mechanosensor on endothelial cells.* Circ Res, 2003. **93**(10): p. e136-42.

202. Shi, Z.D., H. Wang, and J.M. Tarbell, *Heparan sulfate proteoglycans mediate interstitial flow mechanotransduction regulating MMP-13 expression and cell motility via FAK-ERK in 3D collagen.* PLoS One, 2011. **6**(1): p. e15956.

203. Shi, Z.D., G. Abraham, and J.M. Tarbell, *Shear stress modulation of smooth muscle cell marker genes in 2-D and 3-D depends on mechanotransduction by heparan sulfate proteoglycans and ERK1/2.* PLoS One, 2010. **5**(8): p. e12196.

204. Swartz, M.A. and A.W. Lund, *Lymphatic and interstitial flow in the tumour microenvironment: linking mechanobiology with immunity.* Nat Rev Cancer, 2012. **12**(3): p. 210-9.

205. Miteva, D.O., et al., *Transmural flow modulates cell and fluid transport functions of lymphatic endothelium.* Circ Res, 2010. **106**(5): p. 920-31.

206. Helm, C.L., et al., *Synergy between interstitial flow and VEGF directs capillary morphogenesis in vitro through a gradient amplification mechanism.* Proc Natl Acad Sci U S A, 2005. **102**(44): p. 15779-84.

207. Dvorak, H.F., et al., *Vascular permeability factor/vascular endothelial growth factor, microvascular hyperpermeability, and angiogenesis.* Am J Pathol, 1995. **146**(5): p. 1029-39.

208. Boucher, Y. and R.K. Jain, *Microvascular pressure is the principal driving force for interstitial hypertension in solid tumors: implications for vascular collapse.* Cancer Res, 1992. **52**(18): p. 5110-4.

209. Shields, J.D., et al., *Autologous chemotaxis as a mechanism of tumor cell homing to lymphatics via interstitial flow and autocrine CCR7 signaling.* Cancer cell, 2007. **11**(6): p. 526-38.

210. Geer, C.P. and S.A. Grossman, *Interstitial fluid flow along white matter tracts: a potentially important mechanism for the dissemination of primary brain tumors.* J Neurooncol, 1997. **32**(3): p. 193-201.

211. Kingsmore, K.M., et al., *Interstitial flow differentially increases patient-derived glioblastoma stem cell invasion via CXCR4, CXCL12, and CD44-mediated mechanisms.* Integrative Biology, 2016. **8**(12): p. 1246-1260.

212. Piotrowski-Daspit, A.S., J. Tien, and C.M. Nelson, *Interstitial fluid pressure regulates collective invasion in engineered human breast tumors via Snail, vimentin, and E-cadherin.* Integrative Biology, 2016. **8**(3): p. 319-331.

213. Tchafa, A.M., et al., *EMT Transition Alters Interstitial Fluid Flow-Induced Signaling in ERBB2-Positive Breast Cancer Cells.* Mol Cancer Res, 2015. **13**(4): p. 755-64.

214. Polacheck, W.J., J.L. Charest, and R.D. Kamm, *Interstitial flow influences direction of tumor cell migration through competing mechanisms.* Proc Natl Acad Sci U S A, 2011. **108**(27): p. 11115-11120.

215. Pedersen, J.A., S. Lichter, and M.A. Swartz, *Cells in 3D matrices under interstitial flow: effects of extracellular matrix alignment on cell shear stress and drag forces.* J Biomech, 2010. **43**(5): p. 900-905.

216. Shieh, A.C., et al., *Tumor cell invasion is promoted by interstitial flow-induced matrix priming by stromal fibroblasts.* Cancer Res, 2011. **71**(3): p. 790-800.

217. Qazi, H., et al., *Cancer cell glycocalyx mediates mechanotransduction and flow-regulated invasion.* Integr Biol (Camb), 2013. **5**(11): p. 1334-43.

218. Qazi, H., Z.D. Shi, and J.M. Tarbell, *Fluid shear stress regulates the invasive potential of glioma cells via modulation of migratory activity and matrix metalloproteinase expression.* PloS one, 2011. **6**(5): p. e20348.

219. Tomasek, J.J., et al., *Myofibroblasts and mechano-regulation of connective tissue remodelling.* Nat Rev Mol Cell Biol, 2002. **3**(5): p. 349-63.

220. Kalluri, R. and M. Zeisberg, *Fibroblasts in cancer.* Nat Rev Cancer, 2006. **6**(5): p. 392-401.

221. Ng, C.P., B. Hinz, and M.A. Swartz, *Interstitial fluid flow induces myofibroblast differentiation and collagen alignment in vitro.* J Cell Sci, 2005. **118**(20): p. 4731-9.

222. Brown, L.F., et al., *Vascular permeability factor/vascular endothelial growth factor: a multifunctional angiogenic cytokine.* EXS, 1996: p. 233-69.

223. Jain, R.K., *Transport of molecules in the tumor interstitium: a review.* Cancer Res, 1987. **47**(12): p. 3039-51.

224. Shields, J.D., et al., *Chemokine-mediated migration of melanoma cells towards lymphatics–a mechanism contributing to metastasis.* Oncogene, 2007. **26**(21): p. 2997-3005.

225. Sterpetti, A.V., et al., *Shear stress modulates the proliferation rate, protein synthesis, and mitogenic activity of arterial smooth muscle cells.* Surgery, 1993. **113**(6): p. 691-9.

226. Wilson, E., et al., *Mechanical strain induces growth of vascular smooth muscle cells via autocrine action of PDGF.* J Cell Biol, 1993. **123**(3): p. 741-7.

227. Ferguson, S.J., K. Ito, and L.P. Nolte, *Fluid flow and convective transport of solutes within the intervertebral disc.* J Biomech, 2004. **37**(2): p. 213-21.

228. Jain, R.K. and L.T. Baxter, *Mechanisms of heterogeneous distribution of monoclonal antibodies and other macromolecules in tumors: significance of elevated interstitial pressure.* Cancer Res, 1988. **48**(24 Part 1): p. 7022-32.

229. Tarbell, J.M. and M.Y. Pahakis, *Mechanotransduction and the glycocalyx.* J Intern Med, 2006. **259**(4): p. 339-50.

230. Weinbaum, S., J.M. Tarbell, and E.R. Damiano, *The structure and function of the endothelial glycocalyx layer.* Annu Rev Biomed Eng, 2007. **9**: p. 121-67.

231. Tarbell, J.M. and Z.D. Shi, *Effect of the glycocalyx layer on transmission of interstitial flow shear stress to embedded cells.* Biomech Model Mechanobiol, 2013. **12**(1): p. 111-21.

232. Zigmond, S.H., *Ability of polymorphonuclear leukocytes to orient in gradients of chemotactic factors.* J Cell Biol, 1977. **75**(2): p. 606-16.

233. Garcia, A.M., et al., *Contributions of fluid convection and electrical migration to transport in cartilage: relevance to loading.* Arch Biochem Biophys, 1996. **333**(2): p. 317-25.

234. Kholodenko, B.N., *Cell-signalling dynamics in time and space.* Nat Rev Mol Cell Biol, 2006. **7**(3): p. 165-76.

235. Munson, J.M., R.V. Bellamkonda, and M.A. Swartz, *Interstitial flow in a 3D microenvironment increases glioma invasion by a CXCR4-dependent mechanism.* Cancer Res
2013. **73**(5): p. 1536-46.

236. Shyy, J.Y. and S. Chien, *Role of integrins in endothelial mechanosensing of shear stress.* Circ Res, 2002. **91**(9): p. 769-775.

237. Paszek, M.J., et al., *Tensional homeostasis and the malignant phenotype.* Cancer cell, 2005. **8**(3): p. 241-254.

238. Paszek, M.J., et al., *Integrin clustering is driven by mechanical resistance from the glycocalyx and the substrate.* PLoS Comput Biol, 2009. **5**(12): p. e1000604.

239. Chung, L.W., et al., *Molecular insights into prostate cancer progression: the missing link of tumor microenvironment.* J Urol, 2005. **173**(1): p. 10-20.

240. Jain, R.K., *Transport of molecules, particles, and cells in solid tumors.* Annu Rev Biomed Eng, 1999. **1**: p. 241-63.

241. Polacheck, W.J., I.K. Zervantonakis, and R.D. Kamm, *Tumor cell migration in complex microenvironments.* Cell Mol Life Sci, 2013. **70**(8): p. 1335-56.

242. Whiteside, T.L., *The tumor microenvironment and its role in promoting tumor growth.* Oncogene, 2008. **27**(45): p. 5904-12.

243. Polacheck, W.J., J.L. Charest, and R.D. Kamm, *Interstitial flow influences direction of tumor cell migration through competing mechanisms.* Proc Natl Acad Sci U S A, 2011. **108**(27): p. 11115-20.

244. Shieh, A.C. and M.A. Swartz, *Regulation of tumor invasion by interstitial fluid flow.* Phys Biol, 2011. **8**(1): p. 015012.

245. Polacheck, W.J., et al., *Mechanotransduction of fluid stresses governs 3D cell migration.* Proc Natl Acad Sci U S A, 2014. **111**(7): p. 2447-52.

246. Munson, J.M., R.V. Bellamkonda, and M.A. Swartz, *Interstitial flow in a 3D microenvironment increases glioma invasion by a CXCR4-dependent mechanism.* Cancer Res, 2013. **73**(5): p. 1536-46.

247. Shields, J.D., et al., *Chemokine-mediated migration of melanoma cells towards lymphatics--a mechanism contributing to metastasis.* Oncogene, 2007. **26**(21): p. 2997-3005.

248. Ferlay, J., et al., *Cancer incidence and mortality worldwide: sources, methods and major patterns in GLOBOCAN 2012.* Int J Cancer, 2015. **136**(5): p. E359-86.

249. Siegel, R., D. Naishadham, and A. Jemal, *Cancer statistics, 2013.* CA Cancer J Clin, 2013. **63**(1): p. 11-30.

250. Society, A.C. *Liver Cancer*. 2013 [cited 2013; 1/18/2013:[http://www.cancer.org/acs/groups/cid/documents/webcontent/003114-pdf.pdf].

251. Kondo, Y. and K. Wada, *Intrahepatic metastasis of hepatocellular carcinoma: a histopathologic study.* Hum Pathol, 1991. **22**(2): p. 125-30.

252. Katyal, S., et al., *Extrahepatic metastases of hepatocellular carcinoma.* Radiology, 2000. **216**(3): p. 698-703.

253. Bruix, J. and M. Sherman, *Management of hepatocellular carcinoma: an update.* Hepatology, 2011. **53**(3): p. 1020-2.

254. Tung-Ping Poon, R., S.T. Fan, and J. Wong, *Risk factors, prevention, and management of postoperative recurrence after resection of hepatocellular carcinoma.* Ann Surg, 2000. **232**(1): p. 10-24.

255. Zhu, A.X., *Development of sorafenib and other molecularly targeted agents in hepatocellular carcinoma.* Cancer, 2008. **112**(2): p. 250-9.

256. Venook, A.P., et al., *The incidence and epidemiology of hepatocellular carcinoma: a global and regional perspective.* Oncologist, 2010. **15 Suppl 4**: p. 5-13.

257. Wells, R.G. and D.E. Discher, *Matrix elasticity, cytoskeletal tension, and TGF-beta: the insoluble and soluble meet.* Sci Signal, 2008. **1**(10): p. pe13.

258. Polacheck, W.J., I.K. Zervantonakis, and R.D. Kamm, *Tumor cell migration in complex microenvironments.* Cellular and Molecular Life Sciences, 2012: p. 1-22.

259. Hori, K., et al., *Increased tumor tissue pressure in association with the growth of rat tumors.* Jpn J Cancer Res, 1986. **77**(1): p. 65-73.

260. Liu, H., et al., *Roles of chemokine receptor 4 (CXCR4) and chemokine ligand 12 (CXCL12) in metastasis of hepatocellular carcinoma cells.* Cell Mol Immunol, 2008. **5**(5): p. 373-8.

261. Schimanski, C.C., et al., *Dissemination of hepatocellular carcinoma is mediated via chemokine receptor CXCR4.* Br J Cancer, 2006. **95**(2): p. 210-7.

262. Shibuta, K., et al., *Regional expression of CXCL12/CXCR4 in liver and hepatocellular carcinoma and cell-cycle variation during in vitro differentiation.* Jpn J Cancer Res, 2002. **93**(7): p. 789-97.

263. Xiang, Z.L., et al., *Chemokine receptor CXCR4 expression in hepatocellular carcinoma patients increases the risk of bone metastases and poor survival.* BMC Cancer, 2009. **9**: p. 176.

264. Gearhart, T.L. and M.J. Bouchard, *The hepatitis B virus X protein modulates hepatocyte proliferation pathways to stimulate viral replication.* J Virol, 2010. **84**(6): p. 2675-86.

265. Risks, N.I.o.H.O.f.P.f.R. and N.I.o.H.O.o.L.A. Welfare, *Public Health Service policy on humane care and use of laboratory animals*. 2002: Office of Laboratory Animal Welfare, National Institutes of Health, Department of Health and Human Services.

266. Albus, U., *Guide for the Care and Use of Laboratory Animals (8th edn).* Laboratory Animals, 2012. **46**(3): p. 267-268.

267. Tchafa, A.M., et al., *Three-dimensional Cell Culture Model for Measuring the Effects of Interstitial Fluid Flow on Tumor Cell Invasion.* J Vis Exp, 2012(65).

268. Siggers, J.H., et al., *Mathematical model of blood and interstitial flow and lymph production in the liver.* Biomech Model Mechanobiol, 2014. **13**(2): p. 363-78.

269. Brand, S., et al., *CXCR4 and CXCL12 are inversely expressed in colorectal cancer cells and modulate cancer cell migration, invasion and MMP-9 activation.* Exp Cell Res, 2005. **310**(1): p. 117-30.

270. Schmidt, C.M., et al., *Increased MAPK expression and activity in primary human hepatocellular carcinoma.* Biochem Biophys Res Commun, 1997. **236**(1): p. 54-8.

271. Wiesenauer, C.A., et al., *Multiple anticancer effects of blocking MEK-ERK signaling in hepatocellular carcinoma.* J Am Coll Surg, 2004. **198**(3): p. 410-21.

272. Ueki, T., et al., *Usefulness of tumor pressure as a prognostic factor in cases of hepatocellular carcinoma where the diameter of the tumor is 3 cm or less.* Cancer, 2002. **95**(3): p. 596-604.

273. Liang, Z., et al., *CXCR4/CXCL12 axis promotes VEGF-mediated tumor angiogenesis through Akt signaling pathway.* Biochem Biophys Res Commun, 2007. **359**(3): p. 716-22.

274. Domanska, U.M., et al., *A review on CXCR4/CXCL12 axis in oncology: no place to hide.* Eur J Cancer, 2013. **49**(1): p. 219-30.

275. Mitra, P., et al., *Loss of chemokine SDF-1alpha-mediated CXCR4 signalling and receptor internalization in human hepatoma cell line HepG2.* Cell Signal, 2001. **13**(5): p. 311-9.

276. Sutton, A., et al., *Stromal cell-derived factor-1/chemokine (C-X-C motif) ligand 12 stimulates human hepatoma cell growth, migration, and invasion.* Mol Cancer Res, 2007. **5**(1): p. 21-33.

277. Callejas, N.A., et al., *Expression of cyclooxygenase-2 promotes the release of matrix metalloproteinase-2 and -9 in fetal rat hepatocytes.* Hepatology, 2001. **33**(4): p. 860-7.

278. Mayoral, R., et al., *Prostaglandin E2 promotes migration and adhesion in hepatocellular carcinoma cells.* Carcinogenesis, 2005. **26**(4): p. 753-61.

279. Seo, H.R., *Roles of Tumor Microenvironment in Hepatocelluar Carcinoma.* Current Medicinal Chemistry, 2015. **11**(2): p. 82-93.

280. Chen, Y.Y., et al., *Bufalin inhibits migration and invasion in human hepatocellular carcinoma SK-Hep1 cells through the inhibitions of NF-kB and matrix metalloproteinase-2/-9-signaling pathways.* Environ Toxicol, 2015. **30**(1): p. 74-82.

281. Yeh, C.B., et al., *Antimetastatic effects of norcantharidin on hepatocellular carcinoma by transcriptional inhibition of MMP-9 through modulation of NF-kB activity.* PLoS One, 2012. **7**(2): p. e31055.

282. Li, X., et al., *Overexpression of Bmi-1 contributes to the invasion and metastasis of hepatocellular carcinoma by increasing the expression of matrix metalloproteinase (MMP)2, MMP-9 and vascular endothelial growth factor via the PTEN/PI3K/Akt pathway.* Int J Oncol, 2013. **43**(3): p. 793-802.

283. Cheng, J.C., et al., *Radiation-enhanced hepatocellular carcinoma cell invasion with MMP-9 expression through PI3K/Akt/NF-kappaB signal transduction pathway.* Oncogene, 2006. **25**(53): p. 7009-18.

284. Bonfil, R.D., et al., *Inhibition of human prostate cancer growth, osteolysis and angiogenesis in a bone metastasis model by a novel mechanism-based selective gelatinase inhibitor.* Int J Cancer, 2006. **118**(11): p. 2721-6.

285. Brown, S., et al., *Potent and Selective Mechanism-Based Inhibition of Gelatinases.* Journal of the American Chemical Society, 2000. **122**(28): p. 6799-6800.

286. Shah, A.D., M.J. Bouchard, and A.C. Shieh, *Interstitial Fluid Flow Increases Hepatocellular Carcinoma Cell Invasion through CXCR4/CXCL12 and MEK/ERK Signaling.* PLoS One, 2015. **10**(11): p. e0142337.

287. Butcher, D.T., T. Alliston, and V.M. Weaver, *A tense situation: forcing tumour progression.* Nat Rev Cancer, 2009. **9**(2): p. 108-22.

288. Smith, M.L., et al., *Force-induced unfolding of fibronectin in the extracellular matrix of living cells.* PLoS Biol, 2007. **5**(10): p. e268.

289. Nelson, A.R., et al., *Matrix metalloproteinases: biologic activity and clinical implications.* J Clin Oncol, 2000. **18**(5): p. 1135-49.

290. Garanich, J.S., M. Pahakis, and J.M. Tarbell, *Shear stress inhibits smooth muscle cell migration via nitric oxide-mediated downregulation of matrix metalloproteinase-2 activity.* Am J Physiol Heart Circ Physiol, 2005. **288**(5): p. H2244-52.

291. Preaux, A.M., et al., *Matrix metalloproteinase-2 activation in human hepatic fibrosis regulation by cell-matrix interactions.* Hepatology, 1999. **30**(4): p. 944-50.

292. Roy, R., J. Yang, and M.A. Moses, *Matrix metalloproteinases as novel biomarkers and potential therapeutic targets in human cancer.* J Clin Oncol, 2009. **27**(31): p. 5287-97.

293. Hatfield, K.J., H. Reikvam, and O. Bruserud, *The crosstalk between the matrix metalloprotease system and the chemokine network in acute myeloid leukemia.* Curr Med Chem, 2010. **17**(36): p. 4448-61.

294. Bauvois, B., *New facets of matrix metalloproteinases MMP-2 and MMP-9 as cell surface transducers: outside-in signaling and relationship to tumor progression.* Biochim Biophys Acta, 2012. **1825**(1): p. 29-36.

295. Cauwe, B., P.E. Van den Steen, and G. Opdenakker, *The biochemical, biological, and pathological kaleidoscope of cell surface substrates processed by matrix metalloproteinases.* Crit Rev Biochem Mol Biol, 2007. **42**(3): p. 113-85.

296. Sato, H., et al., *A matrix metalloproteinase expressed on the surface of invasive tumour cells.* Nature, 1994. **370**(6484): p. 61-5.

297. Knäuper, V., et al., *Biochemical Characterization of Human Collagenase-3.* Journal of Biological Chemistry, 1996. **271**(3): p. 1544-1550.

298. d'Ortho, M.P., et al., *Membrane-type matrix metalloproteinases 1 and 2 exhibit broad-spectrum proteolytic capacities comparable to many matrix metalloproteinases.* Eur J Biochem, 1997. **250**(3): p. 751-7.

299. Ohuchi, E., et al., *Membrane Type 1 Matrix Metalloproteinase Digests Interstitial Collagens and Other Extracellular Matrix Macromolecules.* Journal of Biological Chemistry, 1997. **272**(4): p. 2446-2451.

300. Yana, I. and M. Seiki, *MT-MMPs play pivotal roles in cancer dissemination.* Clin Exp Metastasis, 2002. **19**(3): p. 209-15.

301. Ip, Y.-C., et al., *Mechanism of metastasis by membrane type 1-matrix metalloproteinase in hepatocellular carcinoma.* World Journal of Gastroenterology : WJG, 2005. **11**(40): p. 6269-6276.

302. Fattovich, G., et al., *Hepatocellular carcinoma in cirrhosis: incidence and risk factors.* Gastroenterology, 2004. **127**(5 Suppl 1): p. S35-50.

303. Schrader, J., et al., *Matrix stiffness modulates proliferation, chemotherapeutic response, and dormancy in hepatocellular carcinoma cells.* Hepatology, 2011. **53**(4): p. 1192-205.

304. Levental, K.R., et al., *Matrix crosslinking forces tumor progression by enhancing integrin signaling.* Cell, 2009. **139**(5): p. 891-906.

305. Cox, T.R. and J.T. Erler, *Remodeling and homeostasis of the extracellular matrix: implications for fibrotic diseases and cancer.* Dis Model Mech, 2011. **4**(2): p. 165-78.

306. Erler, J.T. and V.M. Weaver, *Three-dimensional context regulation of metastasis.* Clin Exp Metastasis, 2009. **26**(1): p. 35-49.

307. Ng, M.R. and J.S. Brugge, *A stiff blow from the stroma: collagen crosslinking drives tumor progression.* Cancer Cell, 2009. **16**(6): p. 455-7.

308. DuFort, C.C., M.J. Paszek, and V.M. Weaver, *Balancing forces: architectural control of mechanotransduction.* Nat Rev Mol Cell Biol, 2011. **12**(5): p. 308-19.

309. Lu, P., V.M. Weaver, and Z. Werb, *The extracellular matrix: a dynamic niche in cancer progression.* J Cell Biol, 2012. **196**(4): p. 395-406.

310. Provenzano, P.P., et al., *Matrix density-induced mechanoregulation of breast cell phenotype, signaling and gene expression through a FAK-ERK linkage.* Oncogene, 2009. **28**(49): p. 4326-4343.

311. Masuzaki, R., et al., *Prospective risk assessment for hepatocellular carcinoma development in patients with chronic hepatitis C by transient elastography.* Hepatology, 2009. **49**(6): p. 1954-61.

312. Rombouts, K. and V. Carloni, *The fibrotic microenvironment as a heterogeneity facet of hepatocellular carcinoma.* Fibrogenesis Tissue Repair, 2013. **6**(1): p. 17.

313. Roy, R., A. Boskey, and L.J. Bonassar, *Processing of Type I Collagen Gels Using Non-Enzymatic Glycation.* J Biomed Mater Res A, 2010. **93**(3): p. 843-51.

314. Roy, R., A.L. Boskey, and L.J. Bonassar, *Non-enzymatic glycation of chondrocyte-seeded collagen gels for cartilage tissue engineering.* J Orthop Res, 2008. **26**(11): p. 1434-9.

315. Mosher, D.F. and P.E. Schad, *Cross-linking of fibronectin to collagen by blood coagulation Factor XIIIa.* J Clin Invest, 1979. **64**(3): p. 781-7.

316. Schnider, S.L. and R.R. Kohn, *Glucosylation of human collagen in aging and diabetes mellitus.* J Clin Invest, 1980. **66**(5): p. 1179-81.

317. Wiberg, C., et al., *Complexes of matrilin-1 and biglycan or decorin connect collagen VI microfibrils to both collagen II and aggrecan.* J Biol Chem, 2003. **278**(39): p. 37698-704.

318. Perepelyuk, M., et al., *Normal and Fibrotic Rat Livers Demonstrate Shear Strain Softening and Compression Stiffening: A Model for Soft Tissue Mechanics.* PLoS ONE, 2016. **11**(1): p. e0146588.

319. Okazaki, I., *Novel Cancer-targeting Agents/Application Strategies Developed from MMP Science.* Anticancer Agents Med Chem, 2012.

320. Provenzano, P.P., et al., *Collagen reorganization at the tumor-stromal interface facilitates local invasion.* BMC Med, 2006. **4**(1): p. 38.

321. Ben-Baruch, A., *The multifaceted roles of chemokines in malignancy.* Cancer Metastasis Rev, 2006. **25**(3): p. 357-71.

322. Stover, D.G., B. Bierie, and H.L. Moses, *A delicate balance: TGF-beta and the tumor microenvironment.* J Cell Biochem, 2007. **101**(4): p. 851-61.

323. Reigle, K.L., et al., *Non-enzymatic glycation of type I collagen diminishes collagen-proteoglycan binding and weakens cell adhesion.* Journal of cellular biochemistry, 2008. **104**(5): p. 1684-1698.

324. Yin, M., et al., *Assessment of hepatic fibrosis with magnetic resonance elastography.* Clin Gastroenterol Hepatol, 2007. **5**(10): p. 1207-1213.e2.

325. Georges, P.C., et al., *Increased stiffness of the rat liver precedes matrix deposition: implications for fibrosis.* Am J Physiol Gastrointest Liver Physiol, 2007. **293**(6): p. G1147-54.

326. Ulrich, P. and A. Cerami, *Protein glycation, diabetes, and aging.* Recent Prog Horm Res, 2001. **56**: p. 1-21.

327. Brett, J., et al., *Survey of the distribution of a newly characterized receptor for advanced glycation end products in tissues.* Am J Pathol, 1993. **143**(6): p. 1699-712.

328. Kemeny, S.F., et al., *Glycated collagen alters endothelial cell actin alignment and nitric oxide release in response to fluid shear stress.* J Biomech, 2011. **44**(10): p. 1927-35.

329. Figueroa, D.S., S.F. Kemeny, and A.M. Clyne, *Glycated Collagen Impairs Endothelial Cell Response to Cyclic Stretch.* Cellular and Molecular Bioengineering, 2011. **4**(2): p. 220.

330. Hirose, A., et al., *Advanced glycation end products increase endothelial permeability through the RAGE/Rho signaling pathway.* FEBS Lett, 2010. **584**(1): p. 61-6.

331. Basta, G., *Receptor for advanced glycation endproducts and atherosclerosis: From basic mechanisms to clinical implications.* Atherosclerosis, 2008. **196**(1): p. 9-21.

332. Herrmann, K.L., A.D. McCulloch, and J.H. Omens, *Glycated collagen cross-linking alters cardiac mechanics in volume-overload hypertrophy.* Am J Physiol Heart Circ Physiol, 2003. **284**(4): p. H1277-84.

333. Hasegawa, G., A.J. Hunter, and A.S. Charonis, *Matrix nonenzymatic glycosylation leads to altered cellular phenotype and intracellular tyrosine phosphorylation.* J Biol Chem, 1995. **270**(7): p. 3278-83.

334. Liang, Y., et al., *A cell-instructive hydrogel to regulate malignancy of 3D tumor spheroids with matrix rigidity.* Biomaterials, 2011. **32**(35): p. 9308-9315.

335. Matsusue, R., et al., *Hepatic stellate cells promote liver metastasis of colon cancer cells by the action of SDF-1/CXCR4 axis.* Ann Surg Oncol, 2009. **16**(9): p. 2645-53.

336. Gentilini, A., et al., *Role of the stromal-derived factor-1 (SDF-1)-CXCR4 axis in the interaction between hepatic stellate cells and cholangiocarcinoma.* J Hepatol, 2012. **57**(4): p. 813-20.

337. Miranti, C.K. and J.S. Brugge, *Sensing the environment: a historical perspective on integrin signal transduction.* Nat Cell Biol, 2002. **4**(4): p. E83-90.

338. Ng, M.R. and J.S. Brugge, *A Stiff Blow from the Stroma: Collagen Crosslinking Drives Tumor Progression.* Cancer Cell, 2009. **16**(6): p. 455-457.

339. Reigle, K.L., et al., *Non-enzymatic glycation of type I collagen diminishes collagen-proteoglycan binding and weakens cell adhesion.* J Cell Biochem, 2008. **104**(5): p. 1684-98.

340. Schrader, J., et al., *Matrix stiffness modulates proliferation, chemotherapeutic response, and dormancy in hepatocellular carcinoma cells.* Hepatology, 2011. **53**(4): p. 1192-1205.

341. Zaman, M.H., et al., *Migration of tumor cells in 3D matrices is governed by matrix stiffness along with cell-matrix adhesion and proteolysis.* Proc Natl Acad Sci U S A, 2006. **103**(29): p. 10889-94.

342. Mierke, C.T., et al., *Integrin α5β1 facilitates cancer cell invasion through enhanced contractile forces.* Journal of Cell Science, 2011. **124**(3): p. 369-383.

343. Pellegrin, S. and H. Mellor, *Actin stress fibres.* J Cell Sci, 2007. **120**(Pt 20): p. 3491-9.

344. Riento, K. and A.J. Ridley, *Rocks: multifunctional kinases in cell behaviour.* Nat Rev Mol Cell Biol, 2003. **4**(6): p. 446-56.

345. Hagerty, L., et al., *ROCK1 phosphorylates and activates zipper-interacting protein kinase.* J Biol Chem, 2007. **282**(7): p. 4884-93.

346. Fukui, K., et al., *Expression and prognostic role of RhoA GTPases in hepatocellular carcinoma.* Journal of Cancer Research and Clinical Oncology, 2006. **132**(10): p. 627-633.

347. Provenzano, P.P., et al., *Contact Guidance Mediated Three-Dimensional Cell Migration is Regulated by Rho/ROCK-Dependent Matrix Reorganization.* Biophysical Journal, 2008. **95**(11): p. 5374-5384.

348. Yangben, Y.-z., et al., *Effects of substrate rigidity on human hepatic and hepatocellular carcinoma cell migration behavior.* J Med Biol Eng. **33**(2): p. 199-206.

349. Blatter, C., et al., *In vivo label-free measurement of lymph flow velocity and volumetric flow rates using Doppler optical coherence tomography.* 2016. **6**: p. 29035.

350. Kang, N., G.J. Gores, and V.H. Shah, *Hepatic stellate cells: Partners in crime for liver metastases?* Hepatology, 2011. **54**(2): p. 707-713.

351. Matsusue, R., et al., *Hepatic Stellate Cells Promote Liver Metastasis of Colon Cancer Cells by the Action of SDF-1/CXCR4 Axis.* Annals of Surgical Oncology, 2009. **16**(9): p. 2645-2653.

352. Bertran, E., et al., *Role of CXCR4/SDF-1 alpha in the migratory phenotype of hepatoma cells that have undergone epithelial-mesenchymal transition in response to the transforming growth factor-beta.* Cell Signal, 2009. **21**(11): p. 1595-606.

353. Werb, Z., *ECM and Cell Surface Proteolysis: Regulating Cellular Ecology.* Cell, 1997. **91**(4): p. 439-442.